A STUDY OF SAND-ASPHALT MIXTURES: A CONSTITUTIVE MODEL BASED ON A THERMOMECHANICAL FRAMEWORK AND EXPERIMENTAL CORROBORATION

A Dissertation

by

PARAG RAVINDRAN

Submitted to the Office of Graduate Studies of
Texas A&M University
in partial fulfillment of the requirements for the degree of

DOCTOR OF PHILOSOPHY

August 2006

Major Subject: Mechanical Engineering

A STUDY OF SAND-ASPHALT MIXTURES: A CONSTITUTIVE MODEL BASED ON A THERMOMECHANICAL FRAMEWORK AND EXPERIMENTAL CORROBORATION

A Dissertation

by

PARAG RAVINDRAN

Submitted to the Office of Graduate Studies of
Texas A&M University
in partial fulfillment of the requirements for the degree of

DOCTOR OF PHILOSOPHY

Approved by:

Chair of Committee,	K. R. Rajagopal
Committee Members,	N. K. Anand
	D. N. Little
	E. Masad
	J. R. Walton
Head of Department,	D. O'Neal

August 2006

Major Subject: Mechanical Engineering

ABSTRACT

A Study of Sand-Asphalt Mixtures:
A Constitutive Model Based on a Thermomechanical Framework and Experimental Corroboration. (August 2006)
Parag Ravindran, B.E., Bangalore University;
M.S.,Texas A&M University
Chair of Advisory Committee: Dr. K. R. Rajagopal

Asphalt bound mixtures have been put to diverse uses. The complicated nature of the material and the demanding conditions under which it is used preclude complete solutions to questions on load bearing capability under field conditions. In proportion to the quantity of its usage and in acknowledgment of modeling complexity, the material has been interrogated by many researchers using a variety of mechanical tests, and a plethora of linear viscoelastic models have been developed. Most models are intended to account for specific classes of problems.

This work addresses the conspicuous absence of systematic documentation of normal forces generated as a result of shear. The normal force generated during simple shear is a clear indication of the nonlinear nature of the material. The effect of fillers (hydrated lime and limestone), air voids, aggregate gradation, asphalt source and step loading on normal force generation during torsion is experimentally investigated.

Based on experimental evidence, a non-linear thermomechanical model for sand-asphalt mixtures based on the idea of multiple natural configurations is developed. The model accounts for the fact that the mixture has a natural configuration (stress-free configuration) which evolves as it is subjected to loads. Assumptions are made regarding the manner in which the material stores and dissipates energy. A key

assumption is that among the various constitutive relations possible, the one that is chosen is the one that maximizes the rate of entropy production. The model that is developed accounts for the anisotropic nature of the response.

The experimental results show that asphalt bound mixtures generate significant normal forces even at low rotation rates. The source of asphalt, aggregate gradation, fillers and air voids have a pronounced effect on normal stress generation. The model is corroborated against data from torsion experiments.

To Mother, Father and Sourabh

ACKNOWLEDGMENTS

As one phase of my learning process comes to an end, I take this opportunity to express my gratitude to the people who made this journey possible and worthwhile.

I thank Professor Rajagopal who has been a big influence on me as a researcher and as a person. It was a great privilege to have a man with his depth and breadth of knowledge as my advisor. His classes on mechanics were exhilarating. The span of his interests from poetry to philosophy have left a deep and lasting impression. I thank him for his guidance and support. Without his key inputs this work would not have come to fruition.

I thank Prof. Anand who helped me in many way during my days in College Station. I thank him for his support. I thank Prof. Walton for his beautifully explained classes and his ability to answer questions with illuminating insight, both I greatly enjoyed. I thank him for taking the time to serve on my committee. I thank Prof. Little for spending time guiding me in my work. He was a pleasure to work with. I thank Prof. Masad whose class on bituminous materials guided my early steps into asphalt mechanics. I appreciate the time he has given me and his help with this work.

I thank Prof. Murali Krishnan who patiently guided me through many problems that arose in the course of this work. Truly without him this work would not have been started or completed. His work ethic, incredible drive, energy and vision will always be a source of motivation.

I owe much to Dr. Luoyi Tao. His wisdom, simplicity and incisive intelligence will always inspire me. He has given of his time and knowledge freely and generously. It was a joy to learn from him.

I thank Dr. Rita Caso who supported me and encouraged me at a crucial time during the course of this work.

I thank Mr. Rick Canatella, who was very helpful and aided me in sample preparation for my experiments.

I thank my friends (in alphabetical order!) Seungik Baek, Craig Bridges, Shankar Coimbatore, Pradeep Hariharakumar, Jae-Taek Im, Saradhi Koneru, Krishna Kannan, Waqar Malik, Anand Mohan, Sharat Prasad and Umakanthan Saravanan who helped me in many ways and made my stay in College Station a happy one. The wonderful conversations I had with them sharpened my thinking and improved my understanding of life and mechanics.

I thank my teachers from school who taught me to think. I learnt much from them. In particular I thank Mr. Jayakar.

My deepest thanks to my mother, my father and my brother Sourabh. This work is the result of their love, sacrifices and support. Without their constant encouragement I would have never started or finished this journey. I owe everything to them.

I thank God for the giving me the opportunity to learn and explore.

TABLE OF CONTENTS

Page

LIST OF TABLES

LIST OF FIGURES

FIGURE Page

FIGURE Page

FIGURE Page

FIGURE Page

CHAPTER I

INTRODUCTION

A. Introduction

Asphalt has had an interesting role in the growth of human civilization. Its most widespread and visible use today is in road construction. A recent review by Murali Krishnan and Rajagopal [1] traces the rich and fascinating history, uses and modeling of asphalt from ancient to modern times. An account of the history of roads can be found in [2],[3]. From tool making to mummification to storing nuclear waste, asphalt has served as a versatile engineering material. The Shell bitumen handbook lists about 250 known uses of asphalt [4].

Today asphalt holds together approximately 2.3 million miles of American hard surfaced roadways. The importance of roads can be gauged from the fact that Americans traveled 2.7 trillion vehicle miles in the year 2000 [5] and 54 percent of total freight transport by weight and 83 percent by value in 1998 occurred over highways [5]. The size of the asphalt industry can be gauged from the fact that Europe and USA produced 800 million tons of hot mix asphalt in the year 2003 [6].

The class of materials under study here are asphalt-bound mixtures. It consists of aggregates of different sizes (decided on the basis of intended use) held together by asphalt. The final mixture laid on the field (and specimens made in the laboratory) include air voids. Aggregates finer than 75 microns that are added to the mixture are classified as fillers. Asphalt together with intimately mixed fillers/fine aggregates is called mastic. The effect of fillers on mixture properties is through the mastic. This is unlike the behavior of the larger aggregates. It is recognized that fillers play a very

---

The journal model is *IEEE Transactions on Automatic Control.*

important role in determining the properties of asphalt paving mixes. The addition of fillers 'stiffens' the mix. It may also influence the long term behavior of the mix (aging), the response of the mix to the presence of moisture and other properties.

Sand asphalt is distinguished from asphalt concrete in that the size of the aggregates is small.

A major goal of asphalt mechanics is be to able to solve initial-boundary value problems to predict the the behavior of asphalt-concrete pavements over their lifetime under the influence of a host of mechanical, thermal and environmental stimuli. The important first step towards this is to perform experiments that capture the essential nature of the mixture. One of the aims of this dissertation is to generate data for a phenomenological model that globally captures the influence of its constituents. Although continuum models do not explicitly incorporate microstructural information, a good understanding of the constituents of sand asphalt is extremely important to performing reasonable experiments and developing constitutive models.

B. Focus of Research

Although it is known that asphalt bound mixtures exhibit non-linear response, linear viscoelastic models are widely used to describe its mechanical response (see the review article by Murali Krishnan and Rajagopal [1] for an extensive list of references).

The goal of this dissertation is two pronged. One to provide conclusive experimental evidence that asphalt bound mixtures are non-linear in nature. The second, to develop an appropriate large deformation model to explain the experimental results.

The above goals were targeted by studying the response of sand asphalt specimens under torsion. The development of normal forces during torsion is evidence of the non-linear response of the material. A systematic experimental documentation

of some of the different factors that influence normal force development was carried out. The following factors were examined:

1. The effect of fillers: That fillers have significant influence on asphalt mix behavior is well documented. One filler of special interest is hydrated lime. Many researchers have documented the beneficial effects of hydrated lime (see for example [7]). Some investigations have also generated evidence to the contrary (see for example. [8]). In this study hydrated lime is compared to limestone and asphalt without fillers.

2. Source of asphalt: Asphalt is graded using the SUPERPAVE PG[1] system. It provides a method for selecting asphalt binders. It aims to prevent fatigue cracking, low temperature cracking and permanent deformation. The PG system assumes that asphalt behaves as a linear viscoelastic material. The properties of asphalt are specified using viscosity measurements, tensile tests and bending tests. Although the PG system is a vast improvement on previous grading methods, there is plenty of room for further improvement. In tests carried out here, the response of specimens differing only in the asphalt used (graded the same but from diverse crude sources) is examined. Asphalts from different sources even when graded the same have different amounts of constituents and this in turn dictates their ability to react chemically.

3. Effect of Air Voids: The behavior of asphalt concrete depends on its internal structure characterized by air voids. The air voids have to be within a certain range to provide good pavements. The percentage of air voids, changes over the lifetime of the pavement. The air voids are a critical factor both in the short

[1]SUPERPAVE stands for Superior Performing Asphalt Pavements, PG stands for Performance Grade.

term and long term response of asphalt pavements. It determines how porous the mixture is and how the environment interacts with the asphalt.

4. Step loading: Step loading subjects the specimen to one or two cycles of loading followed by rest period. This may enable a clear delineation of the effects of the source of asphalt (microscopic cracks form and coalesce in the asphalt during loading, how these cracks heal during rest periods depends on the nature of the asphalt). This type of loading is motivated also by practical considerations (asphalt pavements are subjected to repeated loads).

5. Aggregate gradation. Aggregates constitute the largest component of asphalt bound mixtures. The influence of aggregates on mix behavior has been studied by many authors (see for example [9]). The gradation of aggregates is particularly important to the mix response. In this study the effect of two different sand gradations on normal stresses is documented.

Using the experimental results a large deformation model for sand asphalt mixtures is developed using the framework put in place by Rajagopal [10] and co-workers to study the response of dissipative bodies.

C. Outline of Dissertation

In chapter II, the notation is introduced. The basic kinematics and balance laws are briefly discussed. The role of natural configurations and dissipation is explicated.

Chapter III presents a survey of the literature in the field. A case is built for carrying out a detailed experimental study of normal stress differences generated in asphalt bound mixtures. The case for an appropriate continuum model to interpret the results is also advanced.

Chapter IV carries a documentation of the experiments that were performed and details of the rheometer that was used.

In Chapter V, a thermo-mechanical framework for developing models for asphalt bound mixtures is presented. The methodology of maximization of the rate of dissipation to obtain models is explained in detail. A specific model for the mixture under study here is developed. The model accounts for the anisotropic response of the material. A comparison of theoretical predictions to previously obtained experimental results is provided.

CHAPTER II

CONTINUUM PRELIMINARIES

A. Notation

The notation used in this dissertation is the standard notation used in continuum mechanics. All vectors are boldfaced lower case Roman alphabets. All second order tensors are bold faced upper case Roman alphabets.

B. Kinematics

Consider the body B, where $\kappa_R(B)$ and $\kappa_{c(t)}(B)$ denote the reference and current configurations. The motion assigns a one-to-one mapping between points $\mathbf{X} \in \kappa_R$ and points $\mathbf{x} \in \kappa_{c(t)}$, at each t, i.e.,

$$\mathbf{x} = \boldsymbol{\chi}_{\kappa_R}(\mathbf{X}, t). \tag{2.1}$$

The motion is assumed to have sufficient smoothness to enable all operations defined subsequently. The deformation gradient, $\mathbf{F}_{\kappa_R}$, and the left and right Cauchy-Green stretch tensors $\mathbf{B}_{\kappa_R}$ and $\mathbf{C}_{\kappa_R}$ are defined through,

$$\mathbf{F}_{\kappa_R} := \frac{\partial \chi_{\kappa_R}}{\partial \mathbf{X}}, \tag{2.2}$$

$$\mathbf{B}_{\kappa_R} := \mathbf{F}_{\kappa_R}\mathbf{F}^T_{\kappa_R}, \tag{2.3}$$

$$\mathbf{C}_{\kappa_R} := \mathbf{F}^T_{\kappa_R}\mathbf{F}_{\kappa_R}. \tag{2.4}$$

If $\det(\mathbf{F}_{\kappa_\mathrm{R}}) \neq 0$, then $\mathbf{F}_{\kappa_R}$ can be decomposed uniquely using the polar decom-

position theorem as,

$$\mathbf{F}_{\kappa_R} = \mathbf{R}_{\kappa_R}\mathbf{U}_{\kappa_R} \tag{2.5}$$

$$= \mathbf{V}_{\kappa_R}\mathbf{R}_{\kappa_R}, \tag{2.6}$$

where $\mathbf{R}_{\kappa_R}$ is a proper orthogonal tensor and $\mathbf{U}_{\kappa_R}$, $\mathbf{V}_{\kappa_R}$ are positive definite symmetric tensors.

The velocity $\mathbf{v}$ of a material point is defined as,

$$\mathbf{v} := \frac{\partial \chi_{\kappa_R}}{\partial t}. \tag{2.7}$$

The velocity gradient, $\mathbf{L}$, is related to the deformation gradient $\mathbf{F}_{\kappa_R}$ through,

$$\mathbf{L} := \text{grad}\mathbf{v} = \dot{\mathbf{F}}_{\kappa_R}\mathbf{F}^{-1}_{\kappa_R}. \tag{2.8}$$

The symmetric part of the velocity gradient is denoted by $\mathbf{D}$ and the skew part by $\mathbf{W}$.

$$\mathbf{D} = \frac{\mathbf{L} + \mathbf{L}^T}{2}, \tag{2.9}$$

$$\mathbf{W} = \frac{\mathbf{L} - \mathbf{L}^T}{2}. \tag{2.10}$$

C. Balance Laws

The balance laws in continuum mechanics are the balance of mass, balance of momentum, balance of angular momentum and balance of energy. All processes within the purview of continuum mechanics have to satisfy the above laws.

The balance of mass in Eulerian form can be written as,

$$\dot{\rho} + \rho \text{div}\mathbf{v} = 0, \tag{2.11}$$

where ρ is the density and $\mathbf{v}$ is the velocity. For an incompressible material this

reduces to

$$\mathrm{div}\mathbf{v} = 0. \tag{2.12}$$

The balance of linear momentum is

$$\rho\left(\frac{\partial \mathbf{v}}{\partial t} + (\mathrm{grad}\mathbf{v})\mathbf{v}\right) = \mathrm{div}\mathbf{T} + \rho\mathbf{g}, \tag{2.13}$$

where $\mathbf{T}$ is the Cauchy stress and $\mathbf{g}$ is the acceleration due to gravity.

The balance of angular momentum in the absence of body couples requires that the stress tensor be symmetric.

The conservation of energy is written in the form,

$$\rho\dot{\epsilon} + \mathrm{div}\mathbf{q} = \mathbf{T}\cdot\mathbf{L} + \rho r, \tag{2.14}$$

where ϵ is the specific internal energy, $\mathbf{q}$ is the heat flux vector, $\mathbf{L}$ is the velocity gradient and r is the radiant heating.

D. The Second Law of Thermodynamics

The second law of thermodynamics is commonly used in the form of the Clausius Duhem inequality. Here however it is introduced as a balance law for entropy. This is similar to the approach taken by Green and Naghdi [11] and Rajagopal and Srinivasa [12].

$$\rho\dot{\eta} + \mathrm{div}\left(\frac{\mathbf{q}}{\theta}\right) = \rho\frac{r}{\theta} + \rho\zeta, \tag{2.15}$$

where η is the entropy, θ is the absolute temperature and ζ is the rate of entropy production per unit mass of the material. Combining the balance of energy and balance of entropy, the reduced energy-dissipation equation is obtain,

$$\mathbf{T}\cdot\mathbf{L} - \rho\dot{\epsilon} + \rho\theta\dot{\eta} - \frac{\mathbf{q}\cdot\mathrm{grad}\theta}{\theta} = \rho\theta\zeta = \xi \geq 0, \tag{2.16}$$

where ξ (rate of dissipation) is the rate of entropy production times the temperature per unit volume of the material. Both ζ and ξ are constrained to be non-negative during any process. The radiant heating term has been eliminated from the reduced dissipation equation and the equation places no direct restrictions are placed on the constitutive assumption for the radiant heating term. This issue has been discussed in detail by Rajagopal and Tao [13].

Sometimes the term, rate of dissipation, is used exclusively to denote rate of entropy production associated with mechanical working. But entropy production can take place due to a variety of reasons such as phase change, chemical reaction, heat conduction etc. In this work ξ, is used to encompass all entropy generation mechanisms. The terms rate of dissipation, and rate of entropy production are used interchangeably with the implicit understanding that the two are related through Eq. (2.16). Eq.(2.16) can be rewritten as

$$\mathbf{T}\cdot\mathbf{L}-\rho\dot{\psi}-\rho\eta\dot{\theta}-\frac{\mathbf{q}\cdot\mathrm{grad}\theta}{\theta}=\rho\theta\zeta=\xi\geq 0, \tag{2.17}$$

where ψ is the Helmholtz potential per unit mass of the material and is given by $\psi=\epsilon-\eta\theta$.

E. Natural Configurations

The "natural configurations" may be thought of as a configuration from which kinematical measurements maybe made which help determine the stress in the body. It is customary to choose a stress free configuration as the natural configuration.

In continuum mechanics it is usual to express the stress explicitly in terms of the history of the density and various kinematical quantities. Implicit relation between the history of the stress, its derivative, the density and kinematical quantities have

also been proposed. Many constitutive relations, among them some of the most historically successful, fall within the ambit of simple materials as defined by Noll [14]. In simple materials the stress at a point depends only on the history of quantities measured with respect to a single reference configuration. This assumption is too restrictive for many real materials of practical importance. Indeed it has been long recognized (see Eckart [15]) that bodies that display inelastic behavior possess more than one configurations in which they are stress free. The implications with regard to symmetry are particularly striking. For a simple material if the symmetry is known in any configuration, then its symmetry in any other configuration is known through Noll's rule. But for many materials with multiple stress free configurations, the corresponding symmetry groups may not be related by Noll's rule.

The work of Eckart has been clarified and greatly expanded on by Rajagopal and co-workers, in terms of how the natural configurations come into play in determining stresses, appropriate measures of strain from these configurations and evolution of these configurations.

Asphalt bound mixtures, when modeled as a homogenized continua demand as much latitude as possible. The microstructure of asphalt mixtures change as it is subjected to deformation. These changes maybe due to reduction in air voids, changes in the properties of asphalt in response to environmental stimuli, rearrangement of aggregate particles etc. Clearly the associated natural configuration may change. Distinct symmetry groups unrelated by Noll's rule may exist for each of these configurations. Overly restrictive constitutive assumptions impede or worse preclude solutions. The framework put in place by Rajagopal and co-workers provides an ideal setting to deal with asphalt mixtures.

F. The Role of Dissipation

All processes maybe classified as reversible or irreversible. Reversible processes, are characterized by a zero rate of entropy production and irreversible processes are characterized by a positive rate of entropy production. Entropy may be produced by a variety of mechanisms. For e.g. viscous effects, heat conduction, structural rearrangement, phase change etc. In this work we assumed that ξ can be split into two parts, the first rate of entropy production due to heat conduction and the second, rate of entropy production due to other mechanisms. Furthermore each of these two mechanisms are assumed to be non-negative i.e.,

$$\xi = \xi_d + \xi_c, \qquad \xi_d > 0, \xi_c > 0. \tag{2.18}$$

Here ξ_c/θ is the rate of entropy production per unit volume due to conduction and ξ_d/θ the rate of entropy production per unit volume due to other mechanisms. In the work here the ξ_d/θ is associated with the rate of entropy production per unit volume due to mechanical working. The term $(\mathbf{q} \cdot \text{grad}\theta/\theta^2)$ is identified as the term accounting for the rate of entropy production due to conduction. Therefore the following equations are obtained,

$$\xi_c = -\frac{\mathbf{q} \cdot \text{grad}\theta}{\theta}, \tag{2.19}$$

$$\mathbf{T} \cdot \mathbf{D} - \rho\dot{\psi} - \rho\eta\dot{\theta} = \xi_d \geq 0. \tag{2.20}$$

The reduced energy-dissipation equation (2.20) is used to place restrictions on the constitutive equations.

CHAPTER III

ASPHALT MIX OVERVIEW

A five year, $150 million research project labeled the Strategic Highway Research Program (SHRP) was established by Congress in 1987. The SHRP came up with a specification called SUPERPAVE (Superior Performing Asphalt Pavements). It lays down the specification for the design and analysis of asphalt pavements. SUPERPAVE characterizes asphalt mixes and provides designs to resist rutting, low temperature cracking and fatigue cracking. Standard tests have been established to characterize the response of asphalt mixtures to the above mentioned distress mechanisms. Tests within the purview of the original SUPERPAVE specifications [16] and further tests recommended in NCHRP-465[1] [17], data reduce by assuming that asphalt/asphalt-concrete is a linear viscoelastic material.

Modeling of the mix behavior has attracted considerable attention due to wide applications. Early models for asphalt bound mixtures include those developed by Lee and Marwick [18], Nijboer [19], Saal [20], Secor and Monismith [21], Pagan [22], Moavenzadeh and Soussou [23], Perl et al. [24] among others.

More recently models have been developed by Kim and Little [25], Lee et al. [26], Gibson et al. [27] and Masad et al. [28]. Ideas from mixture theory which explicitly account for multiple constituents (asphalt, matrix and air voids) in asphalt bound mixtures have also been used (see for example [29]).

The correspondence principle due to Schapery [30] that allows migration of solutions from non-linear elasticity to viscoelasticity has found favor among workers in asphalt modeling. But it has been shown that this principle is in general incor-

[1]NCHRP stands for National Cooperative Highway Research Program.

rect (Rajagopal and Srinivasa [31]) when large deformations are involved as models obtained by using it fail to satisfy the balance of angular momentum.

A brief description of constituents that go into the asphalt bound mixtures is provided in the following paragraphs.

A. Asphalt

Asphalt and bitumen are often used interchangeably in literature. This issue has been discussed by Murali Krishnan and Rajagopal [1]. The term asphalt will be used in this work. Asphalt is a complex chemical mixture. A lot of work has been carried out to understand the link between the chemistry of asphalt and its rheological properties. A detailed chemical analysis reveals the presence of thousands of compounds.

Techniques to separate asphalt into fractions that exhibit distinct properties include solvent precipitation and chromatographic methods.

The Corbett procedure is a common method used to separate asphalt into distinct fractions. Each fraction is a mixture of hundreds of individual compounds. The fractions separated have distinct properties. The fractions from the Corbett method are asphaltenes, saturates, napthelene aromatics and polar aromatics.

Size exclusion chromatography (SEC) is used to fractionate asphalt into components of different molecular weights. Ion exchange chromatography (IEC) separates asphalt by chemical composition.

Yields of the fractions are often a function of the procedure used. For e.g. the yield of asphaltenes is a function of the precipitating solvent [32]. The relation of the chemistry to rheology of asphalt is more qualitative than quantitative.

Polar molecules present in asphalt strongly influence its properties. The polar molecules interact with each other and tend to form cluster of molecules. Organized

structures formed as a result of charge separation on molecules, alters the physical properties of asphalt. More energy is required to break these polar associations. This makes the asphalt more viscous.

Oxidatitive aging is a serious problem associated with asphalt. Asphalt exposed to atmospheric conditions oxidizes and its chemical composition changes. Oxidation results in an increase in the viscosity of asphalt and could lead to pavement embrittlement. In the laboratory two techniques are used to simulate oxidation, one the RTFOT (Rolling Thin Film Oven Test) and the other the PAV (Pressure Aging Vessel). The RTFO is used to simulate plant mixing and the PAV is used to simulate oxidation over years in the field.

In addition to oxidative hardening, asphalt also shows steric hardening. Steric hardening is a reversible (reversible in the sense that the hardening observed disappears on heating) process wherein the polar molecules try to attain the most favorable configuration.

Nellensteyn [33] describes asphalt as a colloid. Models to explain the distribution of the various components in the mixture have also been proposed by Pfieffer and Saal [34] and Petersen [35].

As early as 1903 Trouton [36] concluded that pitch is a non-Newtonian fluid.

B. Aggregates

The factors that usually affect aggregate behavior are gradation, shape, angularity and surface texture of the aggregates.

Quantification of these aggregate properties can either be done using physical measurements on aggregates, visual classification methods (i.e direct methods) or index tests (indirect methods) which use empirical relations between properties such

as porosity and aggregate shape, size and surface texture. A review of the various methods of characterizing these properties is presented in [37].

Size of the particle can be expressed in terms of an 'equivalent diameter'. Most popular methods of characterizing size are using sieving and microscopic measurements. Sieving also gives the size distribution of the aggregates.

Description of aggregate shape is based on measurements of aggregate dimension. The descriptions used include flatness ratio, elongation ratio, shape factor and sphericity of the aggregate particle (see for example [38]). Roundness indicates whether the edges are sharp or rounded [39]. Details on how roundness can be quantified can be found in Krumbein [40]. Wadell [39] describes the shape of a particle in terms of sphericity and roundness.

Other measures include surface texture and angularity. Image analysis is also a technique to identify and determine the characteristics of the aggregate [41].

Indirect methods of inferring the aggregate characteristics usually do not distinguish between shape, size and texture and lump them together as an index (example particle index, rugosity etc).

C. Fillers

Fillers are an important component in asphalt mixes. They are added to enhance the properties of the mixture. One filler that has attracted particular attention is hydrated lime. The term filler is usually used to describe a fraction of the mineral material aggregate that passes sieve no. 200 (75 microns). Tunnicliff [42] has a detailed discussion on what may be classified as a filler. The influence of fillers on the response of asphalt mixes is well studied. As early as the first decade of the 1900s Richardson [43] notes 'That it is of the greatest value, especially in surface exposed

to heavy traffic is now known. The difference in penetration, ductility and resistance to stress of the same bitumen with and without filler can be readily shown'.

Among the early studies on the effects of fillers are those due to Traxler and Miller [44],[45], Traxler [46], Mitchell and Lee [47], and Rigden [48]. Tunnicliff [49] has written a review on the effects of fillers. The problem has also been looked into by Warden et al. [50], Anderson and Goetz [51] among others.

Rigden [52] addresses the problem of finding a relation between the flow properties of two-phase systems and the amount and characteristics of the solid phase present. He relates the void structure in dry powder (Rigden voids, which are measured using permeability through the powder) to flow behavior at high solids concentration.

Tunnicliff [42] concludes that the viscosity of filler-asphalt systems depend on the filler (both concentration and characteristics). As filler concentration increases binder viscosity increases.

Anderson and Goetz [51] conclude that asphalt (filled and unfilled) is a linear viscoelastic material at sufficiently low strains. They show that complex compliance is independent of load level, at given frequency and temperature, and that superposition is satisfied. Thus they study the efficacy of fillers in a linear viscoelastic setting.

Craus et al. [53] have carried out a thorough investigation of the physico-chemical interactions in paving mixes. They studied aspects such as geometric characteristics of fillers, adsorption intensity and selective sorption. They evaluated different mastics. Sand-asphalt specimens were compared on the basis of Marshall stability, resilient modulus etc.

Petersen et al. [54] studied the change in properties due to addition of hydrated lime to asphalt in terms of the complex dynamic shear viscosity, storage modulus and loss modulus. They also carried out tensile elongation tests at low temperatures.

They conclude that hydrated lime treatment increases the resistance to deformation of the mixture, and that it maybe desirable in reducing permanent deformation. They also conclude that the effect of hydrated lime depends on the type of asphalt, hydrated lime reduces age-hardening, improves fatigue life and low-temperature properties.

Plancher et al. [55] conclude that hydrated lime treatment reduces age-hardening in asphalt. They studied the mechanical properties by making viscosity measurements at a fixed rate and temperature and by using the resilient modulus.

Shashidhar and coworkers [56],[57] consider the factors affecting the behavior of fillers. They study the problem in terms of the maximum packing fraction Φ_m and the generalized Einstein coefficient, K_E. They explain the stiffening based on Neilsen modified Kerner's equation.

Lesueur and Little [7] concluded that hydrated lime is an active filler (active in the sense of reacting with the asphalt chemically), improving properties both at high and low temperatures. They also found that hydrated lime reduced age hardening.

Other studies on fillers include those due to Kavussi and Hicks [58], Cooley et al. [59] etc.

CHAPTER IV

EXPERIMENTAL INVESTIGATIONS

A. Introduction

Most of the experimental measurements for asphalt mixtures are made in the load-deformation ranges in which the material behavior is linear. However, in the field, asphalt mixtures are subjected to substantial axle loads that lead to the material exhibiting non-linear characteristics.

The development of normal force as a result of simple shear is a characteristic feature of non-linear response. This is well recognized in non-linear elasticity (as Poynting effect [60]), non-Newtonian fluid mechanics (as Weissenberg effect [61]) and the response of granular materials (as dilatancy [62]). Asphalt mixes being composed of granular materials infused with a non-linear viscoelastic fluid maybe expected to generate significant normal forces. Plausible physical mechanism for normal stress generation in asphalt bound mixtures include relative motion between the aggregates coated with asphalt, particularly such events as particles gliding past each other and climbing over one another, due to the relative motion of the asphalt mastic and interactions between the fillers and the asphalt. The need for measuring the normal stresses for asphalt is articulated best by Anderson et al. [63], "Edge fracture is associated with differences in the first and second normal forces, but unfortunately, such measurements were beyond the capabilities of the available equipments for this study. . . Further study of this anomaly is warranted but will require very sophisticated testing with the measurement of normal forces". The experimental study carried out here provides evidence for the development of such normal stresses. Systematic experimental results that may enable the characterization of the non-linear behavior of

asphalt bound mixtures is documented.

A survey of the asphalt literature reveals that a large number of tests are used to study the behavior of asphalt mixes. Among the tests are uniaxial tests, triaxial tests, shear tests, indirect tensile tests, etc [17]. shear tests are important because they can provide an easy and clear distinction between linear and non-linear behavior.

Shear tests on asphalt mixtures have often been used to characterize permanent deformation in asphalt pavements. Some of the recommended tests for assessing the properties of asphalt are simple shear test and repeated shear tests (see SHRP standard method of test M-003 [16]). The measurement of normal forces in simple shear is one of the recommended tests within the SUPERPAVE specifications [64]. Sousa et al. [65] have reported measurement of the axial force needed to maintain the specimen height in asphalt bound specimens subjected to simple shear. But there exists little systematic documentation of the normal forces crucial to characterizing the mechanical properties of asphalt mixtures. It is also noted that within the framework setup by SUPERPAVE the information from normal force measurements is not incorporated in an appropriate large deformation non-linear model. The fact that asphalt mastic subjected to shear (in confined or unconfined mode) generates significant normal forces is not considered in much of the literature on asphalt mixtures. In the case of non-linear materials normal stresses that develop during shear are more important in characterizing the material than even the shear forces (see Truesdell and Noll [66]).

Justification is now provided for using torsional tests as opposed to simple shear tests for the study carried out here. The main reason is that simple shear tests on rectangular blocks are difficult to set up and there are additional complications due to end effects, etc. On the other hand torsion corresponds to locally shearing motion and is easier to investigate experimentally. The measurements obtained from the torsion test are relevant from a practical standpoint albeit in an indirect way (loading

due to traffic does not cause torsion of pavements), since in real life applications asphalt pavements are subjected both to compression and shear stresses due to loading caused by traffic. A pneumatic tire under vertical load produces shear stresses in the pavement (see for example [67]).

The first torsional tests on asphalt bound specimens which measured the normal forces generated were performed by Kasula et al. [68]. Kasula et al. [68] recognize its crucial importance to asphalt mixture behavior. Their results clearly show that significant normal forces are developed even at low shear rates and even in the unconfined mode.

Various kinds of rheometers (for example capillary viscometers, rotational viscometers, sliding plate viscometers, falling body viscometers etc) have been used used to study, different materials (see [69],[70],[71] for details). Among rotational viscometers, coaxial cylinder type, coni-cylindrical viscometers, and cone and plate viscometers are popular. From a theoretical standpoint, the flow between parallel plates is a well studied problem. For a detailed review refer to Rajagopal [72]. Rheometers, in particular torsional rheometers have been used to study the nonlinear response of polymers (see for example [73],[74]).

In the course of the study here the following cases were investigated:

1. Comparison of the effect of limestone and hydrated lime fillers on an asphalt graded as PG64-22. Different combinations of loading rates and duration were studied.

2. Comparison of specimens which differ with respect to the asphalt used. Three asphalts graded as AC-30 were used.

3. Comparison of sand-asphalt specimens which differ with respect to the filler used. Two fillers hydrated lime and limestone were compared. Four asphalts

all graded as AC-30 were used.

4. The effect of step loading. Specimens composed of similar constituents except for the asphalt used were compared under conditions of multiple step-loading. Three asphalts all graded as PG 64-22 were used.

5. The influence of the gradation of sand on similarly specimens except for the sand used was studied. ASTM graded sand and ASTM 20-30 sand were used.

B. The Torsional Rheometer: Description

The torsional rheometer(see Figure 1) used to conduct the experiments essentially consists of two disks, sharing a common axis. One of the disks rotates at a constant rate and the other is held fixed. The motion engendered in the specimen between the two disks is a locally shearing motion. A load cell attached to the top disk measures the normal force. The lower shaft is driven by a DC motor through a speed reducer that provides rotation rates as low as one revolution in 60 minutes. The torque was measured using a torque sensor. The data acquisition was done using a 6023E card (from National Instruments). The front end signal conditioning was carried out using a SCXI system (consisting of a SCXI-1000 chassis, installed with 2 modules: SCXI-1141 and SCXI-1120). The specimen was held between the two holders using glue (DP 460 from 3M). Initial tests were performed to ensure that the glue did not fail due to the applied torque. The test was performed as follows: the top disk was held stationary and the bottom disk was rotated at a very slow fixed rate (say 60 min/rev) for a fixed duration (say 90 sec). Beyond this point the two disks were held stationary thus holding the strain fixed. The normal force generated and the torque required, during torsion and stress relaxation, were measured. The stress relaxation data was collected for 45 minutes. The rates and durations of rotation were chosen such that

the specimen did not sustain any visible damage.

C. Materials

Two fillers were studied, hydrated lime (supplied by Austin Lime Co.) and crushed limestone. The fillers were sieved to obtain the component passing sieve number 200 (75 microns). Asphalt graded PG 64-22 (called Asphalt Number 8) and four asphalts graded AC 30 (called Asphalt Number 1, Asphalt Number 2, Asphalt Number 3, Asphalt Number 4) were used. For step loading experiments another three asphalts graded as PG64-22 (identified as Asphalt Number 5, Asphalt Number 6, Asphalt Number 7) were used. Other materials used were Ottawa sand (furnished by U.S Silica company, conforming to ASTM designation C778) and ground silica (Sil-Co-Sil ground silica supplied by U.S. Silica Company). Two types of Ottawa sand were used, namely ASTM 20-30 sand and ASTM graded sand. The gradations of the Ottawa sands used are given in Tables I and II. The ground silica used was sieved to meet the following criteria: 100% passing sieve number 100 (150 microns) and 100% retained on sieve number 200 (75 microns).

D. Preparation of Specimens

The asphalt was heated and mixed with the filler. This mastic was then added to the Ottawa sand and ground silica heated separately to the mixing temperature. The ratio of the mastic (asphalt plus filler) to the total mixture was maintained at 8% by weight, the ratio of the Ottawa sand to the total mixture was fixed at 80% by weight and the ratio of ground silica to the total mixture was fixed at 12% by weight, for all the specimens. Two filler to asphalt ratios were used: 10% by weight and 23% (10% by volume) by weight. These details are summarized in Table III. The

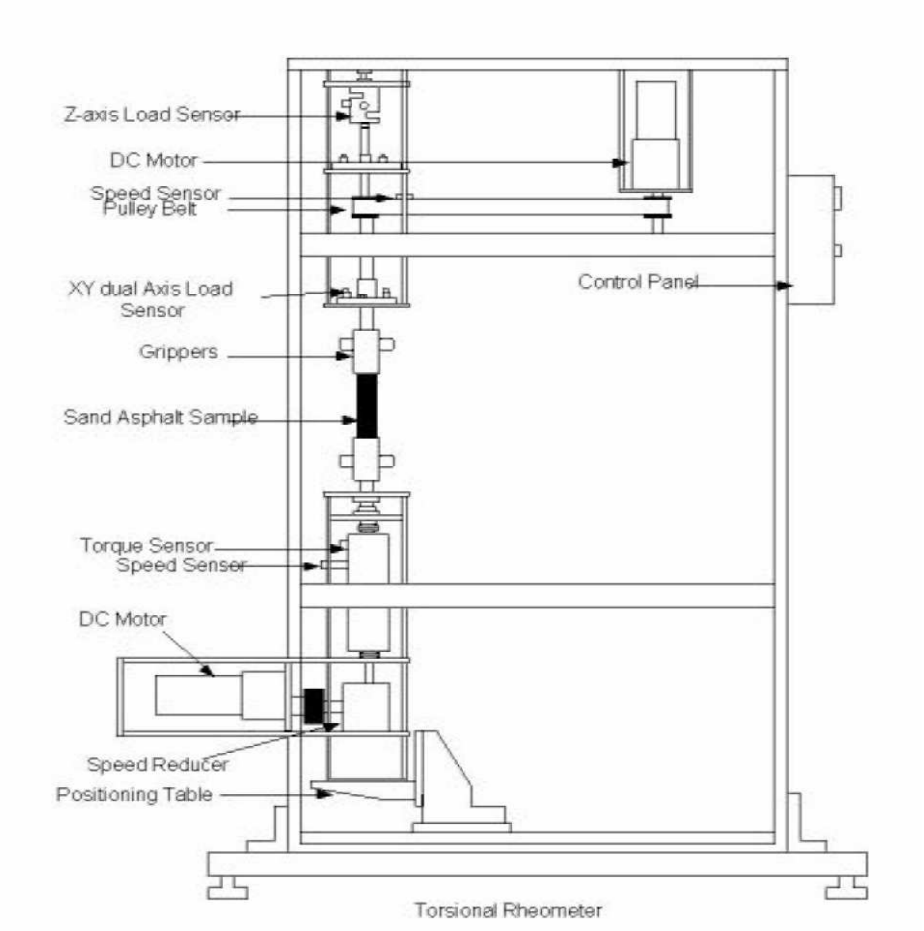

Fig. 1. Torsional rheometer. Reprinted from *Mechanics Research Communications*, vol 32, Kasula et al., Normal stress and stress relaxation data for sand asphalt undergoing torsional flow, pg. 45, Copyright 2005, with permission from Elsevier [68].

Table I. Gradation of ASTM graded Ottawa sand (Supplied by U.S. Silica Co.).

Mesh	% **Passing Cumulative**
16	100.0
30	98.0
40	70.0
50	25.0
100	2.0
Pan	0.0

Table II. Gradation of Ottawa sand (ASTM 20/30 Sand) (Supplied by U.S. Silica Co.).

Mesh	% **Passing Cumulative**
16	100.0
20	99.0
30	2.0
Pan	0.0

compaction was done using a gyratory compactor to obtain 6 inch by 3 inch specimens with the desired air-voids (7.5% and 9.5%). The Rice specific gravity and the bulk density were measured following the standard procedure [75]. Specimens 0.75 inches in diameter by 1.5 inches in height that were used for testing were cored out from the larger specimen. After being glued to the experimental setup the unconfined length of the specimen was 1 inch.

E. Testing

Five series of tests were run. In the first set the same asphalt was used and the effect of limestone and hydrated lime fillers was studied. ASTM 20-30 sand was used for the first set of experiments.

In the second set of experiments the behavior of different asphalts graded as AC 30 was studied. ASTM graded Ottawa sand was used for the second set of experiments.

In the third set the same asphalt was used and the effect of limestone and hydrated lime fillers was studied. This was done for four different asphalts all graded as AC 30.

In the fourth set of experiments three asphalts all graded as PG64-22 were compared under multiple step-loading cycles. Two different cycles were studied namely 90-270-90 (90 seconds of loading, followed by 270 seconds of rest, followed by 90 second of loading, followed by 30 minutes of rest) and 60-450-60-450-60 (60 seconds of loading, followed by 450 seconds of rest, followed by 60 second of loading, followed by 450 seconds of rest, followed by 60 seconds of loading, followed by about 20 minutes of rest).

The final set of experiments were run with sands of different gradation, ASTM

20-30 sand and ASTM graded Ottawa sand.

The testing conditions are summarized in Tables IV, V, VI, VII and VIII.

F. Measurement Error

All measurements are subjected to uncertainties. Error Analysis is a technique to enable the estimation of the uncertainties. (see for example [76],[77],[78]). Data acquisition has to be carefully done to minimize these errors [79].

The sources of error in measurement are many. They could be due to equipment calibration errors, least count of the equipment, mistakes by the experimenter etc. The least count of an instrument is the smallest value that it can resolve. Measurements are correct only upto the least count.

Accuracy refers to how closely a measured value agrees with the true value. Precision refers to how closely the values agree with each other.

Measurements could suffer from both random errors and due to systematic errors. Random errors can be treated statistically. Errors may follow a Gaussian distribution and thus become amenable to a host of techniques.

The propagation of errors is an important issue and it may be treated in a simple manner using a Kline and McClintock analysis. (see [80]).

For the experimental measurements performed in this study the least count of the normal load sensor was $\pm 0.02\%$ of the full scale reading(0.02% of 100 lb). and the least count of the torque sensor was $\pm 0.02\%$ of 100 lb-in. The torque sensor was sent to the manufacturer and calibrated. The calibration sheet is provided in appendix A. The normal load sensor was calibrated at Texas A&M University and the calibration curve which was obtained is shown in Figure 4. Two samples were tested for each test condition. The values reported (graphically as well as in the tables) are the averages

Table III. The composition of the asphalt bound mixtures tested.

Component	**Percentage**
Ottawa sand	80% by mass
Ground Silica (Passing No. 100 and retained on No. 200)	12 %
Filler + Asphalt	8% by mass
Filler/Asphalt Ratio	10% by mass and 23% by mass (10% by Volume)

of the two samples. On an average the error in the normal force measurement was 11.5% and the error in torque measurement was 8.8%. Figures 2 and 3 show the torque and normal force for a particular case with the error bars plotted.

G. Experimental Results

The results obtained are summarized in Figures 5 through 34. The normal force in all cases is compressive, i.e., the normal force acting on the specimen compresses it to maintain its height. Figures 5 and 6 show the influence of air voids, all other variables being comparable, in mixtures containing limestone filler. It is clearly seen that specimens with lower air voids generate larger normal force and require higher torque. Less porous materials show high resistance to local shear resulting in development of high normal force. The fact that asphalt mixtures that have less air voids show significant normal stress is not surprising since the tendency for the particles to climb past each other is greater in more dense material and consequently the resistance to deformation is significant. The peak value of the force for the two cases, 7.5% and 9.5% air voids, are different by as much as 32% and the maximum torque by

Table IV. Summary of testing conditions for the first set of experiments. The asphalt used was Asp No 8 (PG64-22). The sand used was ASTM 20-30 sand.

Filler	**Loading rate**	**Loading Duration**
Hydrated Lime 7.5% air voids	30 min/rev	45, 90 sec
Hydrated Lime 7.5% air voids	60 min/rev	60, 120 sec
Limestone 7.5 % air voids	30min/rev	45, 90 sec
Limestone 7.5 % air voids	60min/rev	60, 120 sec
Limestone 9.5 % air voids	30min/rev	45, 90 sec
Limestone 9.5 % air voids	60min/rev	60, 120 sec
No filler, 7.5% air voids	30min/rev	45, 90 sec
No filler, 7.5% air voids	60 min/rev	60, 120 sec

Table V. Summary of testing conditions for the second set of experiments.No filler was used and air voids were maintained at 9.5%.

Asphalt	**Loading Rate, Duration**
AC-30 Asp No 1	60min/rev, 120 sec
AC-30 Asp No 2	60min/rev, 120 sec
Ac-30 Asp No 3	60min/rev, 120 sec

Table VI. Summary of testing conditions for the third set of experiments. All tests were done at 60 minutes/revolution. Loading duration was 120 seconds. The Asphalt+Filler content was 8% of the mix. The ratio of Filler to Asphalt was 23% by mass. ASTM graded Ottawa sand was used.

Asphalt	**Filler**
AC-30 Asp No 1	Hydrated Lime, 9.5% Air voids
AC-30 Asp No 1	Limestone, 9.5% Air voids
AC-30 Asp No 2	Hydrated Lime, 9.5% Air voids
AC-30 Asp No 2	Limestone, 9.5% Air voids
AC-30 Asp No 3	Hydrated Lime, 9.5% Air voids
AC-30 Asp No 3	Limestone, 9.5% Air voids
AC-30 Asp No 4	Hydrated Lime, 9.5% Air voids
AC-30 Asp No 4	Limestone, 9.5% Air voids

Table VII. Summary of testing conditions for the fourth set of experiments. All tests were done at 90 minutes/revolution.No filler was used. ASTM graded Ottawa sand was used in all cases.

Asphalt	**Loading Duration in sec**
Asp No 5	90(load)-270(rest)-90(load)
Asp No 5	60(load)-450(rest)-60(load)-450(rest)-60(load)
Asp No 6	90(load)-270(rest)-90(load)
Asp No 6	60(load)-450(rest)-60(load)-450(rest)-60(load)
Asp No 7	90(load)-270(rest)-90(load)
Asp No 7	60(load)-450(rest)-60(load)-450(rest)-60(load)

Table VIII. Summary of testing conditions for the fifth set of experiments. No filler was used. The asphalt used was Asp No 8 (PG64-22).

Sand Used	**Loading rate**	**Loading Duration**
ASTM graded Ottawa sand	30 min/rev	60 sec
ASTM 20-30 sand	30 min/rev	60 sec
ASTM graded Ottawa sand	60min/rev	90 sec
ASTM 20-30 sand	60min/rev	90 sec
ASTM graded Ottawa sand	60min/rev	120 sec
ASTM 20-30 sand	60 min/rev	120 sec

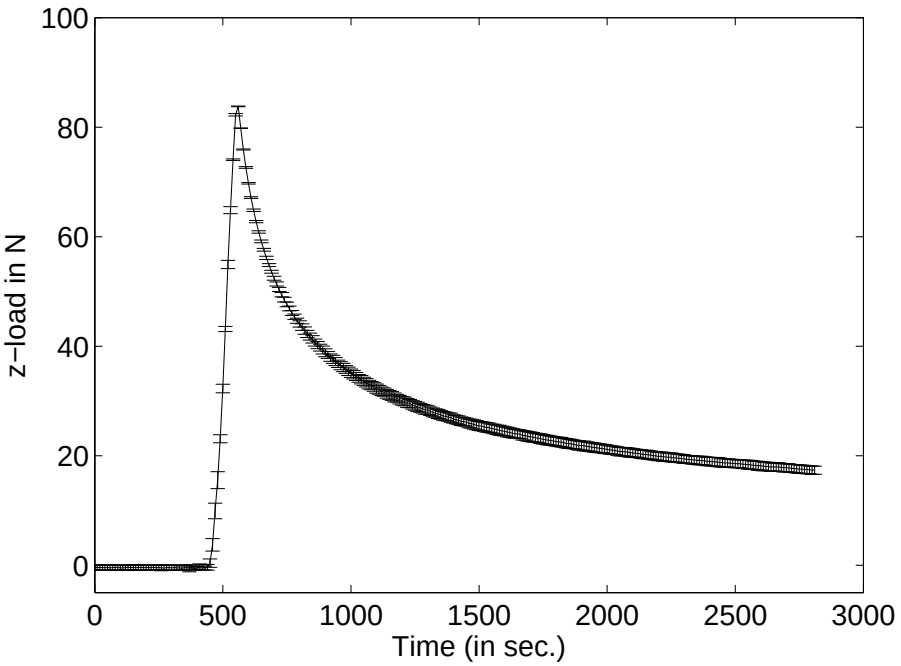

Fig. 2. Error (shown by error bars) in normal force measurement. The sand-asphalt specimens are fabricated using PG64-22 asphalt with limestone filler, at 7.5 % air voids. The loading rate is 60 min/rev. The duration of loading is 120 seconds (Filler/Asphalt ratio 10% by mass).

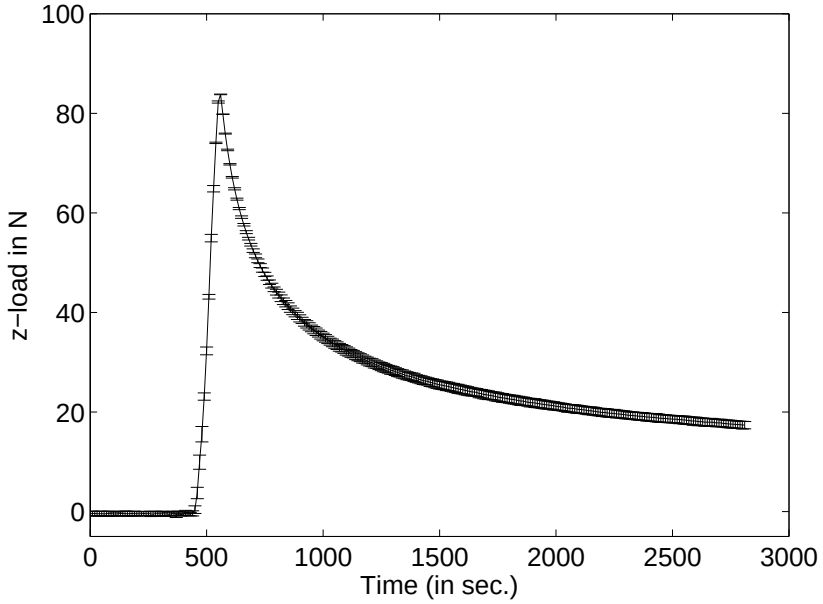

Fig. 3. Error (shown by error bars) in torque measurement. The sand-asphalt specimens are fabricated using PG64-22 asphalt with limestone filler, at 7.5 % air voids. The loading rate is 60 min/rev. The duration of loading is 120 seconds (Filler/Asphalt ratio 10% by mass).

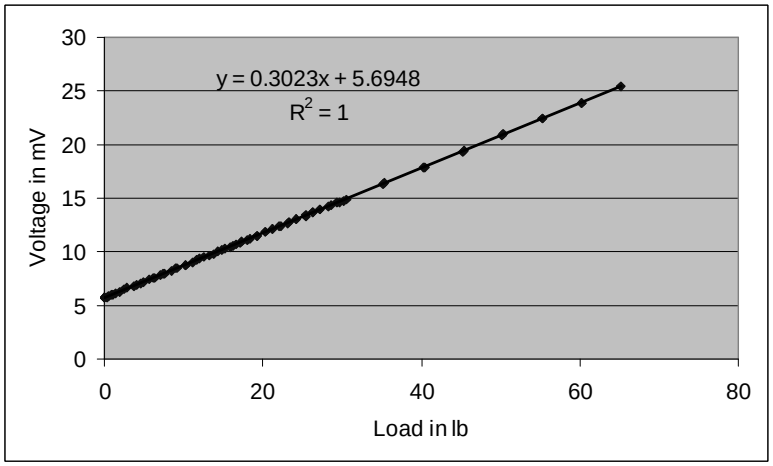

Fig. 4. Calibration curve for the normal force sensor.

26%. Figures 7 through 10 depict the behavior of the specimens with limestone filler (with 7.5% air voids) loaded at different rates and for different durations. It is clearly seen that the initial portions of the graphs for specimens at the same loading rates coincide well. This is also observed during the experiments performed using hydrated lime as filler and for specimens fabricated with PG64-22 asphalt with no filler. Figures 11 through 18 contrast the response of sand-asphalt specimens containing PG64-22 asphalt without filler to that of specimens containing PG64-22 asphalt with fillers hydrated lime and limestone. The presence of the filler leads to a larger normal force and requires a higher torque. This trend was observed for all loading rate-loading duration combinations at which tests were carried out. Figures 19 and 20 compare the behavior of asphalts from different sources graded as AC-30 with no fillers. Clearly the response (peak stress and relaxation behavior) of asphalts from different sources is different although they are all graded as AC-30. The asymptotic value for asphalts from different sources can differ by as much as 50%.

Figures 21 through 24 show the response of comparable specimens differing by asphalts used, which are from different sources but graded the same. In the first figure the loading sequence is 60 seconds (loading)-450 seconds (rest)-60 seconds (loading)-450 seconds (rest)-60 seconds (loading). In the second figure the loading sequence is 90 seconds (loading)-270 seconds (rest)-90 seconds (loading). Clearly the response is dependent upon the source of the asphalt. Also the two figures are consistent with each other in terms of trends observed. Figure 25 and 26 show the effect of hydrated lime filler on different asphalts graded as AC-30. Figures 27 and 28 contrast the effect of limestone filler on different asphalts graded as AC-30. It is clear that hydrated lime has the effect of "stiffening" the asphalts except in the case of the asphalt identified as Asphalt Number 1. This is in agreement with what is to be expected. The results obtained also caution the end user that the chemistry of the

particular asphalt maybe an important variable (inadequately captured by the PG grading system) when considering the effect of hydrated lime as a filler. Figures 29 through 34 compare the behavior of similar specimens differing in the gradation of the sand used. Specimens made with ASTM graded sand generate a higher normal force and torque as compared to specimens made with ASTM 20-30 sand. This is as expected since the percentage of finer sand in ASTM graded sand is higher.

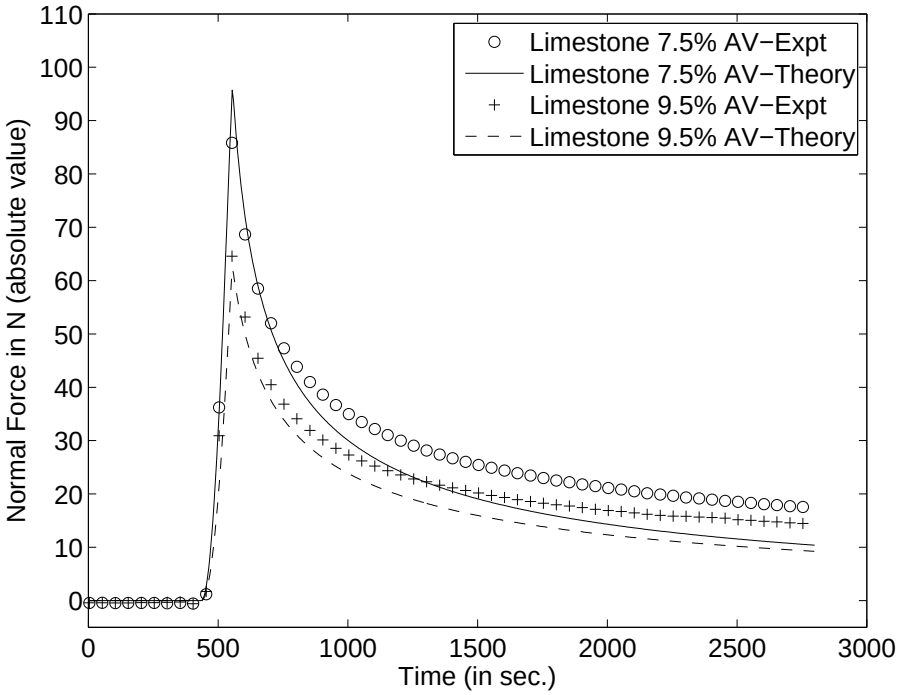

Fig. 5. Comparison of normal force in sand-asphalt specimens fabricated using PG64-22 asphalt with limestone filler, at 7.5% and 9.5% air voids. The loading rate is 60 min/rev. The duration of loading is 120 seconds (Filler/Asphalt ratio 10% by mass).

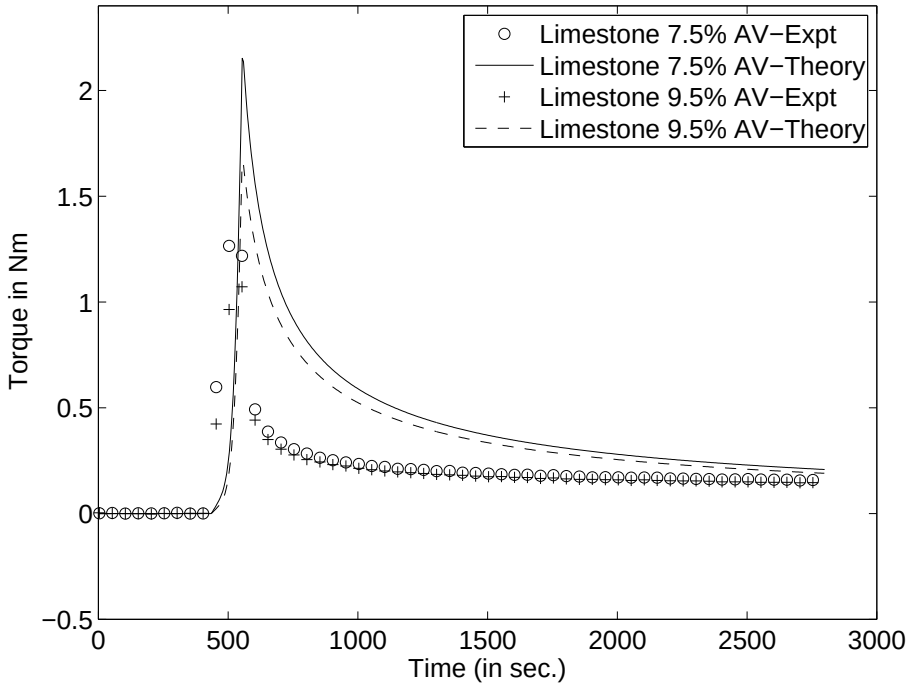

Fig. 6. Comparison of torque in sand-asphalt specimens fabricated using PG64-22 asphalt with limestone filler, at 7.5% and 9.5% air voids. The loading rate is 60 min/rev. The duration of loading is 120 seconds (Filler/Asphalt ratio 10% by mass).

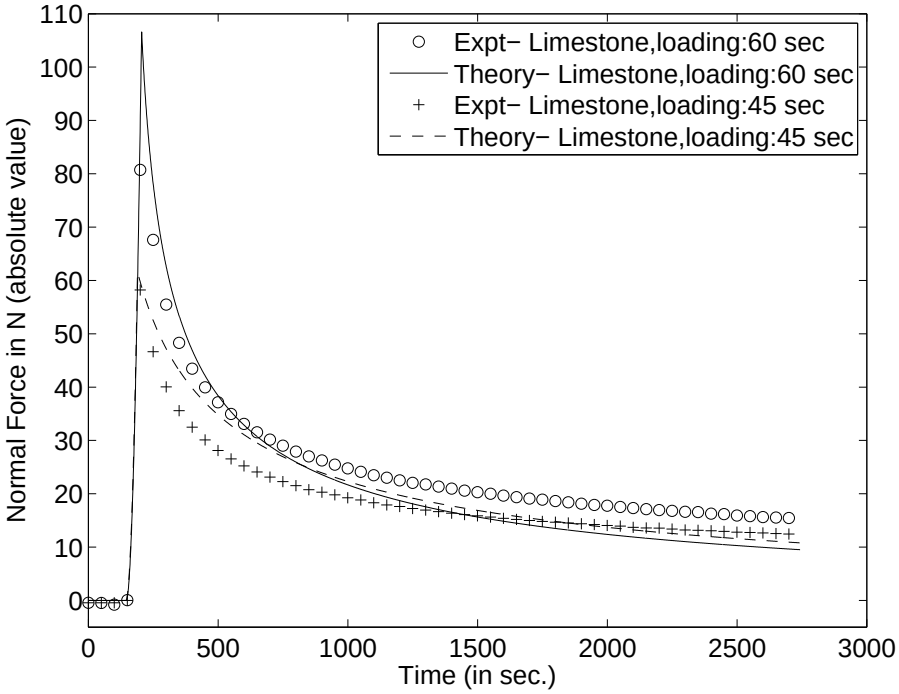

Fig. 7. Comparison of normal force in sand-asphalt specimens fabricated using PG64-22 asphalt with limestone filler, at 7.5% air voids, for different loading durations. The loading rate is 30 min/rev. Filler/Asphalt ratio is 10% by mass.

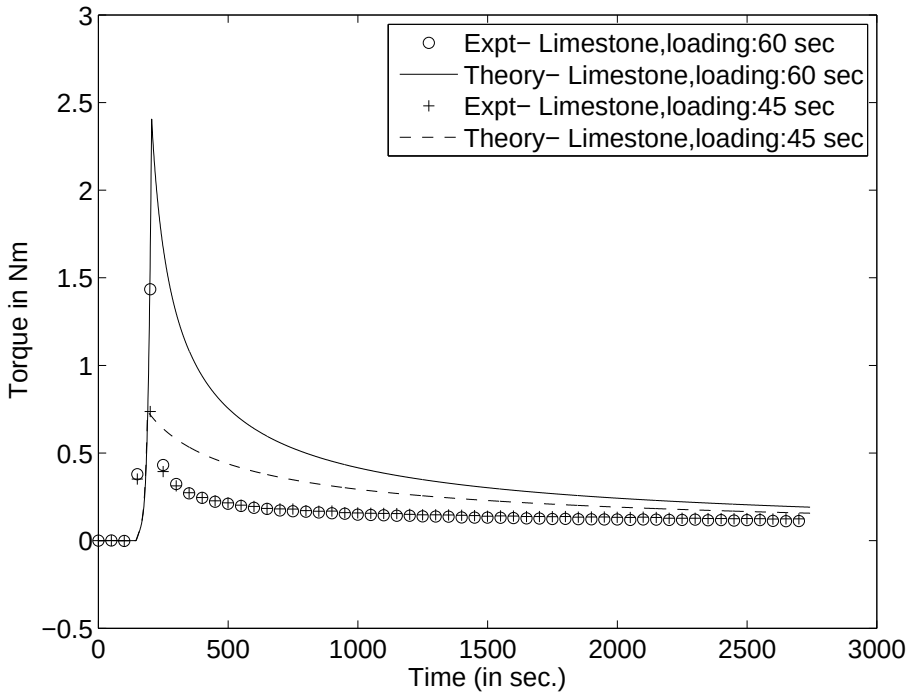

Fig. 8. Comparison of torque in sand-asphalt specimens fabricated using PG64-22 asphalt with limestone filler, at 7.5% air voids, for different loading durations. The loading rate is 30 min/rev. Filler/Asphalt ratio is 10% by mass.

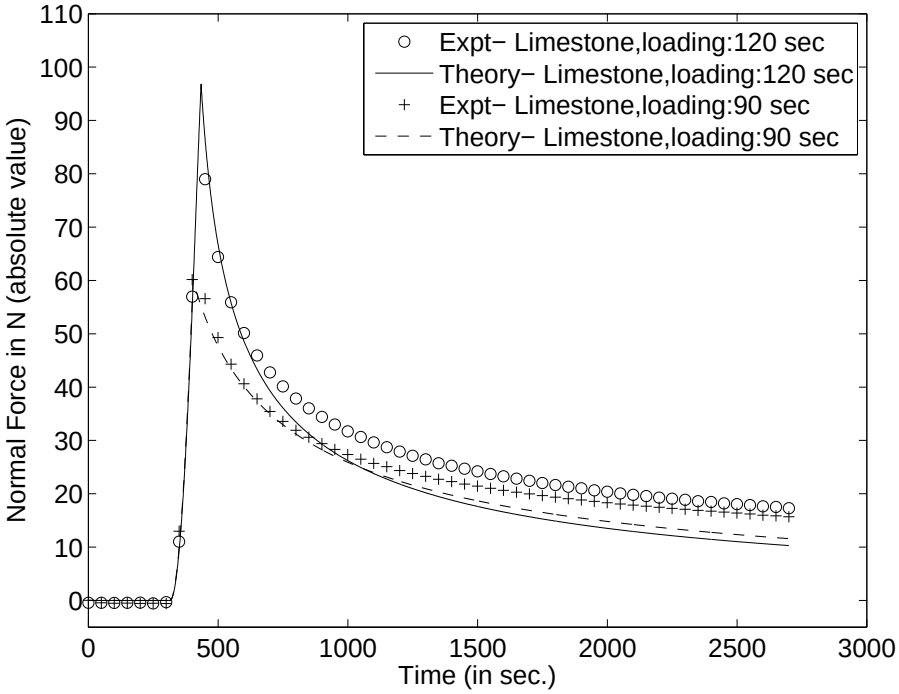

Fig. 9. Comparison of normal force in sand-asphalt specimens fabricated using PG64-22 asphalt with limestone filler, at 7.5% air voids, for different loading durations. The loading rate is 60 min/rev. Filler/Asphalt ratio is 10% by mass.

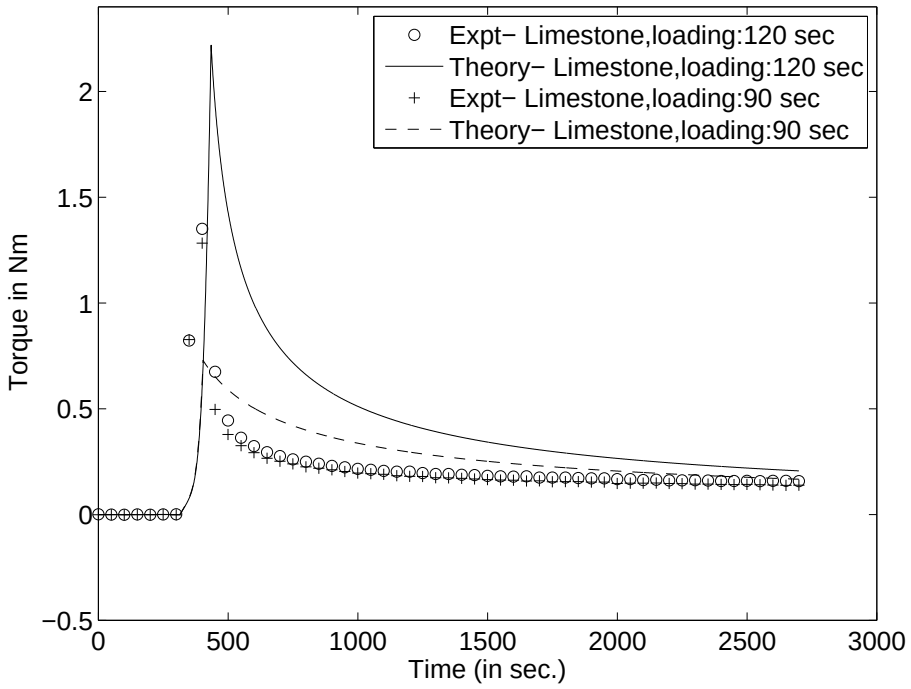

Fig. 10. Comparison of torque in sand-asphalt specimens fabricated using PG64-22 asphalt with limestone filler, at 7.5% air voids, for different loading durations. The loading rate is 60 min/rev. Filler/Asphalt ratio is 10% by mass.

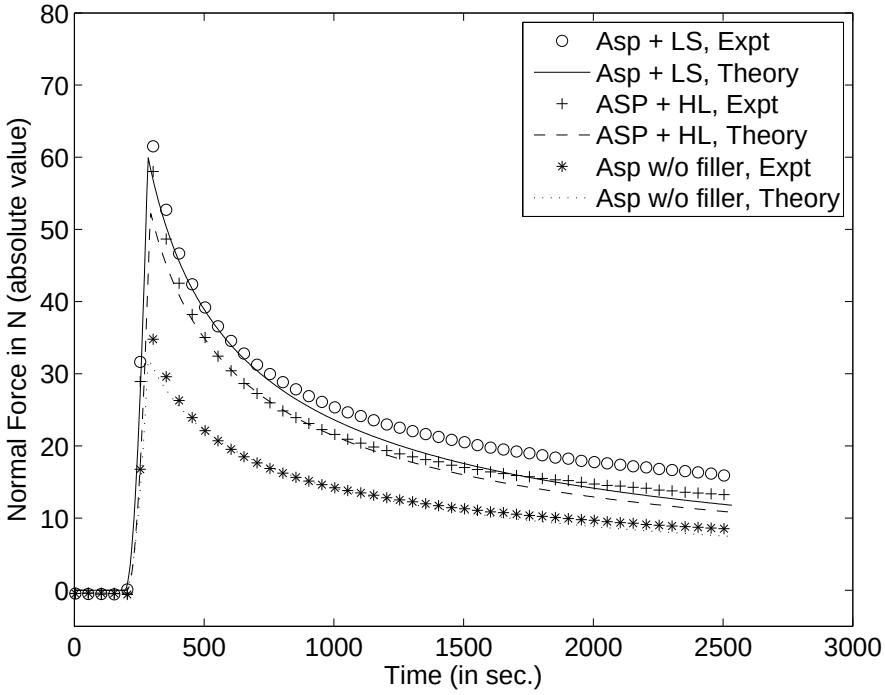

Fig. 11. Comparison of normal force in sand-asphalt specimens fabricated with asphalt(PG64-22) containing hydrated lime filler, asphalt(PG64-22) containing limestone filler and asphalt (PG-64-22) with no filler, at loading rate of 60 min/rev for a loading duration of 90 seconds (Filler/Asphalt ratio 10% by mass).

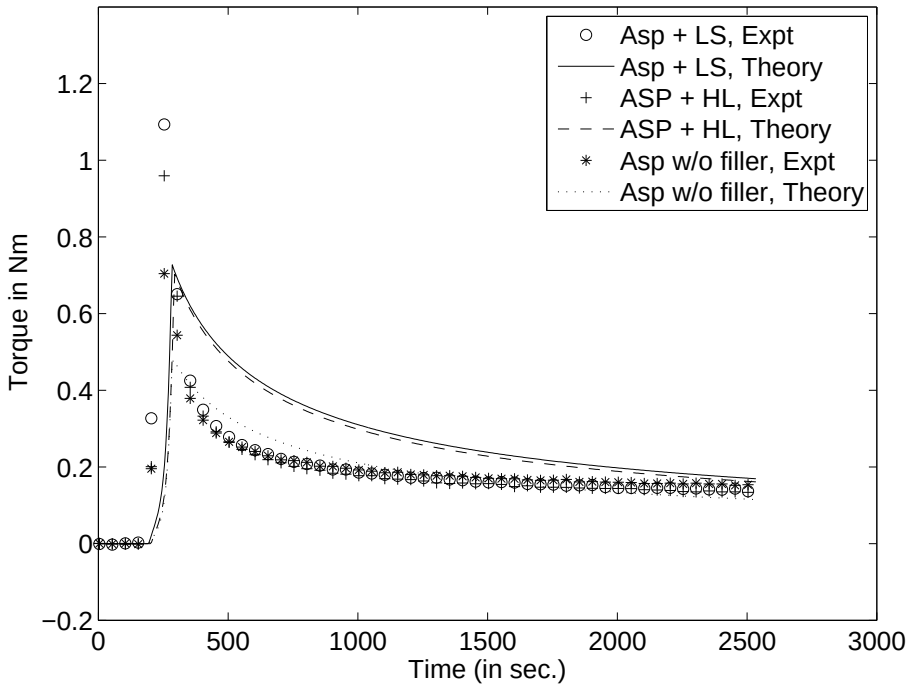

Fig. 12. Comparison of torque in sand-asphalt specimens fabricated with asphalt(PG64-22) containing hydrated lime filler, asphalt(PG64-22) containing limestone filler and asphalt (PG64-22) with no filler, at loading rate of 60 min/rev for a loading duration of 90 seconds (Filler/Asphalt ratio 10% by mass).

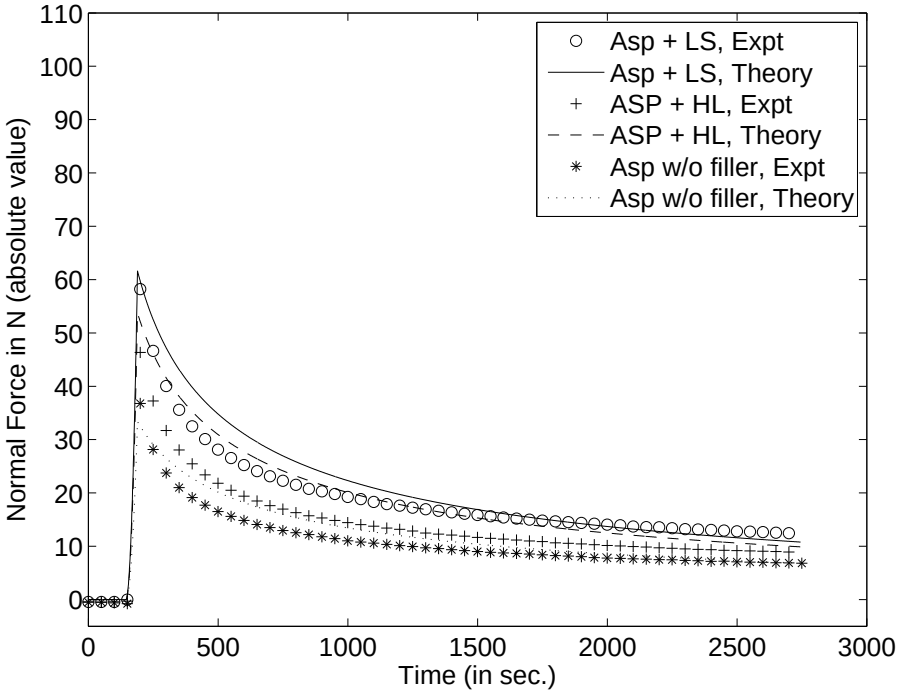

Fig. 13. Comparison of normal force in sand-asphalt specimens fabricated with asphalt(PG64-22) containing hydrated lime filler, asphalt(PG64-22) containing limestone filler and asphalt (PG64-22) with no filler, at loading rate of 30 min/rev for a loading duration of 45 seconds (Filler/Asphalt ratio 10% by mass).

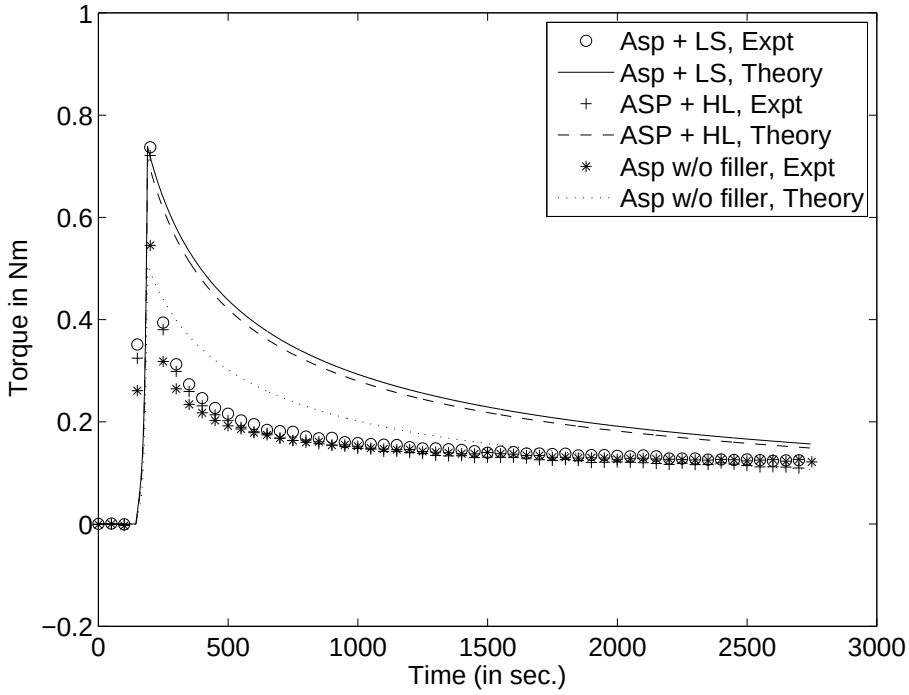

Fig. 14. Comparison of torque in sand-asphalt specimens fabricated with asphalt(PG64-22) containing hydrated lime filler, asphalt(PG64-22) containing limestone filler and asphalt (PG64-22) with no filler, at loading rate of 30 min/rev for a loading duration of 45 seconds (Filler/Asphalt ratio 10% by mass).

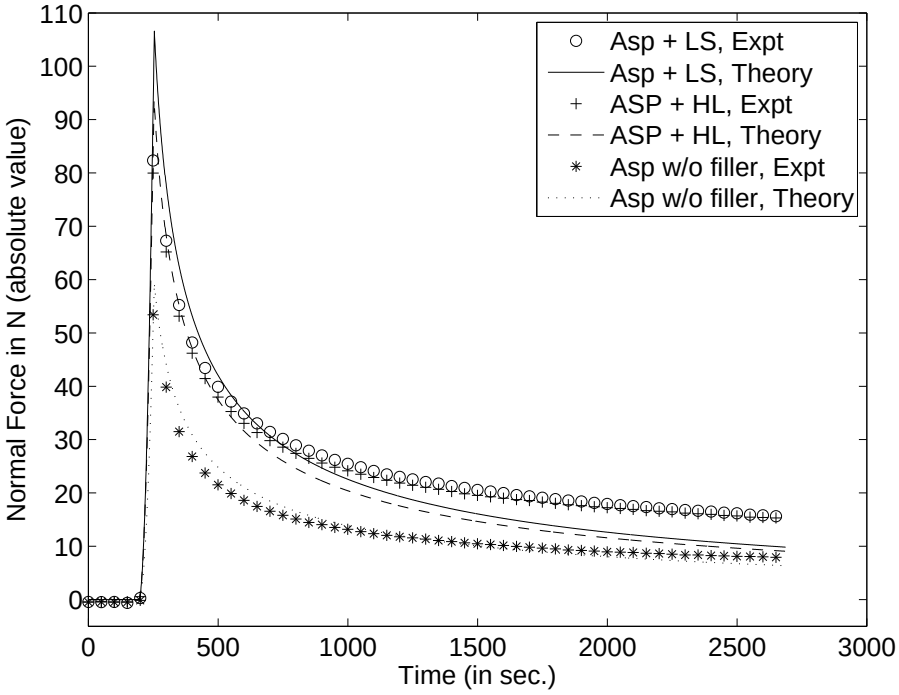

Fig. 15. Comparison of normal force in sand-asphalt specimens fabricated with asphalt(PG64-22) containing hydrated lime filler, asphalt(PG64-22) containing limestone filler and asphalt (PG64-22) with no filler, at loading rate of 30 min/rev for a loading duration of 60 seconds (Filler/Asphalt ratio 10% by mass).

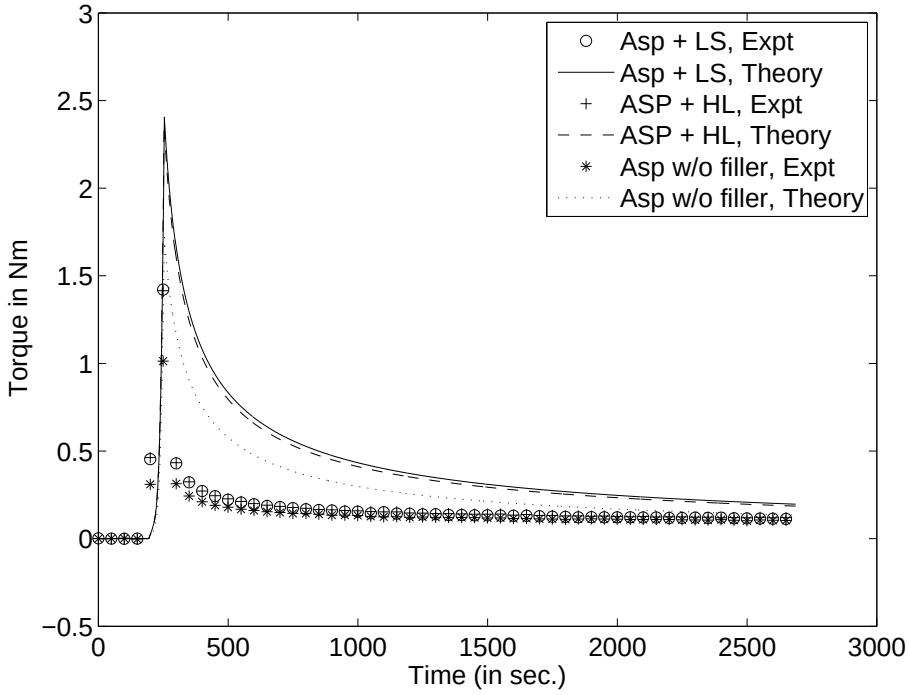

Fig. 16. Comparison of torque in sand-asphalt specimens fabricated with asphalt(PG64-22) containing hydrated lime filler, asphalt(PG64-22) containing limestone filler and asphalt (PG64-22) with no filler, at loading rate of 30 min/rev for a loading duration of 60 seconds (Filler/Asphalt ratio 10% by mass).

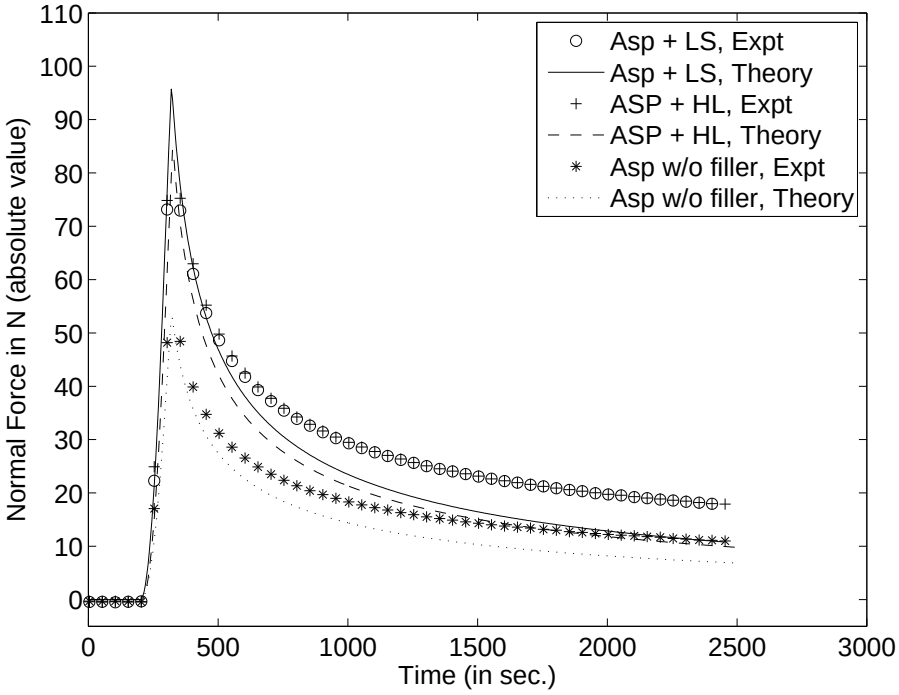

Fig. 17. Comparison of normal force in sand-asphalt specimens fabricated with asphalt(PG64-22) containing hydrated lime filler, asphalt(PG64-22) containing limestone filler and asphalt (PG64-22) with no filler, at loading rate of 60 min/rev for a loading duration of 120 seconds (Filler/Asphalt ratio 10% by mass).

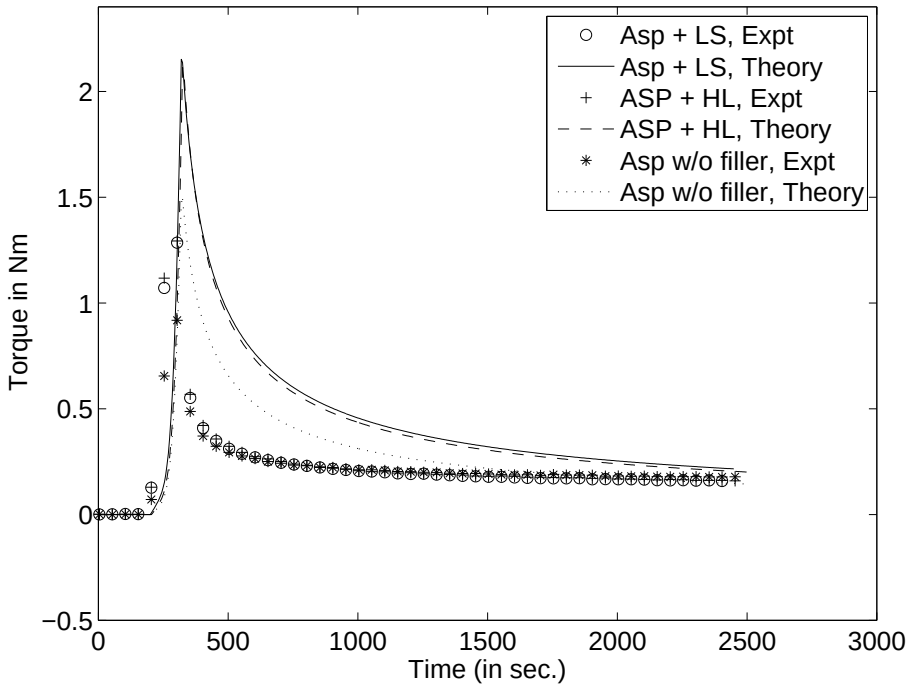

Fig. 18. Comparison of torque in sand-asphalt specimens fabricated with asphalt(PG64-22) containing hydrated lime filler, asphalt(PG64-22) containing limestone filler and asphalt (PG64-22) with no filler, at loading rate of 60 min/rev for a loading duration of 120 seconds (Filler/Asphalt ratio 10% by mass).

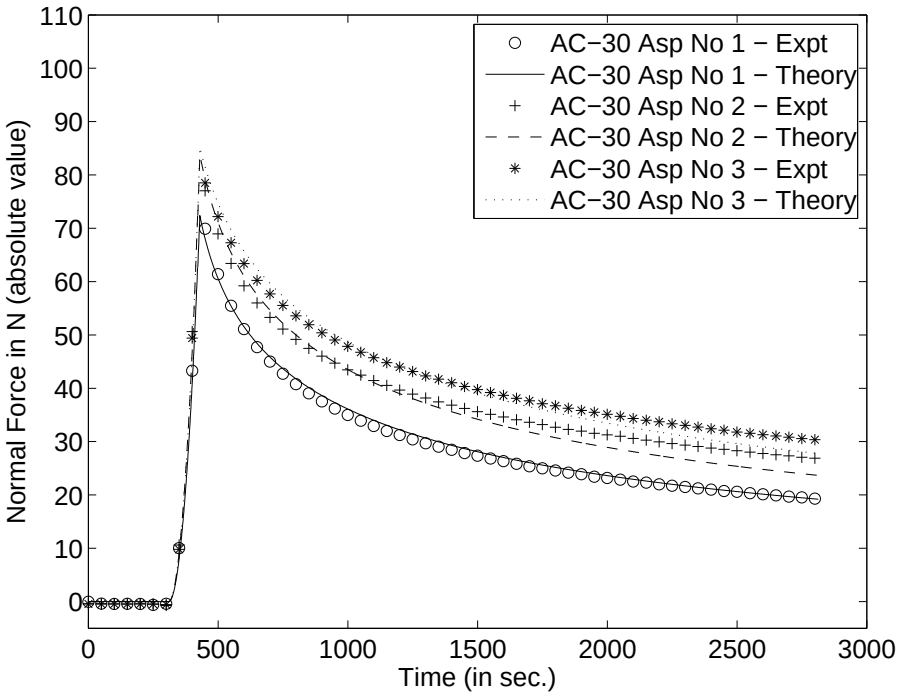

Fig. 19. Comparison of normal force in sand-asphalt specimens fabricated using different asphalts (all graded as AC-30). The loading rate is 60 min/rev and the loading duration is 120 seconds (Filler/Asphalt ratio 23% by mass).

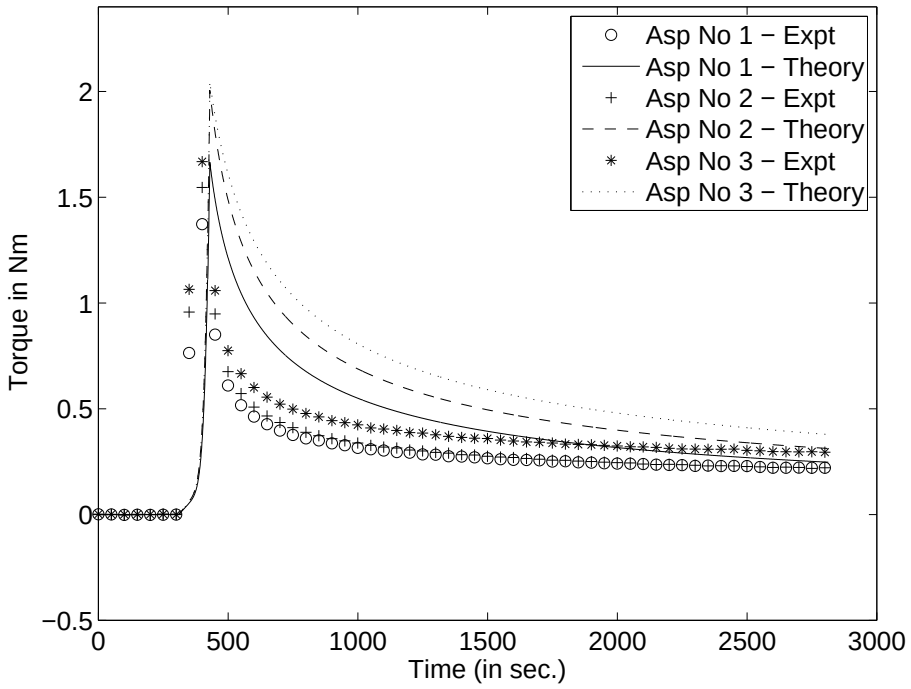

Fig. 20. Comparison of torque in sand-asphalt specimens fabricated using different asphalts (all graded as AC-30). The loading rate is 60 min/rev and the loading duration is 120 seconds (Filler/Asphalt ratio 23% by mass).

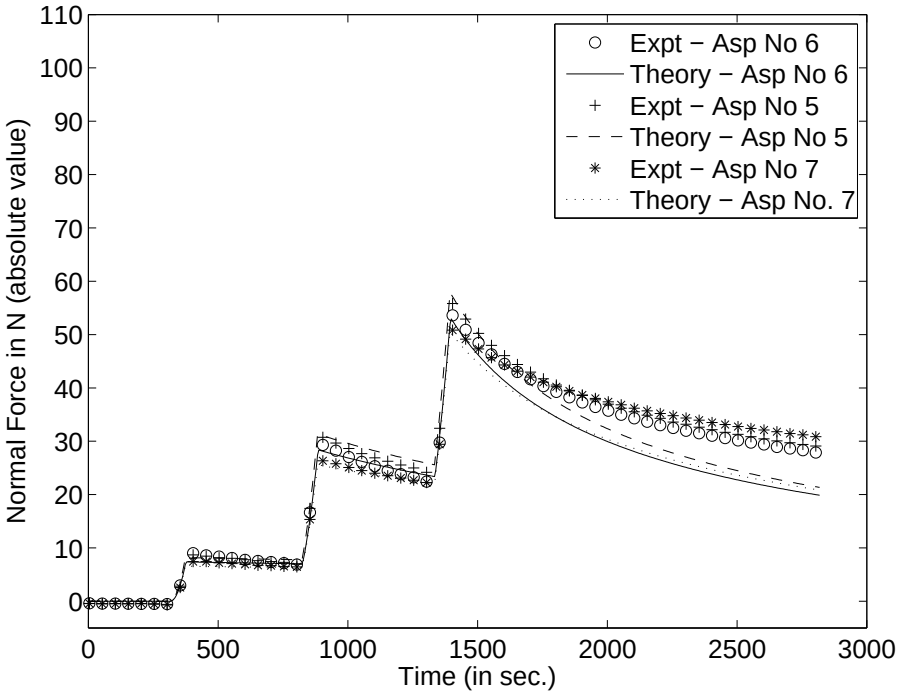

Fig. 21. Comparison of the normal forces in specimens made with three different asphalts graded as PG64-22. The loading cycle is 60-450-60-450-60.

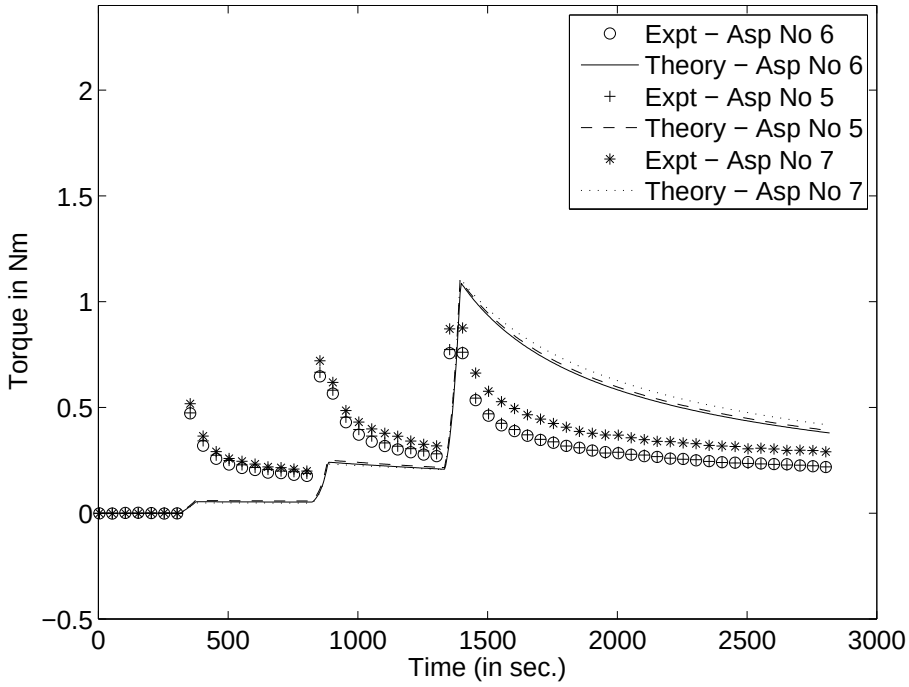

Fig. 22. Comparison of torque in specimens made with three different asphalts graded as PG64-22. The loading cycle is 60-450-60-450-60.

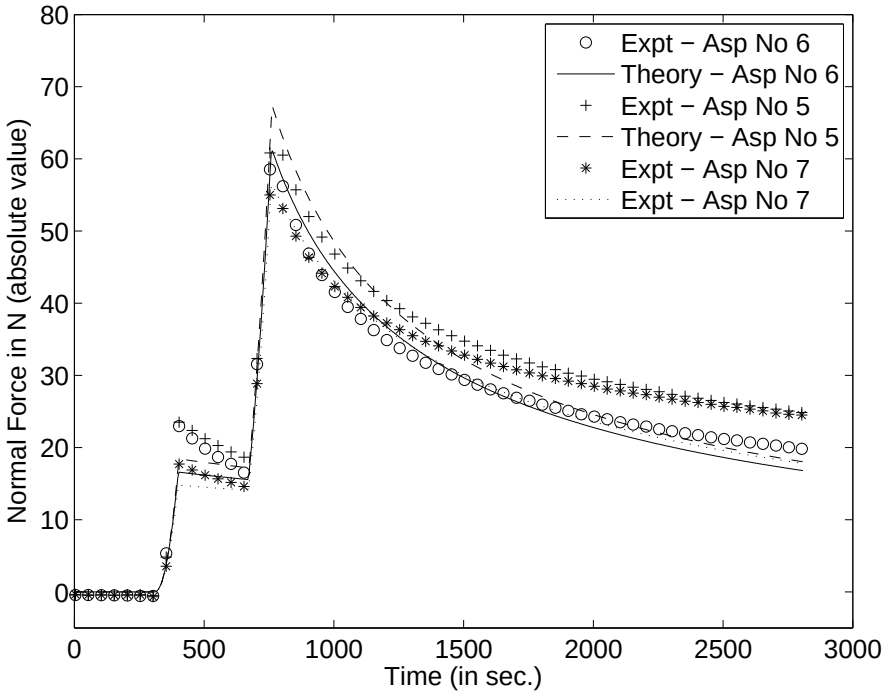

Fig. 23. Comparison of the normal forces in specimens made with three different asphalts graded as PG64-22. The loading cycle is 90-270-90.

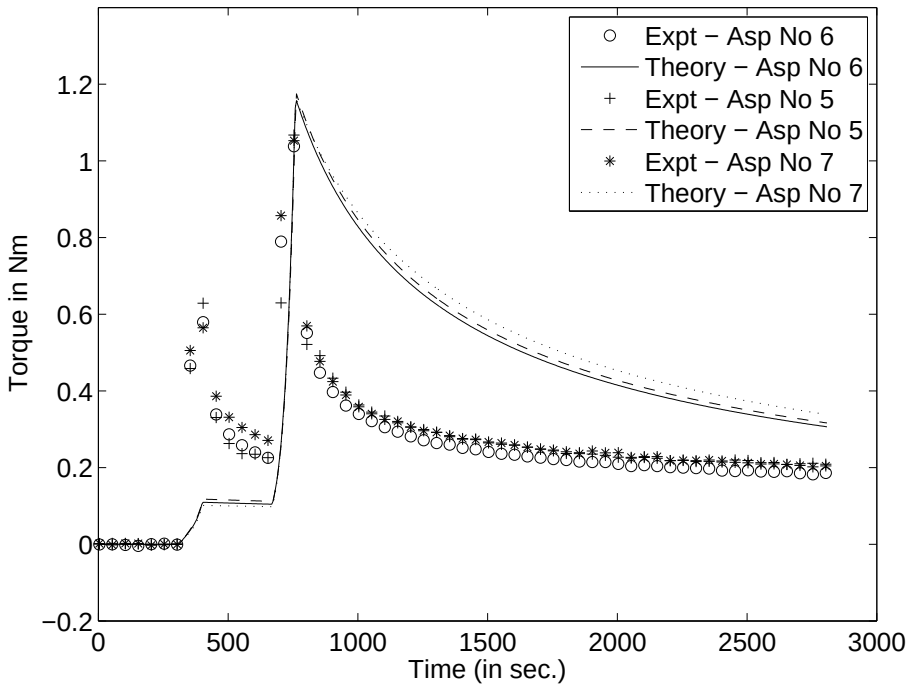

Fig. 24. Comparison of the torques in specimens made with three different asphalts graded as PG64-22. The loading cycle is 90-270-90.

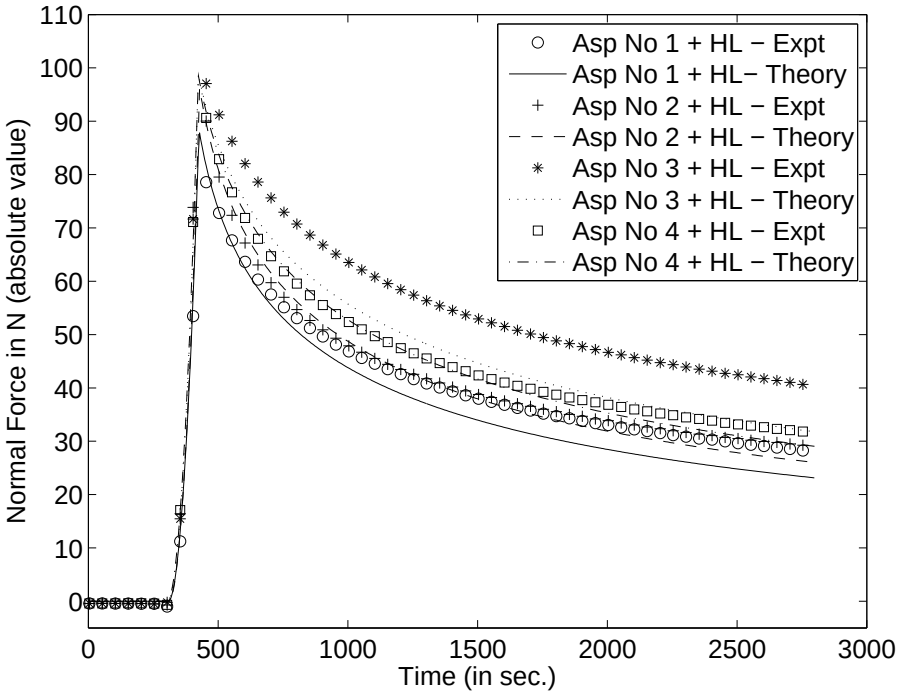

Fig. 25. Comparison of the normal forces in asphalts containing hydrated lime filler. All the asphalts are graded as AC-30.

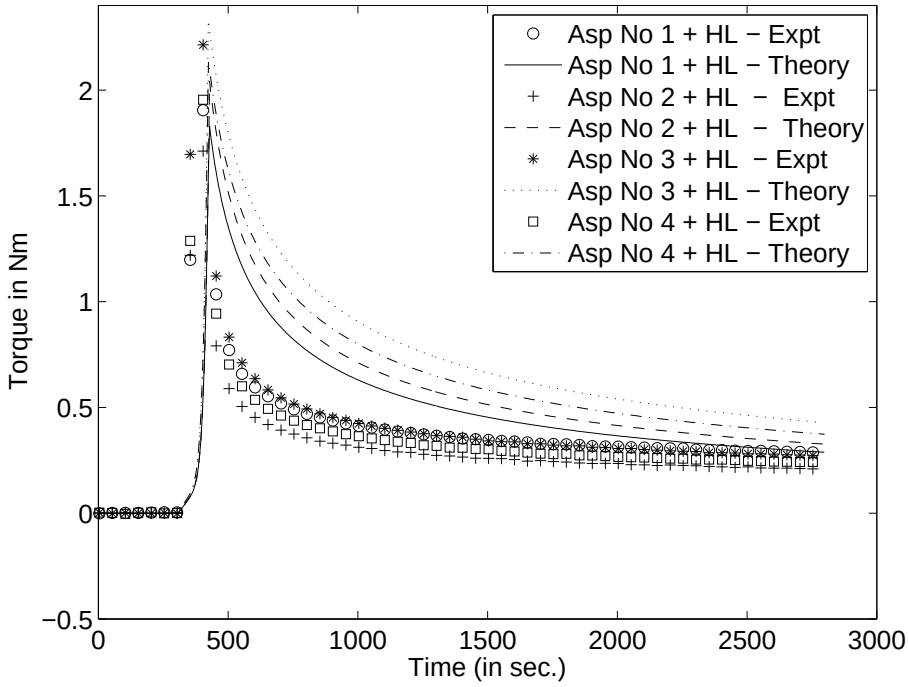

Fig. 26. Comparison of the normal forces in asphalts containing hydrated lime filler. All the asphalts are graded as AC-30.

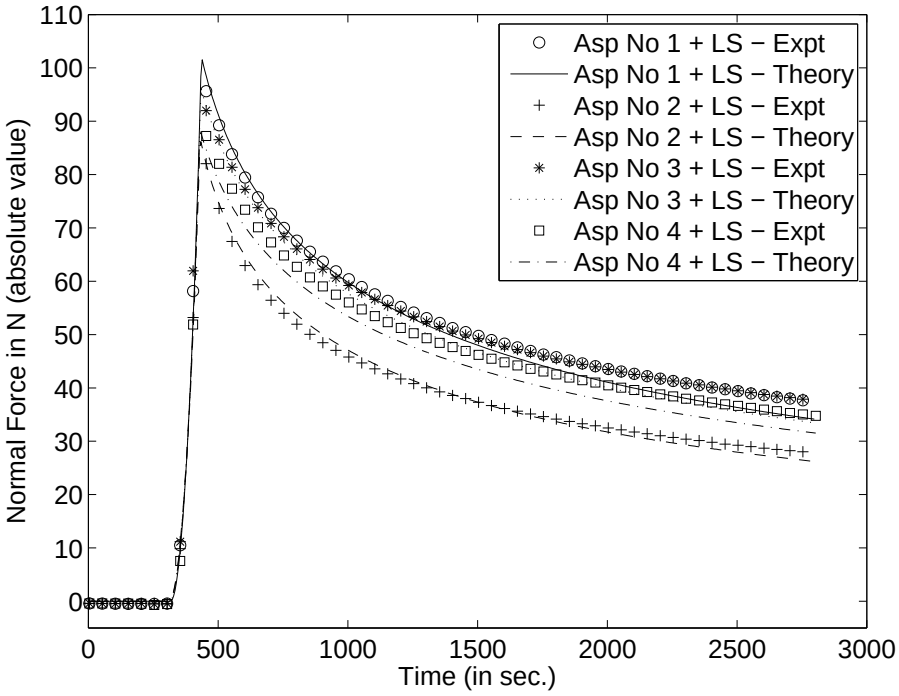

Fig. 27. Comparison of the normal forces in asphalts containing limestone filler. All the asphalts are graded as AC-30.

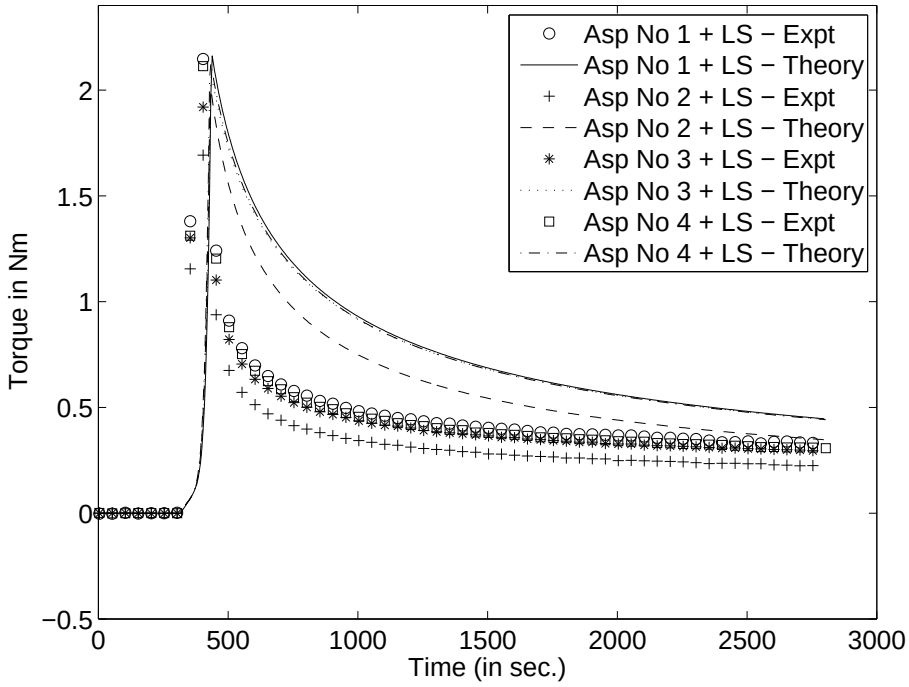

Fig. 28. Comparison of the normal forces in asphalts containing limestone filler. All the asphalts are graded as AC-30.

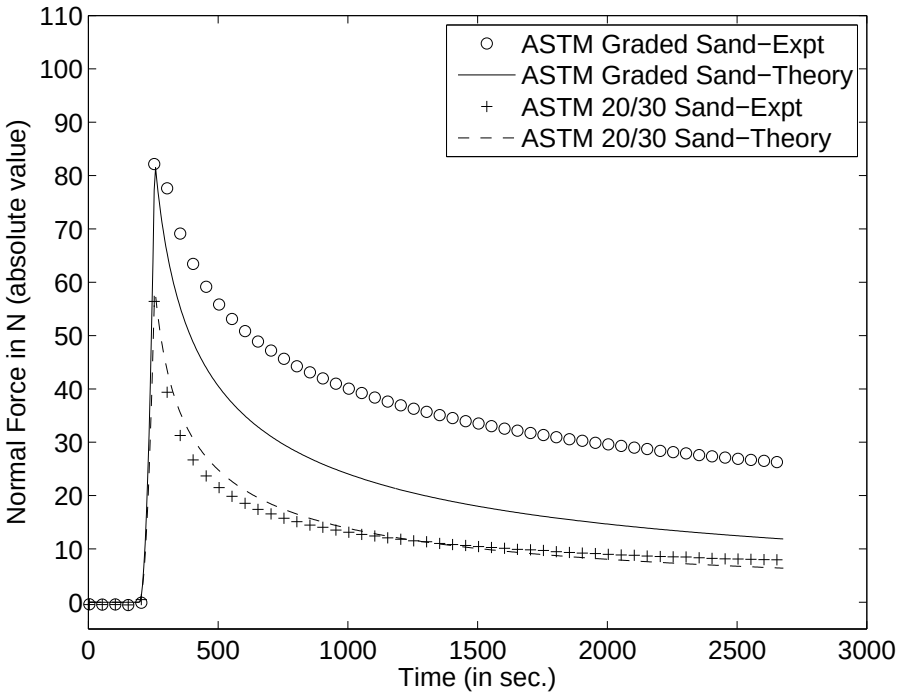

Fig. 29. Comparison of the normal forces in specimens made with sands of different gradation. Loading rate being 30 minutes per rev and duration of loading being 60 seconds.

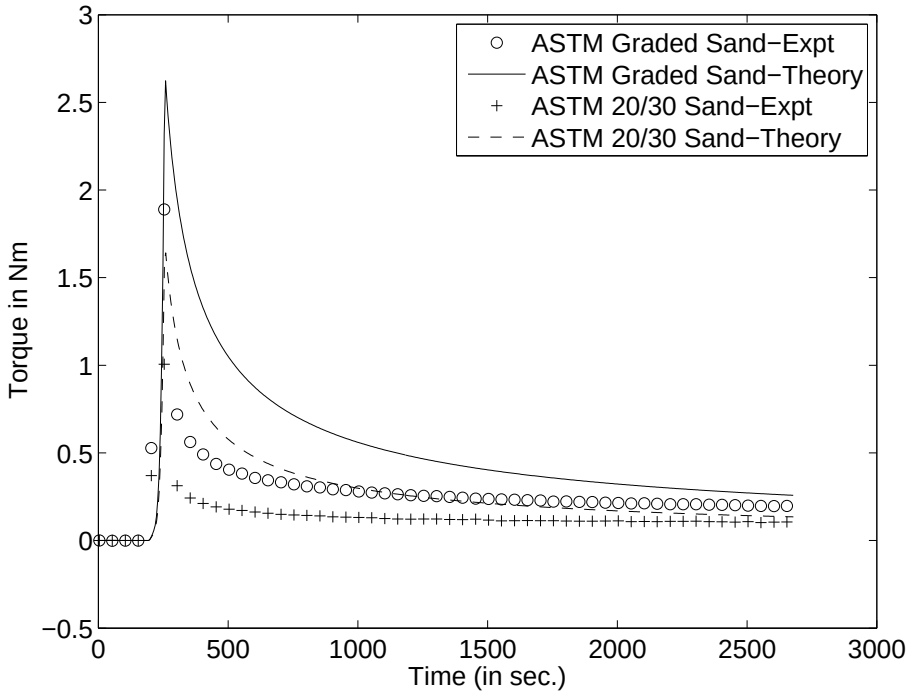

Fig. 30. Comparison of the torques in specimens made with sands of different gradation. Loading rate being 30 minutes per rev and duration of loading being 60 seconds.

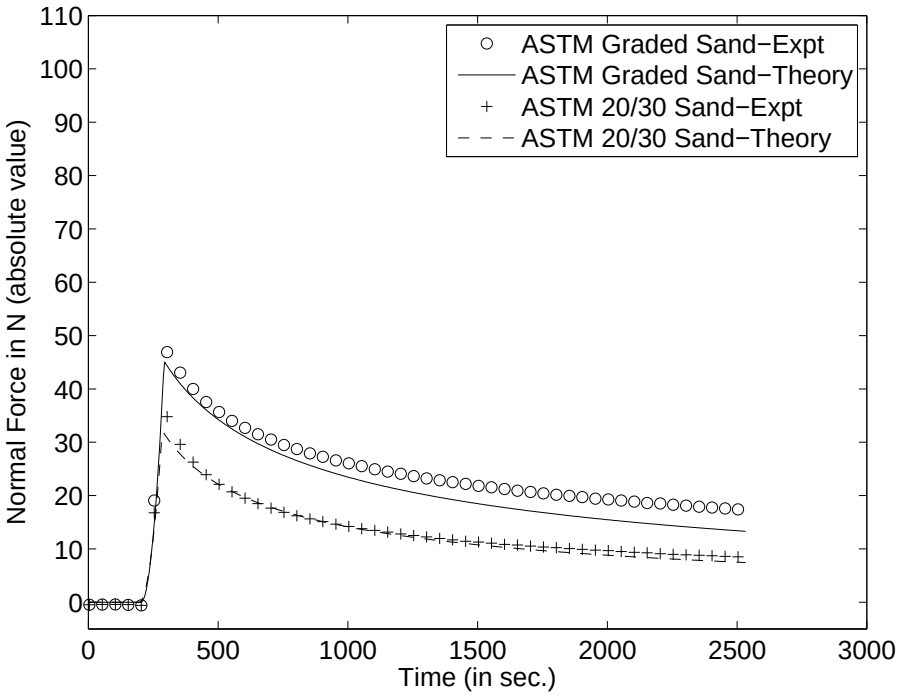

Fig. 31. Comparison of the normal forces in specimens made with sands of different gradation. Loading rate being 60 minutes per rev and duration of loading being 90 seconds.

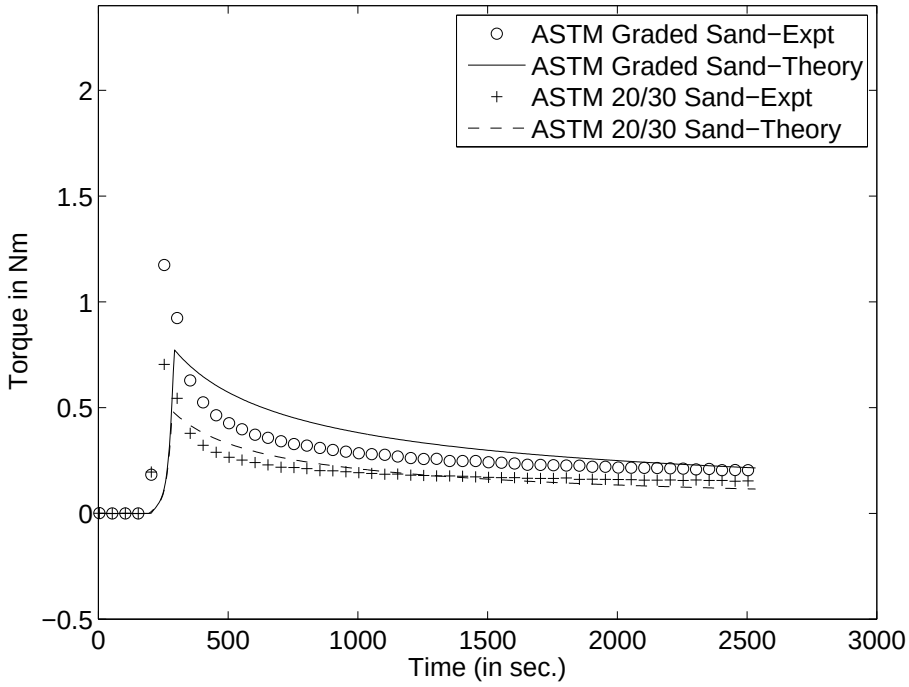

Fig. 32. Comparison of the torques in specimens made with sands of different gradation. Loading rate being 60 minutes per rev and duration of loading being 90 seconds.

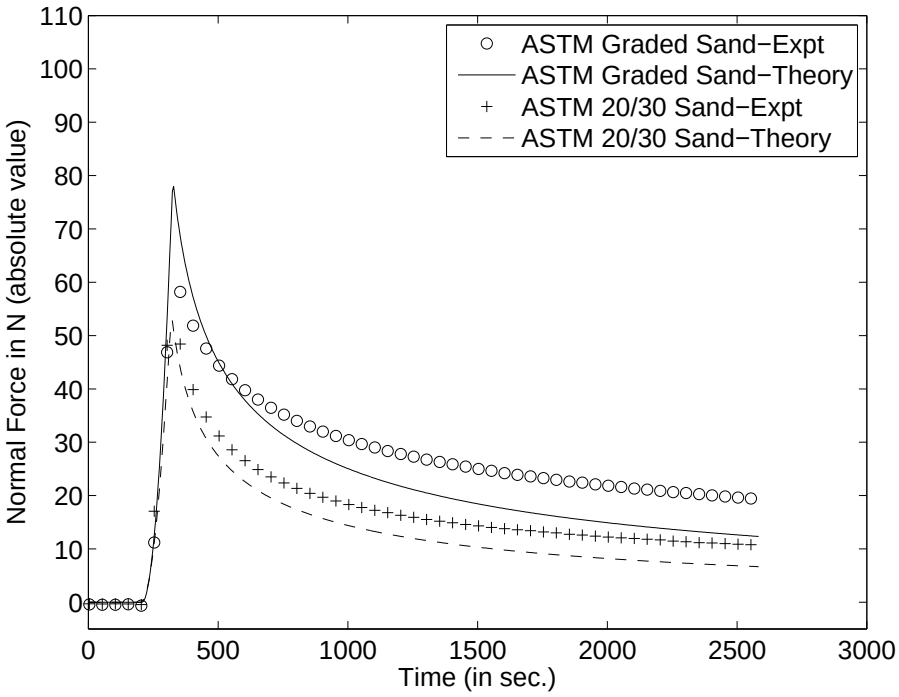

Fig. 33. Comparison of the normal forces in specimens made with sands of different gradation. Loading rate being 60 minutes per rev and duration of loading being 120 seconds.

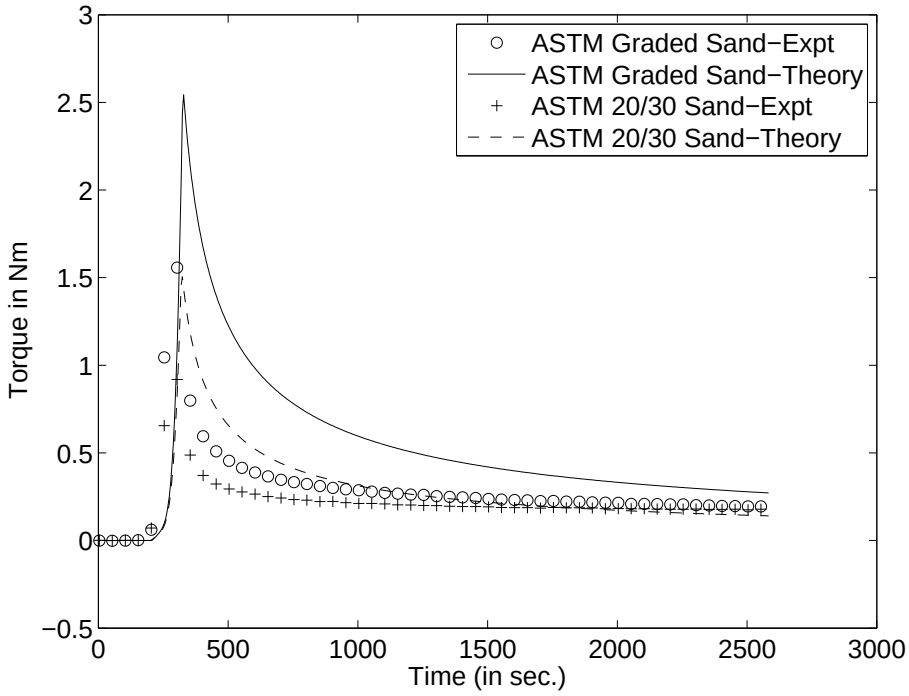

Fig. 34. Comparison of the torques in specimens made with sands of different gradation. Loading rate being 60 minutes per rev and duration of loading being 120 seconds.

CHAPTER V

A MODEL FOR SAND-ASPHALT MIXTURES

Asphalt mixes are three constituent mixtures consisting of an aggregate matrix, a viscous fluid and air-filled voids (Fillers maybe treated together with asphalt as asphalt mastic). The mixture exhibits behavior that ranges from viscoelastic fluid like to viscoelastic solid like to brittle elastic depending on the temperature and loading conditions.

Different test methods tend to activate different response mechanisms. For example the response of asphalt concrete to compressive creep is quite different from its response to tensile creep. This diversity is a reflection of the physics underlying the load carrying and relaxation mechanisms. In compressive tests the aggregate matrix takes up a large share of the load and matrix interlock progressively slows down the rate of deformation. On the other hand in tensile tests the majority of the stress is transmitted through the asphalt mastic.

The air voids play a very important role in asphalt mix behavior. The possibility of microcracks coalescing and propagating is determined by the air void distribution. The air voids also serve to accommodate asphalt movements during deformation.

Sand-asphalt although a member of the extended asphalt concrete family shows characteristics not usually seen in regular mixes. These characteristics such as a less "stiff" aggregate matrix are accounted for through the smaller size and smooth shape of the aggregate particles that make up sand-asphalt mixtures.

For a material as complex as asphalt concrete it is impractical to have a single constitutive relation to determine its mechanical response under all conditions. A very strong case maybe made to allow for a family of models depending upon the class of processes the body is subjected to. This is indeed the basis for the framework

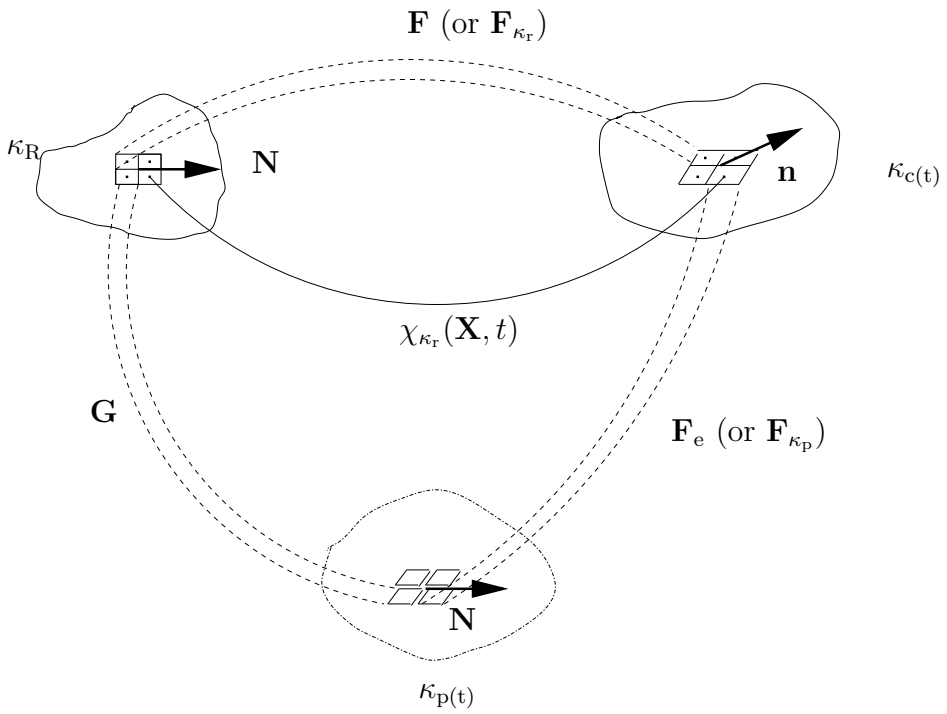

Fig. 35. Diagram showing the notion of multiple natural configuration.

for the study of materials with multiple natural configurations.

A hierarchy of models of increasing sophistication, within the framework of multiple natural configurations has been developed by Krishnan and Rajagopal ([81],[82],[83],[84]) which have been very successful in capturing the behavior of asphalt mixtures subjected to a variety of mechanical tests ranging from uni-axial extension to tri-axial compression. The modeling efforts here are in the same spirit.

It is assumed that the behavior of interest here can be captured by a homogenized, incompressible anisotropic fluid like model. The validity (or lack of it) of these assumptions will be borne out by comparisons to experimental results.

A. Kinematics

As shown in Figure 35, κ_R is the reference configuration and $\kappa_{c(t)}$ is the configuration currently occupied by the material. $\kappa_{p(t)}$ refers to the natural configuration associated

with the material at time t. For homogenous deformations, $\mathbf{F}_{\kappa_{p(t)}}$ (or $\mathbf{F}_{\mathrm{e}}$) denotes the deformation gradient from κ_R to $\kappa_{\mathrm{c(t)}}$. In general this meaning may not be attached to $\mathbf{F}_{\kappa_{p(t)}}$ (see [12]). The mapping $\mathbf{G}$ from κ_R to $\kappa_{\mathrm{p(t)}}$ is defined through,

$$\mathbf{G} := \mathbf{F}_{\mathrm{e}}{}^{-\mathbf{1}}\mathbf{F}. \tag{5.1}$$

Using the polar decomposition theorem,

$$\mathbf{F} = \mathbf{RU} = \mathbf{VR}, \tag{5.2}$$

where $\mathbf{R}$ is a proper orthogonal tensor, $\mathbf{U}$ and $\mathbf{V}$ are the right and left stretch tensors and they are positive definite symmetric tensors. Similarly we define,

$$\begin{aligned} \mathbf{F}_{\mathrm{e}} &= \mathbf{R}_{\mathrm{e}}\mathbf{U}_{\mathrm{e}} && (5.3)\\ &= \mathbf{V}_{\mathrm{e}}\mathbf{R}_{\mathrm{e}} && (5.4)\\ &= \mathbf{R}_{\kappa_{\mathrm{p}}}\mathbf{U}_{\kappa_{\mathrm{p}}} && (5.5)\\ &= \mathbf{V}_{\kappa_{\mathrm{p}}}\mathbf{R}_{\kappa_{\mathrm{p}}}. && (5.6) \end{aligned}$$

$\mathbf{L}_{\mathrm{e}}$ and $\mathbf{L}_{\mathrm{p}}$ are defined through,

$$\mathbf{L}_{\mathrm{e}} = \dot{\mathbf{F}}_{\mathrm{e}}\mathbf{F}_{\mathrm{e}}^{-1}, \tag{5.7}$$

$$\mathbf{L}_{\mathrm{p}} = \dot{\mathbf{G}}\mathbf{G}^{-\mathbf{1}}. \tag{5.8}$$

B. A Constitutive Model for Sand-Asphalt Mixtures

From equation (2.20)

$$\mathbf{T}\cdot\mathbf{L} - \rho\dot{\hat{\psi}} - \rho\eta\dot{\theta} = \xi_d. \tag{5.9}$$

Let,

$$\hat{\psi} = \hat{\psi}(\mathbf{F}_{\mathrm{e}}, \theta). \tag{5.10}$$

Using the previous two equations,

$$\mathbf{T} \cdot \mathbf{L} - \rho \frac{\partial \hat{\psi}}{\partial \mathbf{F}_{\mathrm{e}}} \cdot \dot{\mathbf{F}}_{\mathrm{e}} - \rho \frac{\partial \hat{\psi}}{\partial \theta} \dot{\theta} - \rho \eta \dot{\theta} = \xi_d. \tag{5.11}$$

$$\mathbf{T} \cdot \mathbf{L} - \rho \frac{\partial \hat{\psi}}{\partial \mathbf{F}_{\mathrm{e}}} \cdot \dot{\mathbf{F}}_{\mathrm{e}} - \rho \dot{\theta} (\frac{\partial \hat{\psi}}{\partial \theta} + \eta) = \xi_d. \tag{5.12}$$

Setting,

$$\frac{\partial \hat{\psi}}{\partial \theta} = -\eta, \tag{5.13}$$

in Eq. (5.12), we have,

$$\mathbf{T} \cdot \mathbf{L} - \rho \frac{\partial \hat{\psi}}{\partial \mathbf{F}_{\mathrm{e}}} \cdot \dot{\mathbf{F}}_{\mathrm{e}} = \xi_d. \tag{5.14}$$

From the kinematics,

$$\mathbf{L}_{\kappa_{\mathrm{r}}} = \dot{\mathbf{F}}_{\kappa_{\mathrm{r}}} \mathbf{F}_{\kappa_{\mathrm{r}}}^{-1}. \tag{5.15}$$

$$\begin{aligned} \dot{\mathbf{F}}_{\mathrm{e}} &= \mathbf{F}_{\mathrm{e}}{}' + \overset{\triangledown}{\mathbf{F}}_{\mathrm{e}} = \dot{\mathbf{F}}_{\mathrm{e}}|_{\mathbf{G} \text{ held fixed}} + \dot{\mathbf{F}}_{\mathrm{e}}|_{\mathbf{F}_{\kappa_{\mathrm{r}}} \text{ held constant}} \\ &= \dot{\mathbf{F}}_{\kappa_{\mathrm{r}}} \mathbf{G}^{-1}|_{\mathbf{G} \text{ held fixed}} + \mathbf{F}_{\kappa_{\mathrm{r}}} \dot{\mathbf{G}^{-1}}|_{\mathbf{F}_{\kappa_{\mathrm{r}}} \text{ held constant}} \\ &= \mathbf{L}_{\kappa_{\mathrm{r}}} \mathbf{F}_{\mathrm{e}} - \mathbf{F}_{\mathrm{e}} \mathbf{L}_{\mathrm{p}}. \end{aligned} \tag{5.16}$$

This implies,

$$\mathbf{L} = \mathbf{L}_{\kappa_{\mathrm{r}}} = (\dot{\mathbf{F}}_{\mathrm{e}} + \mathbf{F}_{\mathrm{e}} \mathbf{L}_{\mathrm{p}}) \mathbf{F}_{\mathrm{e}}^{-1} \tag{5.17}$$

$$= (\dot{\mathbf{F}}_{\mathrm{e}} - \overset{\triangledown}{\mathbf{F}}_{\mathrm{e}}) \mathbf{F}_{\mathrm{e}}^{-1}. \tag{5.18}$$

Substituting for $\mathbf{L}_{\kappa_{\mathrm{r}}}$ in Eq. (5.14) we have,

$$\mathbf{T} \cdot (\dot{\mathbf{F}}_{\mathrm{e}} - \overset{\triangledown}{\mathbf{F}}_{\mathrm{e}}) \mathbf{F}_{\mathrm{e}}^{-1} - \rho \frac{\partial \hat{\psi}}{\partial \mathbf{F}_{\mathrm{e}}} \cdot \dot{\mathbf{F}}_{\mathrm{e}} = \xi_d. \tag{5.19}$$

$$(\mathbf{T} - \rho\frac{\partial\hat{\psi}}{\partial\mathbf{F}_{\mathrm{e}}}\mathbf{F}_{\mathrm{e}}^{T}) \cdot \mathbf{L}_{\mathrm{e}} - (\mathbf{T}\mathbf{F}_{\mathrm{e}}^{-T} \cdot \overset{\triangledown}{\mathbf{F}}_{\mathrm{e}}) = \xi_d. \tag{5.20}$$

Using the property that the dot product of a symmetric tensor and a skew tensor is zero, the above equation can be rewritten as,

$$(\mathbf{T} - \rho\frac{\partial\hat{\psi}}{\partial\mathbf{F}_{\mathrm{e}}}\mathbf{F}_{\mathrm{e}}^{T}) \cdot \mathbf{L}_{\mathrm{e}} - \mathbf{T}^{*} \cdot \overset{\triangledown}{\mathbf{V}}_{\mathrm{e}} - \boldsymbol{\tau}^{*} \cdot \boldsymbol{\Omega}_{\mathbf{e}} = \xi_d, \tag{5.21}$$

where,

$$\mathbf{T}^{*} = \frac{1}{2}(\mathbf{T}\mathbf{V}_{\mathrm{e}}{}^{-1} + \mathbf{V}_{\mathrm{e}}{}^{-1}\mathbf{T}), \tag{5.22}$$

$$\boldsymbol{\tau}^{*} = \frac{1}{2}(\mathbf{V}_{\mathrm{e}}\mathbf{T}\mathbf{V}_{\mathrm{e}}{}^{-1} - \mathbf{V}_{\mathrm{e}}{}^{-1}\mathbf{T}\mathbf{V}_{\mathrm{e}}), \tag{5.23}$$

$$\boldsymbol{\Omega}_{\mathbf{e}} = \overset{\triangledown}{\mathbf{R}}_{\mathrm{e}}\mathbf{R}_{\mathrm{e}}{}^{\mathbf{T}}, \tag{5.24}$$

$$\overset{\triangledown}{\mathbf{V}}_{\mathrm{e}} = \dot{\mathbf{V}}_{\mathrm{e}}|_{\mathbf{F}_{\kappa_{\mathrm{r}}} \text{ held fixed}}, \tag{5.25}$$

$$\overset{\triangledown}{\mathbf{R}}_{\mathrm{e}} = \dot{\mathbf{R}}_{\mathrm{e}}|_{\mathbf{F}_{\kappa_{\mathrm{r}}} \text{ held fixed}}. \tag{5.26}$$

It is assumed that the dissipation is of the following form (following Rajagopal and Srinivasa [85]),

$$\xi_d = (\beta_0 \overset{\triangledown}{\mathbf{V}}_{\mathrm{e}} \cdot \overset{\triangledown}{\mathbf{V}}_{\mathrm{e}} + \beta_1 \boldsymbol{\Omega}_{\mathbf{e}} \cdot \boldsymbol{\Omega}_{\mathbf{e}})^{r}. \tag{5.27}$$

Now it is required that the natural configuration evolve in such a way that the rate of entropy prduction is maximized. This is by no means the only possible route. This issue has been discussed in detail by Rajagopal and Srinivasa [86]-[87]. The procedure has been successfully used previously for asphalt bound mixture by Krishnan and Rajagopal [81] and it has worked very well. The maximization of dissipation as a strategy to pick among the many different ways in which the natural configuration could evolve has also been successfully applied to a variety of materials from polymers to single crystals, by Rajagopal and co-workers ([88],[89],[90],[91]).

The reduced energy-dissipation equation acts as a constraint on the maximization

of dissipation. Constraints are also imposed by incompressibility (both of the elastic response and the inelastic response). The suitability of this assumption for asphalt bound bound mixtures is open to debate. Indeed air voids play a crucial role in the reponse of asphalt mixtures and changes in the percentage of air voids over time in pavements is used by practicing engineers as a measure of residual service life of pavements. The assumption of incompressibility is imposed here because for the specific problem on hand air void changes over the duration of the experiment may not be significant. It is also noted that relaxing this constraint of incompressibility presents no difficulty and may be easily carried out.

The standard methods of the calculus of constrained maximization is applied. Lagrange multipliers λ_1, λ_2 and λ_3 are introduced.

$$h = \xi_d - \lambda_1(\mathbf{A}\cdot\mathbf{L}_{\mathrm{e}} - \mathbf{T}^*\cdot\overset{\triangledown}{\mathbf{V}}_{\mathrm{e}} - \boldsymbol{\tau}^*\cdot\boldsymbol{\Omega}_{\mathbf{e}} - \xi_{\mathbf{d}}) - \lambda_2 \mathrm{tr}\mathbf{L}_{\mathrm{e}} - \lambda_3\overset{\triangledown}{\mathbf{V}}_{\mathrm{e}}\cdot\mathbf{V}_{\mathrm{e}}^{-1}, \tag{5.28}$$

where,

$$\mathbf{A} = \mathbf{T} - \rho\frac{\partial\hat{\psi}}{\partial\mathbf{F}_{\mathrm{e}}}\mathbf{F}_{\mathrm{e}}{}^{T}. \tag{5.29}$$

Differentiating h with respect to $\mathbf{L}_{\mathrm{e}}$,

$$\frac{\partial h}{\partial\mathbf{L}_{\mathrm{e}}} = -\lambda_1\mathbf{A} - \lambda_2\mathbf{I} = 0. \tag{5.30}$$

i.e.,

$$\begin{aligned}\mathbf{T} &= -\mathrm{p}\mathbf{I} + \rho\frac{\partial\hat{\psi}}{\partial\mathbf{F}_{\mathrm{e}}}\mathbf{F}_{\mathrm{e}}^{\mathrm{T}} \\ &= -\mathrm{p}\mathbf{I} + 2\rho\mathbf{F}_{\mathrm{e}}\frac{\partial\hat{\psi}}{\partial\mathbf{C}_{\mathrm{e}}}\mathbf{F}_{\mathrm{e}}{}^{\mathrm{T}},\end{aligned} \tag{5.31}$$

where $\mathrm{p} = \frac{\lambda_2}{\lambda_1}$.

Differentiating h with respect to $\overset{\triangledown}{\mathbf{V}}_{\mathrm{e}}$,

$$\frac{\partial h}{\partial \overset{\triangledown}{\mathbf{V}}_{\mathrm{e}}} = (1+\lambda_1)\frac{\partial \xi}{\partial \overset{\triangledown}{\mathbf{V}}_{\mathrm{e}}} - \lambda_3 \mathbf{V}_{\mathrm{e}}^{-1} + \lambda_1 \mathbf{T}^* = \mathbf{0}. \tag{5.32}$$

i.e.,

$$(1+\lambda_1) 2r\beta_0 \overset{\triangledown}{\mathbf{V}}_{\mathrm{e}} \, \xi^{(r-1)/r} - \lambda_3 \mathbf{V}_{\mathrm{e}}^{-1} + \lambda_1 \mathbf{T}^* = \mathbf{0}. \tag{5.33}$$

Differentiating h with respect to $\mathbf{\Omega_e}$,

$$\frac{\partial h}{\partial \mathbf{\Omega_e}} = (1+\lambda_1)\frac{\partial \xi}{\partial \mathbf{\Omega_e}} + \lambda_1 \boldsymbol{\tau}^* = 0. \tag{5.34}$$

i.e.,

$$(1+\lambda_1) 2r\beta_1 \mathbf{\Omega_e} \xi^{(\mathbf{r-1})/\mathbf{r}} + \lambda_{\mathbf{1}} \boldsymbol{\tau}^* = \mathbf{0}. \tag{5.35}$$

By routine manipulations,

$$\begin{aligned} \frac{2r(1+\lambda_1)}{\lambda_1} &= 1 \quad \text{and} \\ \frac{\lambda_3}{\lambda_1} &= \frac{\mathbf{T}^* \cdot \mathbf{V}_{\mathrm{e}}^{-\mathbf{1}}}{\mathbf{V}_{\mathrm{e}}^{-1} \cdot \mathbf{V}_{\mathrm{e}}^{-1}}. \end{aligned} \tag{5.36}$$

From kinematics, the following relation is available,

$$\dot{\mathbf{V}}_e + \mathbf{V}_{\mathrm{e}} \mathbf{W_e} - \mathbf{L}_{\kappa_{\mathrm{r}}} \mathbf{V}_{\mathrm{e}} = \overset{\triangledown}{\mathbf{V}}_{\mathrm{e}} + \mathbf{V}_{\mathrm{e}} \mathbf{\Omega_e}, \tag{5.37}$$

where,

$$\mathbf{W_e} = \dot{\mathbf{R}}_{\mathrm{e}} \mathbf{R}_{\mathrm{e}}{}^T. \tag{5.38}$$

Expression for $\overset{\triangledown}{\mathbf{V}}_{\mathrm{e}}$ and $\mathbf{\Omega_e}$ are available from Eq.(5.33) and Eq.(5.35). After eliminating ξ, the expressions for $\overset{\triangledown}{\mathbf{V}}_{\mathrm{e}}$ and $\mathbf{\Omega_e}$ maybe substituted in the above kinematic

relation to obtain the evolution equation. Using Eq. (5.27), Eq (5.33) and Eq. (5.35),

$$\xi_d = \left(\left(\frac{\lambda_3}{\lambda_1}\mathbf{V}_{\mathrm{e}}^{-1} - \mathbf{T}^*\right) \cdot \left(\frac{\lambda_3}{\lambda_1}\mathbf{V}_{\mathrm{e}}^{-1} - \mathbf{T}^*\right)\frac{1}{\beta_0} + \left(\frac{\boldsymbol{\tau}^* \cdot \boldsymbol{\tau}^*}{\beta_1}\right) \right)^{\frac{r}{\overline{2r-1}}}. \tag{5.39}$$

Therefore the evolution equation becomes,

$$\mathbf{L}_{\kappa_{\mathrm{r}}}\mathbf{V}_{\mathrm{e}} - \dot{\mathbf{V}}_e - \mathbf{V}_{\mathrm{e}}\mathbf{W}_{\mathbf{e}} = \delta^{\frac{1-r}{2r-1}} \left(\left(\mathbf{T}^* - \frac{\lambda_3}{\lambda_1}\mathbf{V}_{\mathrm{e}}^{-1}\right)\frac{1}{\beta_0} + \frac{\mathbf{V}_{\mathrm{e}}\boldsymbol{\tau}^*}{\beta_1} \right), \tag{5.40}$$

where,

$$\delta = \left(\left(\frac{\lambda_3}{\lambda_1}\mathbf{V}_{\mathrm{e}}^{-1} - \mathbf{T}^*\right) \cdot \left(\frac{\lambda_3}{\lambda_1}\mathbf{V}_{\mathrm{e}}^{-1} - \mathbf{T}^*\right)\frac{1}{\beta_0} + \left(\frac{\boldsymbol{\tau}^* \cdot \boldsymbol{\tau}^*}{\beta_1}\right) \right). \tag{5.41}$$

The response of asphalt bound mixtures is anisotropic. This has been documented by Masad et. al. [92]. Guided by these observations a form for the Helmholtz potential is chosen. It is assumed that the response of the asphalt mixture is orthotropic from the natural configuration. This is a reasonable assumption as the fabrication process involves compaction and radial heat transfer. Let $\mathbf{N}$ and $\mathbf{M}$ denote the two mutually perpendicular preferred directions (fixed) in the natural configuration of the material. Let $\mathbf{n}$ and $\mathbf{m}$ correspond to $\mathbf{N}$ and $\mathbf{M}$ respectively in current configuration of the body. Then,

$$\mathbf{n} = \mathbf{F}_{\mathrm{e}}\mathbf{N}, \tag{5.42}$$

$$\mathbf{m} = \mathbf{F}_{\mathrm{e}}\mathbf{M}. \tag{5.43}$$

Two related quantities $\mathbf{n}^*$ and $\mathbf{m}^*$ are also defined where,

$$\mathbf{n}^* = \mathbf{R}_{\mathrm{e}}\mathbf{N}, \tag{5.44}$$

$$\mathbf{m}^* = \mathbf{R}_{\mathrm{e}}\mathbf{M}. \tag{5.45}$$

The Helmholtz potential is assumed to have the following form:

$$\hat{\psi} = \hat{\psi}(\mathrm{I}_1, \mathrm{I}_2, \mathrm{I}_3, \mathrm{I}_4, \mathrm{I}_5, \mathrm{I}_6, \mathrm{I}_7, \theta), \tag{5.46}$$

where,

$$\begin{aligned}
\mathrm{I}_1 &= \mathrm{tr}\mathbf{B}_\mathrm{e} = \mathrm{tr}\mathbf{C}_\mathrm{e}, \\
\mathrm{I}_2 &= \mathrm{tr}(\mathbf{B}_\mathrm{e}^2) = \mathrm{tr}(\mathbf{C}_\mathrm{e}^2), \\
\mathrm{I}_3 &= \mathrm{det}\mathbf{B}_\mathrm{e} = \mathrm{det}\mathbf{C}_\mathrm{e}, \\
\mathrm{I}_4 &= \mathbf{N}\cdot\mathbf{C}_\mathrm{e}\mathbf{N}, \qquad \mathbf{N} = \begin{pmatrix} 1 \\ 0 \\ 0 \end{pmatrix}, \\
\mathrm{I}_5 &= \mathbf{M}\cdot\mathbf{C}_\mathrm{e}\mathbf{M}, \qquad \mathbf{M} = \begin{pmatrix} 0 \\ 0 \\ 1 \end{pmatrix}, \\
\mathrm{I}_6 &= \mathbf{N}\cdot{\mathbf{C}_\mathrm{e}}^2\mathbf{N}, \\
\mathrm{I}_7 &= \mathbf{M}\cdot{\mathbf{C}_\mathrm{e}}^2\mathbf{M}.
\end{aligned}$$

Specifically,

$$\begin{aligned}
\hat{\psi} &= A + B(\theta-\theta_r) - \frac{C_1}{2}(\theta-\theta_r)^2 + C_2(\theta-\theta_r-\theta\ln\frac{\theta}{\theta_r}) \\
&+ \frac{\hat{\mu}_1\theta}{\rho_{\kappa_{p(t)}}\theta_r}(\mathrm{I}_1-3)^q + \frac{\hat{\mu}_2\theta}{2\rho_{\kappa_{p(t)}}\theta_r}(\mathrm{I}_1-3)g(I_4) \\
&+ \frac{\hat{\mu}_3\theta}{\rho_{\kappa_{p(t)}}\theta_r}\mathrm{k}(\mathrm{I}_4) + \frac{\hat{\mu}_5\theta}{2\rho_{\kappa_{\mathrm{p(t)}}}\theta_\mathrm{r}}(\mathrm{I}_1-3)^2 + \frac{\hat{\mu}_6\theta}{\rho_{\kappa_{\mathrm{p(t)}}}\theta_\mathrm{r}}\mathrm{h}(\mathrm{I}_5).
\end{aligned} \tag{5.47}$$

where,

$$g(I_4) = \begin{cases} \omega + \omega(1 - e^{\frac{-(I_4-1)}{\tau}}), & \text{if } \mathrm{I}_4 \geq 1 \\ \omega - \omega(1 - e^{\frac{(I_4-1)}{\tau}}), & \text{if } \mathrm{I}_4 < 1. \end{cases} \tag{5.48}$$

Computations yield,

$$\begin{aligned} \mathbf{T} &= -p\mathbf{I} + 2\hat{\mu}_1 q(I_1-3)^{q-1}\frac{\theta}{\theta_r}\mathbf{B}_\mathrm{e} + 2\hat{\mu}_2\frac{\theta}{\theta_r}(I_1-3)g(I_4)\mathbf{B}_\mathrm{e} \\ &\quad +2\hat{\mu}_2\frac{\theta}{\theta_r}(I_1-3)^2 g'(I_4)(\mathbf{F}_\mathrm{e}\mathbf{N}\otimes\mathbf{F}_\mathrm{e}\mathbf{N}) \\ &\quad +2\hat{\mu}_3\frac{\theta}{\theta_r}k'(I_4)(\mathbf{F}_\mathrm{e}\mathbf{N}\otimes\mathbf{F}_\mathrm{e}\mathbf{N}) + 2\hat{\mu}_5\frac{\theta}{\theta_r}(I_1-3)\mathbf{B}_\mathrm{e} \\ &\quad +2\hat{\mu}_6\frac{\theta}{\theta_r}h'(I_5)(\mathbf{F}_\mathrm{e}\mathbf{M}\otimes\mathbf{F}_\mathrm{e}\mathbf{M}). \end{aligned} \tag{5.49}$$

i.e.,

$$\mathbf{T} = -p\mathbf{I} + \mu_1\mathbf{B}_\mathrm{e} + \mu_2(\mathbf{F}_\mathrm{e}\mathbf{N}\otimes\mathbf{F}_\mathrm{e}\mathbf{N}) + \mu_3(\mathbf{F}_\mathrm{e}\mathbf{M}\otimes\mathbf{F}_\mathrm{e}\mathbf{M}), \tag{5.50}$$

where,

$$\mu_1 = 2(\hat{\mu}_1 q(I_1-3)^{q-1} + \hat{\mu}_2(I_1-3)g(I_4) + \hat{\mu}_5(I_1-3))\frac{\theta}{\theta_r}, \tag{5.51}$$

$$\mu_2 = (2\hat{\mu}_2(I_1-3)^2 g'(I_4) + 2\hat{\mu}_3 k'(I_4))\frac{\theta}{\theta_r}, \tag{5.52}$$

$$\mu_3 = 2\hat{\mu}_6 h'(I_5)\frac{\theta}{\theta_r}. \tag{5.53}$$

C. Application to Torsion

Since the deformation of interest in this study is due to torsion, the following form is assumed for the motion,

$$\begin{aligned} r &= R, \\ \theta &= \Theta + \psi(t)Z, \\ z &= Z. \end{aligned} \tag{5.54}$$

In the interest of clarity it is noted that $\psi(t)$ is the twist per unit length and is not related to the Helmholtz potential $\hat{\psi}$.

The deformation gradient with respect to the reference configuration is found to be,

$$\mathbf{F}_{\kappa_{\mathrm{r}}} = \begin{pmatrix} 1 & 0 & 0 \\ 0 & 1 & \psi \mathrm{R} \\ 0 & 0 & 1 \end{pmatrix}. \tag{5.55}$$

The velocity gradient with respect to the reference configuration is computed to be,

$$\mathbf{L}_{\kappa_{\mathrm{r}}} = \begin{pmatrix} 0 & -\dot{\psi}z & 0 \\ \dot{\psi}z & 0 & r\dot{\psi} \\ 0 & 0 & 0 \end{pmatrix}. \tag{5.56}$$

Solutions of the following form are sought,

$$\mathbf{V}_{\mathrm{e}}(R,t) = \begin{pmatrix} k_1 & 0 & 0 \\ 0 & \dfrac{k_2}{k_1} & \dfrac{k_3}{k_1} \\ 0 & \dfrac{k_3}{k_1} & \dfrac{k_1 + k_3^2}{k_1 k_2} \end{pmatrix}, \tag{5.57}$$

$$\mathbf{R}_{\mathrm{e}}(R,t) = \begin{pmatrix} 1 & 0 & 0 \\ 0 & \cos\alpha & -\sin\alpha \\ 0 & \sin\alpha & \cos\alpha \end{pmatrix}. \tag{5.58}$$

This is essentially a semi-inverse approach to determine the elastic response at each instant. There is no surety on the existence of a solution of this form. The constraint of incompressibility is met by the form assumed for $\mathbf{V}_{\mathrm{e}}$.

The evolution equation now becomes,

$$\begin{aligned} \mathbf{L}_{\kappa_{\mathrm{r}}}\mathbf{V}_{\mathrm{e}} - \dot{\mathbf{V}}_e - \mathbf{V}_{\mathrm{e}}\dot{\mathbf{R}}_e\mathbf{R}_{\mathrm{e}}{}^T &= \delta^{\frac{1-r}{2r-1}}\Bigg\{\frac{1}{\beta_0}\Bigg(\mu_1\mathbf{V}_{\mathrm{e}} + \frac{1}{2}\mu_2\mathbf{V}_{\mathrm{e}}\mathbf{n}^*\otimes\mathbf{n}^* + \frac{1}{2}\mu_3\mathbf{V}_{\mathrm{e}}\mathbf{m}^*\otimes\mathbf{m}^* \\ &\quad -(\frac{3\mu_1+\mu_2+\mu_3}{\mathbf{V}_{\mathrm{e}}^{-1}\cdot\mathbf{V}_{\mathrm{e}}^{-1}})\mathbf{V}_{\mathrm{e}}^{-1} \\ &\quad +\frac{1}{2}\mu_2\mathbf{n}^*\otimes\mathbf{V}_{\mathrm{e}}\mathbf{n}^* + \frac{1}{2}\mu_3\mathbf{m}^*\otimes\mathbf{V}_{\mathrm{e}}\mathbf{m}^*\Bigg) \\ &\quad +\frac{\mathbf{V}_{\mathrm{e}}}{\beta_1}\Bigg(\frac{1}{2}\mu_2\mathbf{V}_{\mathrm{e}}^2\mathbf{n}^*\otimes\mathbf{n}^* + \frac{1}{2}\mu_3\mathbf{V}_{\mathrm{e}}^2\mathbf{m}^*\otimes\mathbf{m}^* \\ &\quad -\frac{1}{2}\mu_2\mathbf{n}^*\otimes\mathbf{V}_{\mathrm{e}}^2\mathbf{n}^* - \frac{1}{2}\mu_3\mathbf{m}^*\otimes\mathbf{V}_{\mathrm{e}}^2\mathbf{m}^*\Bigg)\Bigg\}, \end{aligned} \tag{5.59}$$

where,

$$\mathbf{n}^* = \mathbf{R}_{\mathrm{e}}\mathbf{N} = \begin{pmatrix} 1 \\ 0 \\ 0 \end{pmatrix}, \tag{5.60}$$

$$\mathbf{m}^* = \mathbf{R}_{\mathrm{e}}\mathbf{M} = \begin{pmatrix} 0 \\ -\sin\alpha \\ \cos\alpha \end{pmatrix}, \tag{5.61}$$

Let,

$$\tilde{\Theta} = s(R,\Theta,Z,t), \tag{5.62}$$

where tilde identifies quantities in the natural configuration. It is now assumed that

the terms involving $\dot{s}$ are small enough to be ignored. This assumption leaves us with five equation for the evolution of k_1, k_2, k_3, α. Of these five equations only four are independent. The evolution equations are,

$$\frac{\mathrm{dk_1}}{\mathrm{dt}} = -\delta^{(\frac{1-r}{2r-1})}(\frac{\mu_1 k_1}{\beta_0} + \frac{\mu_2 k_1}{\beta_0} - \frac{\mu_4}{\beta_0 k_1}), \tag{5.63}$$

$$\begin{aligned}\frac{\mathrm{r}\dot{\psi}\mathrm{k_3}}{k_1} - \frac{\mathrm{d}}{\mathrm{dt}}(\frac{k_2}{k_1}) - \frac{\dot{\alpha}k_3}{k_1} &= \delta^{(\frac{1-r}{2r-1})}\Bigg(\frac{\mu_1 k_2}{\beta_0 k_1} + \frac{\mu_3}{\beta_0}(\frac{k_2}{k_1}\sin^2\alpha - \frac{\mathrm{k_3}}{\mathrm{k_1}}\sin\alpha\cos\alpha) \\ &\quad -\frac{\mu_4}{\beta_0}(\frac{k_1+k_3^2}{k_2}) \\ &\quad -\frac{k_3\mu_3}{k_1 2\beta_1}\Big\{(\frac{k_2k_3}{k_1^2} + \frac{k_3(k_1+k_3^2)}{k_1^2k_2})(\cos^2\alpha - \sin^2\alpha) \\ &\quad +(\frac{-(k_2^2+k_3^2)}{k_1^2} + \frac{k_3^2}{k_1^2} + \frac{(k_1+k_3^2)^2}{k_1^2k_2^2})\sin\alpha\cos\alpha\Big\}\Bigg),\end{aligned} \tag{5.64}$$

$$\begin{aligned}\frac{r\dot{\psi}(k_3^2+k_1)}{k_1k_2} - \frac{\mathrm{d}}{\mathrm{dt}}(\frac{k_3}{k_1}) + \frac{k_2}{k_1}\dot{\alpha} &= \delta^{(\frac{1-r}{2r-1})}\Bigg(\frac{\mu_1 k_3}{\beta_0 k_1} + \frac{\mu_4 k_3}{\beta_0} \\ &\quad +\frac{\mu_3}{2\beta_0}\Big(\frac{k_3}{k_1} - (\frac{k_2}{k_1} + \frac{k_3^2+k_1}{k_1k_2})\sin\alpha\cos\alpha\Big) \\ &\quad +\frac{\mu_3 k_2}{2\beta_1 k_1}\Big\{(\frac{k_2k_3}{k_1^2} + \frac{k_3(k_1+k_3^2)}{k_1^2k_2})(\cos^2\alpha - \sin^2\alpha) \\ &\quad +(\frac{k_3^2}{k_1^2} + \frac{(k_1+k_3^2)^2}{k_1^2k_2^2} - \frac{k_2^2+k_3^2}{k_1^2})\cos\alpha\sin\alpha\Big\}\Bigg),\end{aligned} \tag{5.65}$$

$$
\begin{aligned}
-\frac{\mathrm{d}}{\mathrm{dt}}(\frac{k_3}{k_1}) - \dot{\alpha}\frac{k_3^2+k_1}{k_1k_2} &= \delta^{(\frac{1-r}{2r-1})}\Bigg(\frac{\mu_1 k_3}{\beta_0 k_1} + \frac{\mu_4 k_3}{\beta_0} \\
&\quad + \frac{\mu_3}{2\beta_0}\Big(\frac{k_3}{k_1} - (\frac{k_3^2+k_1}{k_1k_2} + \frac{k_2}{k_1})\mathrm{cos}\alpha\mathrm{sin}\alpha\Big) \\
&\quad - \frac{\mu_3}{2\beta_1}(\frac{k_1+k_3^2}{k_1k_2})\Big\{(\frac{k_2k_3}{k_1^2} + \frac{k_3(k_1+k_3^2)}{k_1^2k_2})(\cos^2\alpha - \sin^2\alpha) \\
&\quad + (\frac{k_3^2}{k_1^2} + \frac{(k_1+k_3^2)^2}{k_1^2k_2^2} - \frac{k_2^2+k_3^2}{k_1^2})\mathrm{sin}\alpha\mathrm{cos}\alpha\Big\}\Bigg). \qquad (5.66)
\end{aligned}
$$

where $\frac{\mathrm{d}}{\mathrm{dt}}$ denotes the material time derivative. The initial conditions for these equations are given by,

$$
\begin{aligned}
k_1(R, t=0) &= 1, \qquad (5.67)\\
k_2(R, t=0) &= 1, \qquad (5.68)\\
k_3(R, t=0) &= 0, \qquad (5.69)\\
\alpha(R, t=0) &= 0. \qquad (5.70)
\end{aligned}
$$

The stress $\mathbf{T}$ is given by,

$$
\mathbf{T} = \begin{pmatrix} -\mathrm{p} + \mu_1\mathrm{k}_1^2 + \mu_2\mathrm{k}_1^2 & 0 & 0 \\ 0 & \mathrm{T}_{\theta\theta} & \mathrm{T}_{\theta\mathrm{r}} \\ 0 & \mathrm{T}_{\mathrm{r}\theta} & \mathrm{T}_{\mathrm{zz}} \end{pmatrix}, \qquad (5.71)
$$

where,

$$
\begin{aligned}
\mathrm{T}_{\theta\theta} &= -\mathrm{p} + \mu_1(\frac{\mathrm{k}_2^2}{\mathrm{k}_1^2} + \frac{\mathrm{k}_3^2}{\mathrm{k}_1^2}) + \mu_3(\frac{-\mathrm{k}_2\mathrm{sin}\alpha}{\mathrm{k}_1} + \frac{\mathrm{k}_3\mathrm{cos}\alpha}{\mathrm{k}_1})^2, \qquad (5.72)\\
\mathrm{T}_{r\theta} &= \mathrm{T}_{\theta r} \\
&= \mu_1\Big(\frac{k_2k_3}{k_1^2} + \frac{k_3(k_1+k_3^2)}{k_1^2k_2}\Big) \\
&\quad + \mu_3(-\frac{k_2}{k_1}\mathrm{sin}\alpha + \frac{\mathrm{k}_3}{\mathrm{k}_1}\mathrm{cos}\alpha)(-\frac{\mathrm{k}_3}{\mathrm{k}_1}\mathrm{sin}\alpha + \frac{\mathrm{k}_1+\mathrm{k}_3^2}{\mathrm{k}_1\mathrm{k}_2}\mathrm{cos}\alpha), \qquad (5.73)\\
\mathrm{T}_{zz} &= -\mathrm{p} + \mu_1\Big(\frac{\mathrm{k}_3^2}{\mathrm{k}_1^2} + (\frac{\mathrm{k}_1+\mathrm{k}_3^2}{\mathrm{k}_1\mathrm{k}_2})^2\Big) + \mu_3(\frac{-\mathrm{k}_3}{\mathrm{k}_1}\mathrm{sin}\alpha + \frac{\mathrm{k}_1+\mathrm{k}_3^2}{\mathrm{k}_1\mathrm{k}_2}\mathrm{cos}\alpha)^2. \qquad (5.74)
\end{aligned}
$$

On neglecting body forces and interial terms, the equilibrium equation yields,

$$\mathrm{div}\mathbf{T} = 0. \tag{5.75}$$

i.e.,

$$\frac{\partial T_{rr}}{\partial r} + \frac{1}{r}(T_{rr} - T_{\theta\theta}) = 0. \tag{5.76}$$

i.e,

$$\frac{\partial}{\partial R}(-p + \mu_1 k_1^2 + \mu_2 k_1^2)$$
$$+\frac{1}{R}\Big((\mu_1+\mu_2)k_1^2 - \mu_1(\frac{k_2^2}{k_1^2}+\frac{k_3^2}{k_1^2}) - \mu_3(-\frac{k_2}{k_1}\mathrm{sin}\alpha + \frac{\mathrm{k_3}}{\mathrm{k_1}}\mathrm{cos}\alpha)^2\Big) = 0. \tag{5.77}$$

The boundary conditions for this equation is the traction free condition on the outer surface of the cylinder.

$$\mathrm{T}_{rr}|_{R=R_{outer}} = 0. \tag{5.78}$$

i.e.,

$$\Big(-p + \mu_1 k_1^2 + \mu_2 k_1^2\Big)|_{R=R_{outer}} = 0. \tag{5.79}$$

The evolution and momentum equations are solved (Eq. 5.63, Eq. 5.64, Eq. 5.65, Eq. 5.66 and Eq. 5.77) with the initial and boundary conditions to obtain k_1, k_2, k_3 and α.

The normal force is given by,

$$N = \int_o^R 2\pi R\Big(-p+\mu_1\Big\{\frac{k_3^2}{k_1^2}+(\frac{k_1+k_3^2}{k_1k_2})^2\Big\}+\mu_3(-\frac{k_3}{k_1}\mathrm{sin}\alpha+\frac{\mathrm{k_1}+\mathrm{k_3^2}}{\mathrm{k_1k_2}}\mathrm{cos}\alpha)^2\Big)\mathrm{dR}. \tag{5.80}$$

The torque is given by,

$$\begin{aligned} M &= \int_0^R 2\pi R^2\Big(\mu_1(\frac{k_2k_3}{k_1^2}+\frac{k_3(k_1+k_3^2)}{k_1^2k_2}) \\ &\quad +\mu_3(-\frac{k_2}{k_1}\mathrm{sin}\alpha+\frac{\mathrm{k_3}}{\mathrm{k_1}}\mathrm{cos}\alpha)(\frac{-\mathrm{k3}}{\mathrm{k1}}\mathrm{sin}\alpha+\frac{\mathrm{k_1}+\mathrm{k_3^2}}{\mathrm{k_1k_2}}\mathrm{cos}\alpha)\Big)\mathrm{dR}. \end{aligned} \tag{5.81}$$

The comparison of experimental results to theoretical prediction is provided in Figures 5 through 34. The values of the model parameters used in the theoretical predictions are tabulated in Table IX. In all cases here $\hat{\mu}_3$, $\hat{\mu}_5$ and $\hat{\mu}_6$ are set to 0.0.

D. Parametric Study of Model

Typically asphalt bound mixtures in the laboratory are subjected to stains of the order of .04 to 0.4%, i.e 400 to 4000 microstrain (see for example [93]). The strain measure widely used in literature pertaining to asphalt bound materials is the linearized strain (There are many different strain measures, see for example [94]).

In the experimental study carried out here, the strains encountered were much higher than this. The linearized strain calculated as (rϕ/l) were of the order of 5%. Thus the strains attained were high enough to have damaged the material. This is a possible explanation for the discrepancy between the experimental results and the theoretical prediction of torque values immediately after unloading (the long-term fits are quite good). A large volume of literature exists on damage within the context of asphalt bound mixtures (see for example [27]) and the mechanics of different kinds of materials. (See for example [95],[96],[97],[98])

To further investigate this, a parametric study was carried out to see the effect of small strains on the mix response. The material moduli used for the parametric study were, $\hat{\mu}_1 = 1.2 \times 10^7$, $\hat{\mu}_2 = 1 \times 10^6$, q = 1, r = 0.76, $\beta_0 = 6 \times 10^{10}$ and $\beta_1 = 6 \times 10^{10}$. The results are summarized in Figures 36 through 43.

Table IX. Parameter values used for the different materials. The units of μ are N/m^2 and the units of $(\mu/\beta)^{(r)/(2r-1)}$ are s^{-1}

Material	**Parameter**
Limestone 7.5% air voids, Asp No 8 (PG64-22)	$\omega = \tau = 9 \times 10^{-3}$ $\hat{\mu}_1 = 3 \times 10^{11}$ $\hat{\mu}_2 = 1.5 \times 10^{8}$ $\beta_0 = \beta_1 = 8.5 \times 10^{10}$ q = 3 r = 0.85
Limestone 9.5% air voids, Asp No 8 (PG64-22)	$\omega = \tau = 9 \times 10^{-3}$ $\hat{\mu}_1 = 2.3 \times 10^{11}$ $\hat{\mu}_2 = 0.9 \times 10^{8}$ $\beta_0 = \beta_1 = 7.8 \times 10^{10}$ q = 3 r = 0.85
Hydrated Lime 7.5% air voids, Asp No 8 (PG64-22)	$\omega = \tau = 9 \times 10^{-3}$ $\hat{\mu}_1 = 3 \times 10^{11}$

Table IX. Continued.

Material	**Parameter**
	$\hat{\mu}_2 = 1.3 \times 10^8$ $\beta_0 = \beta_1 = 8 \times 10^{10}$ q = 3 r = 0.85
20-30 Sand and Pure Asphalt, Asp No 8 (PG64-22)	$\omega = \tau = 9 \times 10^{-3}$ $\hat{\mu}_1 = 2.2 \times 10^{11}$ $\hat{\mu}_2 = 0.8 \times 10^8$ $\beta_0 = \beta_1 = 5.5 \times 10^{10}$ q = 3 r = 0.85
Pure Asphalt,Asp No 1, AC-30	$\omega = \tau = 9 \times 10^{-3}$ $\hat{\mu}_1 = 35 \times 10^{12}$ $\hat{\mu}_2 = 9.6 \times 10^7$ $\beta_0 = \beta_1 = 1.5 \times 10^{11}$ q = 4 r = 0.84
Pure Asphalt, Asp No 2, AC-30	$\omega = \tau = 9 \times 10^{-3}$ $\hat{\mu}_1 = 42 \times 10^{12}$ $\hat{\mu}_2 = 1.1 \times 10^8$

Table IX. Continued.

Material	**Parameter**
	$\beta_0 = \beta_1 = 2.0 \times 10^{11}$ q = 4 r = 0.84
Pure Asphalt, Asp No 3, AC-30	$\omega = \tau = 9 \times 10^{-3}$ $\hat{\mu}_1 = 42 \times 10^{12}$ $\hat{\mu}_2 = 1.1 \times 10^{8}$ $\beta_0 = \beta_1 = 2.6 \times 10^{11}$ q = 4 r = 0.84
ASTM graded sand, Pure Asphalt, Asp No 8, PG64-22	$\omega = \tau = 9 \times 10^{-3}$ $\hat{\mu}_1 = 4.2 \times 10^{11}$ $\hat{\mu}_2 = 1.2 \times 10^{8}$ $\beta_0 = \beta_1 = 9 \times 10^{10}$ q = 3 r = 0.85
Pure Asphalt Asp No 5, PG64-22	$\omega = \tau = 9 \times 10^{-3}$ $\hat{\mu}_1 = 1.4 \times 10^{11}$ $\hat{\mu}_2 = 1.0 \times 10^{8}$

Table IX. Continued.

Material	**Parameter**
	$\beta_0 = \beta_1 = 1.35 \times 10^{11}$ q = 3 r = 0.9
Pure Asphalt, Asp No 7, PG64-22	$\omega = \tau = 9 \times 10^{-3}$ $\hat{\mu}_1 = 1.4 \times 10^{11}$ $\hat{\mu}_2 = 0.8 \times 10^{8}$ $\beta_0 = \beta_1 = 1.5 \times 10^{11}$ q = 3 r = 0.9
Pure Asphalt, Asp No 6, PG64-22	$\omega = \tau = 9 \times 10^{-3}$ $\hat{\mu}_1 = 1.4 \times 10^{11}$ $\hat{\mu}_2 = 0.9 \times 10^{8}$ $\beta_0 = \beta_1 = 1.3 \times 10^{11}$ q = 3 r = 0.9
Asp No 3, AC-30 with HL	$\omega = \tau = 9 \times 10^{-3}$ $\hat{\mu}_1 = 50 \times 10^{12}$ $\hat{\mu}_2 = 1.3 \times 10^{8}$ $\beta_0 = \beta_1 = 3.5 \times 10^{11}$

Table IX. Continued.

Material	**Parameter**
	q = 4 r = 0.84
Asp No 3, AC-30 with LS	$\omega = \tau = 9 \times 10^{-3}$ $\hat{\mu}_1 = 42 \times 10^{12}$ $\hat{\mu}_2 = 1.25 \times 10^{8}$ $\beta_0 = \beta_1 = 3.2 \times 10^{11}$ q = 4 r = 0.84
Asp No 4, AC-30 with HL	$\omega = \tau = 9 \times 10^{-3}$ $\hat{\mu}_1 = 44 \times 10^{12}$ $\hat{\mu}_2 = 1.3 \times 10^{8}$ $\beta_0 = \beta_1 = 2.5 \times 10^{11}$ q = 4 r = 0.84
Asp No 4, AC-30 with LS	$\omega = \tau = 9 \times 10^{-3}$ $\hat{\mu}_1 = 46 \times 10^{12}$ $\hat{\mu}_2 = 1.15 \times 10^{8}$ $\beta_0 = \beta_1 = 3.2 \times 10^{11}$ q = 4

Table IX. Continued.

Material	**Parameter**
	r = 0.84
Asp No 2, AC-30 with LS	$\omega = \tau = 9 \times 10^{-3}$ $\hat{\mu}_1 = 44 \times 10^{12}$ $\hat{\mu}_2 = 1.15 \times 10^{8}$ $\beta_0 = \beta_1 = 2.3 \times 10^{11}$ q = 4 r = 0.84
Asp No 2, AC-30 with HL	$\omega = \tau = 9 \times 10^{-3}$ $\hat{\mu}_1 = 44 \times 10^{12}$ $\hat{\mu}_2 = 1.3 \times 10^{8}$ $\beta_0 = \beta_1 = 2.1 \times 10^{11}$ q = 4 r = 0.84
Asp No 1, AC-30 with LS	$\omega = \tau = 9 \times 10^{-3}$ $\hat{\mu}_1 = 46 \times 10^{12}$ $\hat{\mu}_2 = 1.35 \times 10^{8}$ $\beta_0 = \beta_1 = 3.2 \times 10^{11}$ q = 4 r = 0.84

Table IX. Continued.

Material	**Parameter**
Asp No 1, AC-30 with HL	$\omega = \tau = 9 \times 10^{-3}$ $\hat{\mu}_1 = 40 \times 10^{12}$ $\hat{\mu}_2 = 1.2 \times 10^{8}$ $\beta_0 = \beta_1 = 1.8 \times 10^{11}$ q = 4 r = 0.84

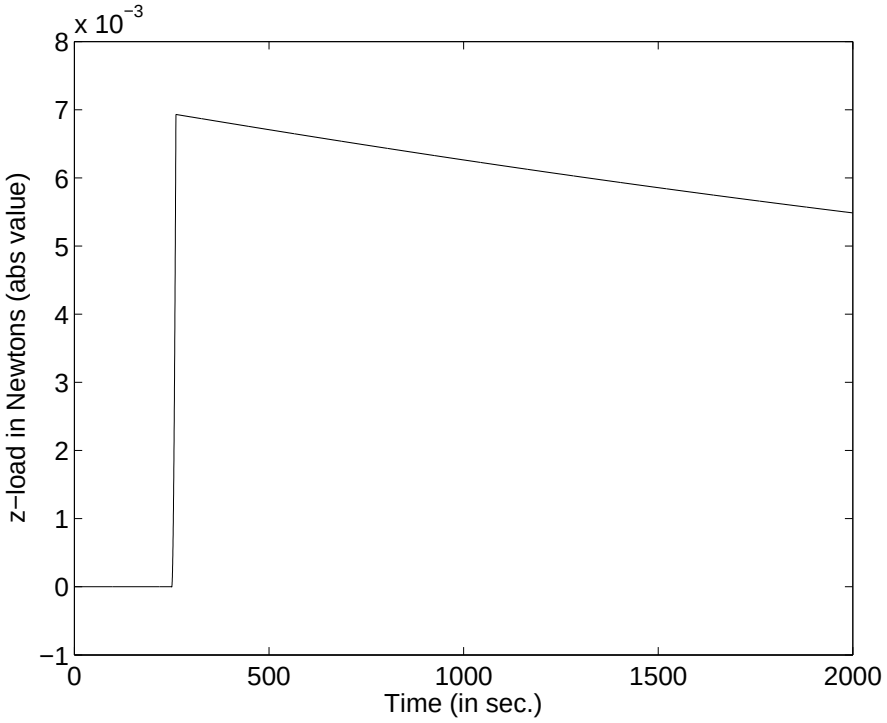

Fig. 36. Normal force for loading rate of 200 minutes per rev and duration of loading being 11 seconds. Linearized strain $\approx 0.2\%$.

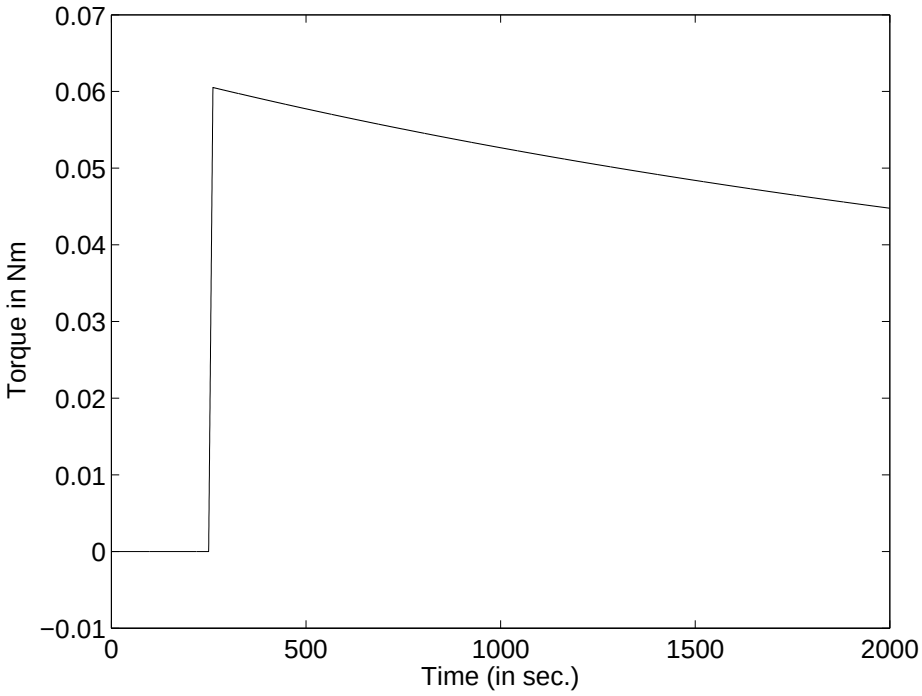

Fig. 37. Torque for loading rate of 200 minutes per rev and duration of loading being 11 seconds. Linearized strain $\approx 0.2\%$.

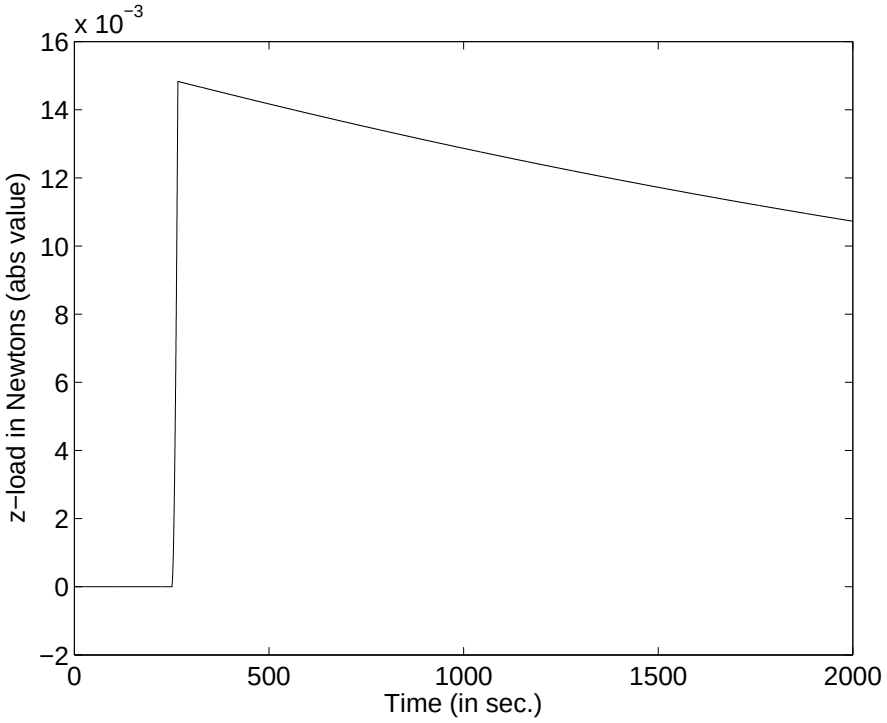

Fig. 38. Normal force for loading rate of 200 minutes per rev and duration of loading being 16 seconds. Linearized strain $\approx 0.3\%$.

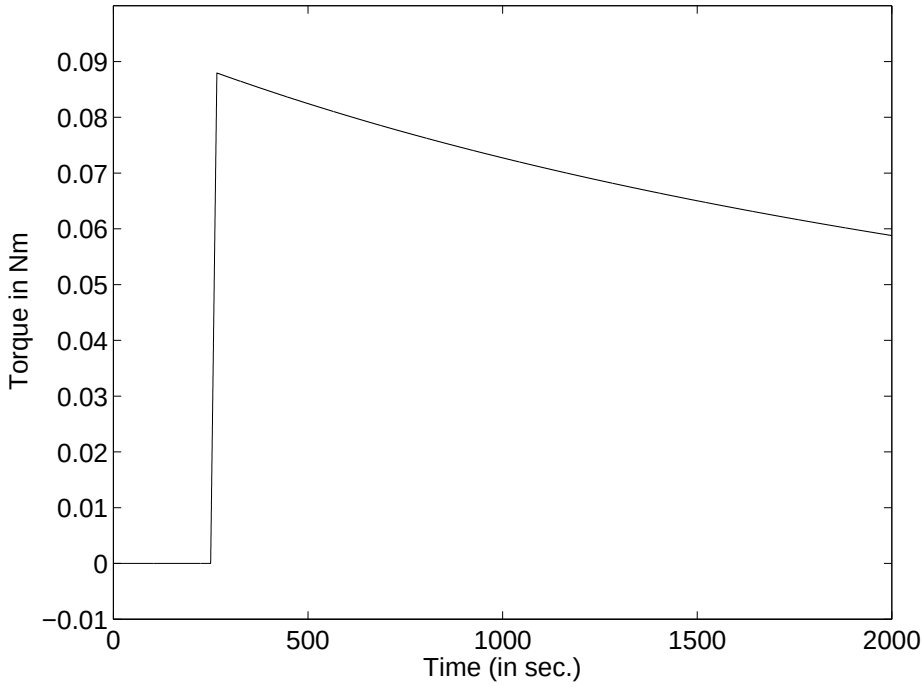

Fig. 39. Torque for loading rate of 200 minutes per rev and duration of loading being 16 seconds. Linearized strain $\approx 0.3\%$.

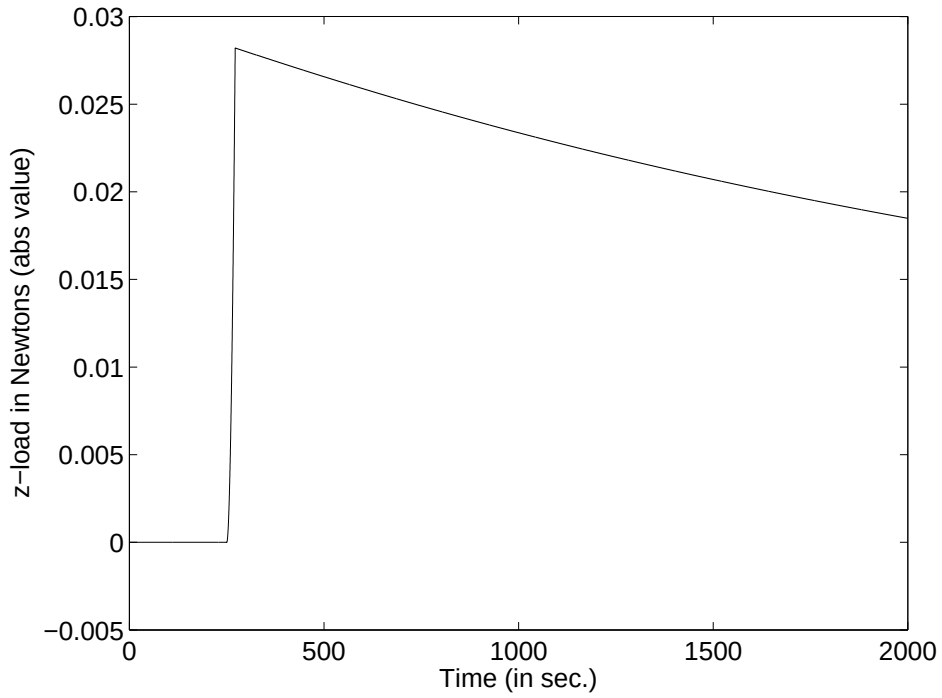

Fig. 40. Normal force for loading rate of 200 minutes per rev and duration of loading being 22 seconds. Linearized strain $\approx 0.4\%$.

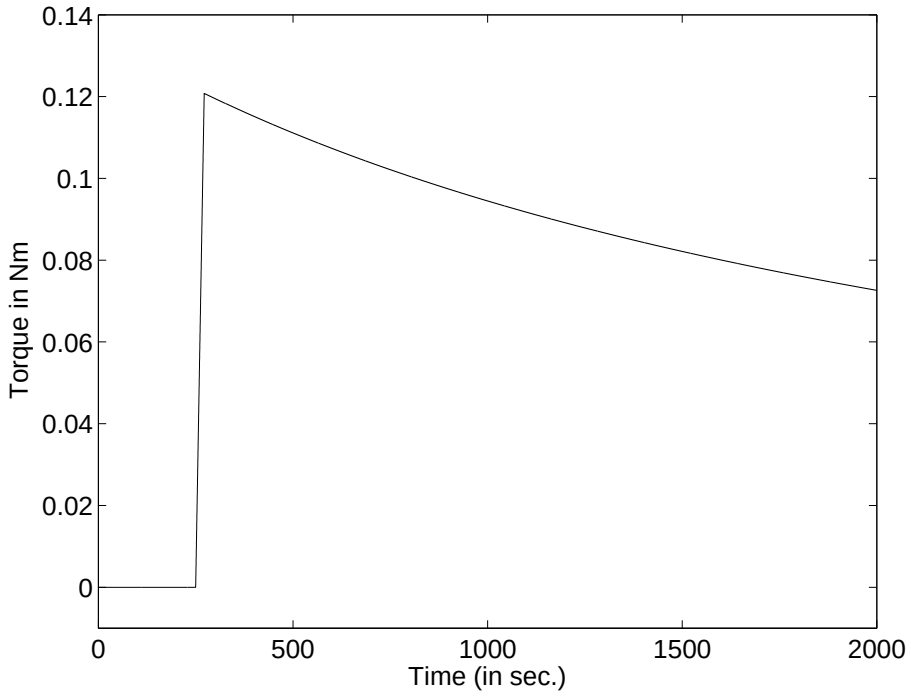

Fig. 41. Torque for loading rate of 200 minutes per rev and duration of loading being 22 seconds. Linearized strain $\approx 0.4\%$.

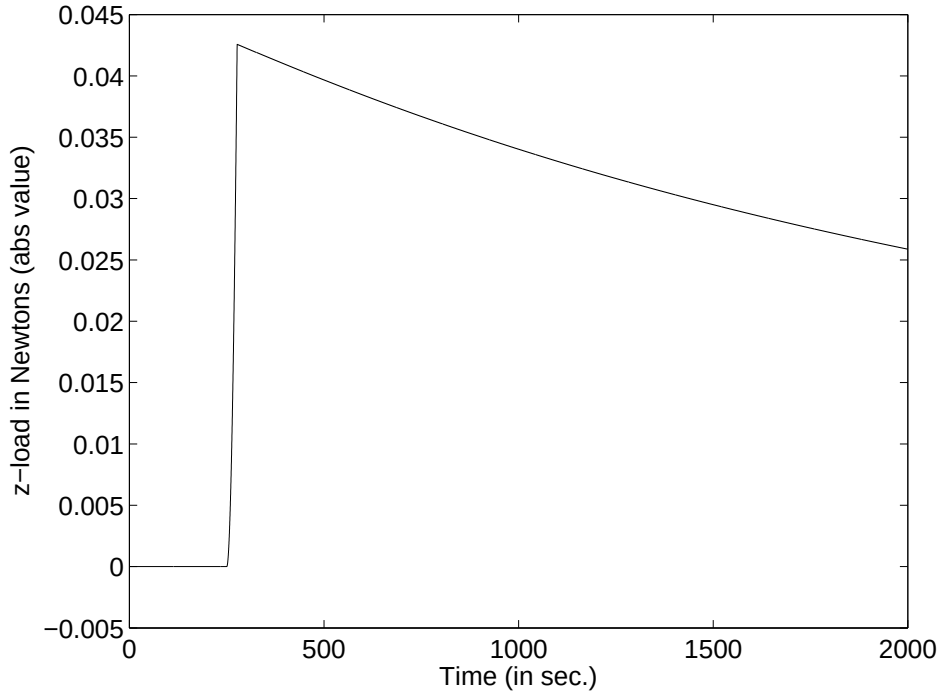

Fig. 42. Normal force for loading rate of 200 minutes per rev and duration of loading being 27 seconds. Linearized strain $\approx 0.5\%$.

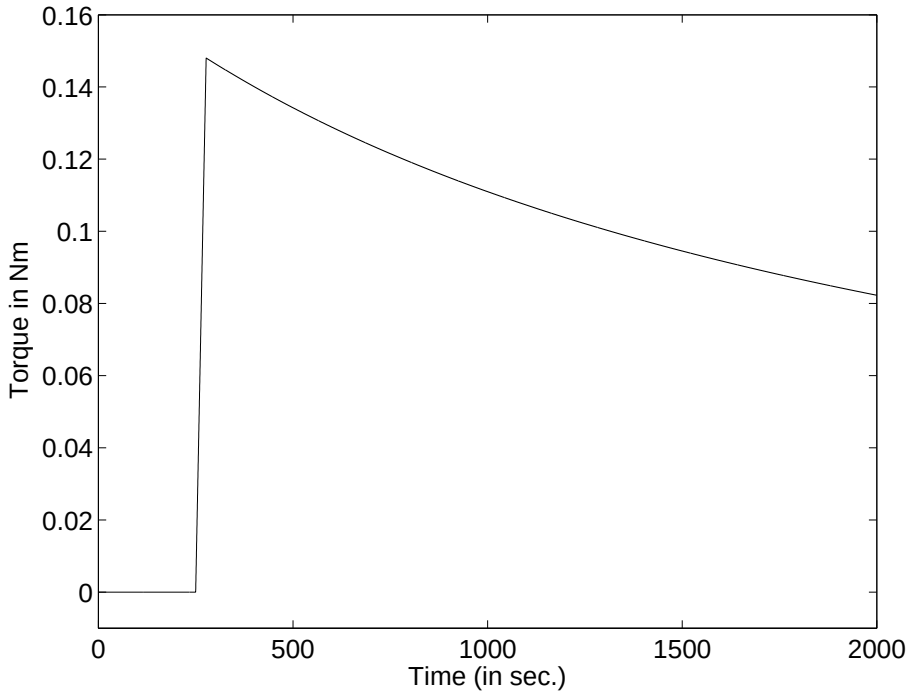

Fig. 43. Torque for loading rate of 200 minutes per rev and duration of loading being 27 seconds. Linearized strain $\approx 0.5\%$.

CHAPTER VI

CONCLUSION

A. Summary

The experimental results clearly showed that asphalt bound mixtures generate significant normal forces even at low rotation rates. The fact that asphalt mixtures show distinct non-linear behavior is no surprise but the fact that even at very low rotation rates, significant amount of normal forces are generated underlines the high non-linearity of the material response. It was also observed that asphalts from different sources but graded the same, behaved differently. The addition of fillers and the reduction of air voids caused the specimens to become stiffer. The effect of gradation of the sand on the normal stress generation is pronounced and along expected lines.

The anisotropic model that was developed was able to predict qualitative trends and obtain reasonable quantitative agreement. The magnitude of the final strain that was induced in specimens in the course of the experiments may have been large enough to damage them. This has to be taken into account in the modeling to obtain better fits.

B. Directions for Future Work

The scope for future work is virtually limitless. Asphalt concrete is an extremely complicated material. Each of its constituents by themselves have defied easy characterization. A model that accounts for damage could be developed. The model that has been developed here can be extended to a constrained mixture model paying cognizance to the fact that the asphalt mastic and aggregate matrix have distinct relaxation and load bearing mechanisms. The constraint of incompressibility could

also be relaxed to obtain a more realistic model. The air void distribution also needs to be taken into account. The model could also be modified to allow for a transition to a viscoelastic solid type response as the temperature drops. The interaction between asphalt and aggregates is a entropy producing process and this also needs to be factored in.

The number of problems arising out of inadequate understanding of asphalt concrete behavior are many. Among these are the problem of aging (including cracking and healing), quantification of the compaction process and fatigue life prediction. The design of pavements could also reap great benefits from successful modeling efforts.

REFERENCES

[1] J. M. Krishnan and K. R. Rajagopal, "Review of the uses and modeling of bitumen from ancient to modern times," *Applied Mechanics Review*, vol. 56, pp. 149–214, 2004.

[2] R. J. Forbes, *Notes on the History of Ancient Roads and Their Construction*. Amsterdam: N.V. Noord-Hollandsche Uitgevers-Mij, 1934.

[3] A. C. Hughes, W. G. Adam, and F. J. E. China, *Tar Roads*. London: Edward Arnold & Co, 1938.

[4] J. Read and D. Whiteoak, *The Shell Bitumen Handbook*, 5th ed. London, United Kingdom: Shell Bitumen, 2003.

[5] FHA, "2002 status of the nation's highways, bridges and transit: Conditions and performance," Report to Congress FHWA-PL-03-003, U.S. Department of Transportation, Federal Highway Administration, Washington, DC, 2003.

[6] EAPA, *Asphalt in Figures 2003*. Breukelen, The Netherlands: European Asphalt Pavement Association, 2004.

[7] D. Lesueur and D. N. Little, "Effect of hydrated lime on rheology, fracture, and aging of bitumen," *Transportation Research Record*, vol. 1661, pp. 93–105, 1999.

[8] L. S. Johansson, J. Branthaver, and R. Robertson, "A study of rheological properties of lime treated paving asphalts aged at 60C in a pressure aging vessel," *Fuel Science and Technology International*, vol. 13, pp. 1317–1343, 1995.

[9] V. P. Puzinauskas, "Influence of mineral aggregate structure on properties of asphalt paving mixtures," *Highway Research Record*, vol. 51, pp. 1–18, 1964.

[10] K. R. Rajagopal, "Multiple configurations in continuum mechanics," University of Pittsburgh, Reports of the Institute for Computational and Applied Mechanics 6, 1995.

[11] A. E. Green and P. M. Naghdi, "On thermodynamics and the nature of the second law," *Proceedings of the Royal Society of London, Series A*, vol. 357, pp. 253–270, 1977.

[12] K. R. Rajagopal and A. R. Srinivasa, "A thermodynamic frame work for rate type fluid models," *Journal of Non-Newtonian Fluid Mechanics*, vol. 88, pp. 207–227, 2000.

[13] K. R. Rajagopal and L. Tao, "Modeling of the microwave drying process of aqueous dielectrics," *Zeitschrift für angewandte Mathematik und Physik*, vol. 53, pp. 923–948, 2002.

[14] W. Noll, "A mathematical theory of the mechanical behavior of continuous media," *Archives for Rational Mechanics and Analysis*, vol. 2, pp. 197–226, 1958.

[15] C. Eckart, "The thermodynamics of irreversible processes iv, the theory of elasticity and anelasticity," *Physical Review*, vol. 73, pp. 373–382, 1948.

[16] E. T. Harrington, R. B. Leahy, and J. S. Youtcheff, "The superpave mix design system manual of specifications, test methods, and practices," SHRP Report (Strategic Highway Research Program) SHRP-A-379, National Research Council, Washington, DC, 1994.

[17] M. W. Witczak, K. Kaloush, T. Pellinen, M. El-Basyouny, and H. L. Quintus, "Simple performance test for superpave mix design," NCHRP Report (National Cooperative Highway Research Program) 465, Transportation Research Board, Washington, DC, 2002.

[18] A. R. Lee and A. H. D. Markwick, "The mechanical properties of bituminous surfacing materials under constant stress," *Journal of Society of Chemical Industry*, vol. 56, pp. 146–156, 1937.

[19] L. Nijboer, *Plasticity as a Factor in the Design of Dense Bituminous Road Carpets*. Amsterdam: Elsevier, 1948.

[20] R. N. J. Saal, "Physical properties of asphaltic bitumen: Rheological properties," in *The Properties of Asphaltic Bitumen*, J. Pfeiffer, Ed. Amsterdam, The Netherlands: Elsevier, 1950, pp. 49–76.

[21] K. E. Secor and C. L. Monismith, "Viscoelastic properties of asphalt concrete," *Highway Research Board Proceedings*, vol. 41, pp. 299–320, 1962.

[22] C. Pagen, "Rhelogical response of bituminous concrete," *Highway Research Record*, vol. 67, pp. 1–26, 1965.

[23] F. Moavenzadeh and J. Soussou, "Viscoelastic constitutive equations for sand-asphalt mixture," *Highway Research Record*, vol. 256, pp. 36–52, 1968.

[24] M. Perl, J. Uzan, and A. Sides, "Visco-elastic-plastic constitutive law for a bituminous mixture under repeated loading," *Transportation Research Record*, vol. 911, pp. 20–27, 1983.

[25] Y. Kim and D. N. Little, "One-dimensional constitutive modeling of asphalt concrete," *Journal of Engineering Mechanics*, vol. 116, pp. 751–772, 1990.

[26] H. J. Lee, J. S. Daniel, and Y. R. Kim, "Continuum damage mechanics based fatigue model of asphalt concrete," *Journal of Materials in Civil Engineering*, vol. 12, pp. 105–112, 2000.

[27] N. H. Gibson, C. W. Schwartz, R. A. Schapery, and M. W. Witczak, "Viscoelastic, viscoplastic, and damage modeling of asphalt concrete in unconfined compression," *Transportation Research Record*, vol. 1860, pp. 3–15, 2003.

[28] E. Masad, L. Tashman, D. Little, and H. Zbib, "Viscoplastic modeling of asphalt mixes with the effects of anisotropy, damage and aggregate characteristics," *Mechanics of Materials*, vol. 37, pp. 1242–1256, 2005.

[29] J. M. Krishnan and C. L. Rao, "Air voids reduction of asphalt concrete using mixture theory," *International Journal of Engineering Science*, vol. 38, pp. 1331–1354, 2000.

[30] R. A. Schapery, "Correspondence principles and a generalized j integral for large defromation and fracture-analysis of viscoelastic media," *International Journal of Fracture*, vol. 25, pp. 195–223, 1984.

[31] K. R. Rajagopal and A. R. Srinivasa, "A note on a correspondence principle in nonlinear viscoelastic materials," *International Journal of Fracture*, vol. 131, pp. 47–52, 2005.

[32] R. B. Girdler, "Constitution of asphaltenes and related studies," *Proceedings of the Association of Asphalt Paving Technologists*, vol. 34, pp. 45–79, 1965.

[33] F. J. Nellensteyn, "The constitution of asphalt," *Journal of the Institution of Petroleum Technologists*, vol. 10, pp. 311–325, 1924.

[34] J. P. Pfeiffer and R. Saal, "Asphaltic bitumen as colloid system," *Journal of Physical Chemistry*, vol. 44, pp. 139–149, 1940.

[35] J. Petersen, "Chemical composition of asphalt as related to asphalt durability: State of the art," *Transportation Research Record*, vol. 999, pp. 13–30, 1984.

[36] F. T. Trouton and E. S. Andrews, "On the viscosity of pitch-like substances," *Proceedings of the Physical Society of London*, vol. 19, pp. 47–57, 1903.

[37] V. C. Janoo, "Quantification of shape, angularity and surface texture of base course materials," Special Report 98-1, U.S. Army Corps of Engineers, Hanover, NH, 1998.

[38] G. Lees, "A new method for determining the angularity of particles," *Sedimentology*, vol. 3, pp. 2–21, 1964.

[39] H. Wadell, "Sphericity and roundness of rock particles," *Journal of Geology*, vol. 41, pp. 310–331, 1933.

[40] W. C. Krumbein, "The effects of abrasion on the size, shape and roundness of rock fragments," *Journal of Geology*, vol. 49, pp. 482–520, 1941.

[41] C. Chandan, K. Sivakumar, E. Masad, and T. Fletcher, "Application of imaging techniques to geometry analysis of aggregate particles," *Journal of Computing in Civil Engineering*, vol. 18, pp. 75–82, 2004.

[42] D. G. Tunnicliff, "Binding effects of mineral filler," *Proceedings of the Association of Asphalt Paving Technologists*, vol. 36, pp. 114–156, 1967.

[43] C. Richardson, *The Modern Asphalt Pavement*, 2nd ed. New York: John Wiley and Sons Inc, 1908.

[44] J. S. Miller and R. N. Traxler, "Some of the fundamental physical characteristics of mineral filler intended for asphalt paving mixtures," *Proceedings of the Association of Asphalt Paving Technologists*, vol. 3, pp. 53–63, 1932.

[45] R. N. Traxler and J. S. Miller, "Mineral powders, their physical properties and stabilizing effects," *Proceedings of the Association of Asphalt Paving Technologists*, vol. 7, pp. 112–123, 1936.

[46] R. N. Traxler, "The evaluation of mineral powders as fillers for asphalts," *Proceedings of the Association of Asphalt Paving Technologists*, vol. 8, pp. 60–67, 1937.

[47] J. G. Mitchell and A. R. Lee, "The evaluation of fillers for tar and other bituminous surfacings," *Journal of the Society of Chemical Industry*, vol. 58, pp. 299–306, 1939.

[48] P. J. Rigden, "The use of fillers in bituminous road surfacings. A study of filler-binder systems in relation to filler characteristics," *Journal of the Society of Chemical Industry*, vol. 66, pp. 299–309, 1947.

[49] D. G. Tunnicliff, "A review of mineral filler," *Proceedings of the Association of Asphalt Paving Technologists*, vol. 31, pp. 118–150, 1962.

[50] W. B. Warden, S. B. Hudson, and H. C. Howell, "Evaluation of mineral fillers in terms of practical pavement performance," *Proceedings of the Association of Asphalt Paving Technologists*, vol. 28, pp. 316–352, 1959.

[51] D. A. Anderson and W. H. Goetz, "Mechanical behavior and reinforcement of mineral filler-asphalt mixtures," *Proceedings of the Association of Asphalt Paving Technologists*, vol. 42, pp. 37–66, 1973.

[52] P. J. Rigden, "The rheology of non-aqueous suspensions," Road Research Technical Paper 28, Road Research Laboratory, London, UK: Her Majesty's Stationary Office, 1954.

[53] J. Craus, I. Ishai, and A. Sides, "Some physico-chemical aspects of the effect and the role of filler in bituminous paving mixtures," *Proceedings of the Association of Asphalt Paving Technologists*, vol. 47, pp. 558–588, 1978.

[54] J. C. Petersen, H. Plancher, and P. Harnsberger, "Lime treatment of asphalt to reduce age hardening and improve flow properties," *Proceedings of the Association of Asphalt Paving Technologists*, vol. 56, pp. 632–653, 1987.

[55] H. Plancher, E. L. Green, and J. C. Petersen, "Reduction of oxidative hardening of asphalts by treatment with hydrated lime- a mechanistic study," *Proceedings of the Association of Asphalt Paving Technologists*, vol. 45, pp. 1–24, 1976.

[56] N. Shashidhar and P. Romero, "Factors affecting the stiffening potential of mineral fillers," *Transportation Research Record*, vol. 1638, pp. 94–100, 1998.

[57] N. Shashidhar, S. P. Needham, B. H. Chollar, and P. Romero, "Prediction of the performance of mineral fillers in stone matrix asphalt," *Proceedings of the Association of Asphalt Paving Technologists*, vol. 68, pp. 222–251, 1999.

[58] A. Kavussi and R. G. Hicks, "Properties of bituminous mixtures containing different fillers," *Proceedings of the Association of Asphalt Paving Technologists*, vol. 66, pp. 153–186, 1997.

[59] L. A. Cooley, M. Stroup-Gardiner, E. R. Brown, D. I. Hanson, and M. O. Fletcher, "Characterization of asphalt-filler mortars with superpave binder

tests," *Proceedings of the Association of Asphalt Paving Technologists*, vol. 67, pp. 42–65, 1998.

[60] J. H. Poynting, "On pressure perpendicular to the shear planes in finite pure shears, and on the lengthening of loaded wires when twisted," *Proceedings of the Royal Society of London*, vol. 82, pp. 546–559, 1909.

[61] K. Weissenberg, "A continuum theory of rheological phenomena," *Nature*, vol. 159, pp. 310–311, 1947.

[62] O. Reynolds, "On the dilatancy of media composed of rigid particles in contact. with experimental illustrations," *The London, Edinburgh, and Dublin Philosophical Magazine and Journal of Science*, vol. 20, no. 127, pp. 469–481, 1885.

[63] D. A. Anderson, Y. M. L. Hir, M. O. Marasteanu, J. P. Planche, D. Martin, and G. Gauthier, "Evaluation of fatigue criteria for asphalt binders," *Transportation Research Record*, vol. 1766, pp. 48–56, 2001.

[64] T. W. Kennedy, G. A. Huber, E. T. Harrington, R. J. Cominsky, C. S. Hughes, H. V. Quintus, and J. S. Moulthrop, "Superior performing asphalt pavements (superpave): The product of the SHRP," SHRP Report (Strategic Highway Research Program) SHRP-A-410, National Research Council, Washington, DC, 1994.

[65] J. Sousa, S. L. Weissman, J. L. Sackman, and C. L. Monismith, "Nonlinear elastic viscous with damage model to predict permanent deformation of asphalt concrete mixes," *Transportation Research Record*, vol. 1384, pp. 80–93, 1993.

[66] C. Truesdell and W. Noll, *Non-Linear Field Theories of Mechanics*. Berlin: Springer-Verlag, 1965.

[67] E. D. Barber, "Shear loads on pavements," in *International Conference on the Structural Design of Asphalt Pavements Proceedings*. Ann Arbor, MI: University of Michigan, 354–357, 1962.

[68] L. R. Kasula, J. M. Krishnan, K. R. Rajagopal, and D. N. Little, "Normal stress and stress relaxation data for sand asphalt undergoing torsional flow," *Mechanics Research Communications*, vol. 32, pp. 43–52, 2005.

[69] E. Hatschek, *The Viscosity of Liquids*. London: G. Bell and Sons Ltd., 1928.

[70] G. Barr, *A Monograph of Viscometry*. London: Oxford University Press, 1931.

[71] A. Dinsdale and F. Moore, *Viscosity and Its Measurement*. London: Chapman and Hall, 1962.

[72] K. R. Rajagopal, "Flow of viscoelastic fluids between rotating disks," *Theoretical and Computational Methods in Fluid Mechanics*, vol. 3, pp. 185–206, 1992.

[73] R. W. Penn and E. A. Kearsley, "The scaling law for finite torsion of elastic cylinders," *Transactions of the Society of Rheology*, vol. 20, pp. 227–238, 1976.

[74] C. R. Schulteisz and G. McKenna, "Nonlinear viscoelastic analysis of the torque, axial normal force, and volume change measured simultaneously in the national institute of standards and technology torsional dilatometer," *Journal of Rheology*, vol. 46, pp. 901–925, 2002.

[75] ASTM, "ASTM Standards 04.03, ASTM D2041, standard test method for theoretical maximum specific gravity and density of bituminous paving mixtures," Philadelphia, PA, pp. 182–189, 2004.

[76] J. R. Taylor, *An Introduction to Error Analysis, The Study of Uncertainties in Physical Measurements*. Mill Valley, CA: University Science Books, 1982.

[77] M. Neuilly and CETAMA, *Modeling and Estimation of Measurement Errors*. Hampshire, UK: Intercept, 1999.

[78] M. Pagano and K. Gauvreau, *Principles of Biostatistics*. Belmont, CA: Duxbury Press, 1992.

[79] G. W. Johnson, *LabVIEW® Graphical Programming - Practical Applications in Instrumentation and Control*, 2nd ed. New York: McGraw Hill, 1997.

[80] S. J. Kline and F. A. McClintock, "Describing uncertainities in single-sample experiments," *Mechanical Engineering*, vol. 75, pp. 3–8, 1953.

[81] J. M. Krishnan and K. R. Rajagopal, "On the mechanical behavior of asphalt," *Mechanics of Materials*, vol. 37, pp. 1085–1100, 2005.

[82] J. M. Krishnan, K. R. Rajagopal, E. Masad, and D. N. Little, "Thermomechanical framework for constitutive modeling of asphalt concrete," *International Journal of Geomechanics*, vol. 6, pp. 36–45, 2006.

[83] J. M. Krishnan and K. R. Rajagopal, "Triaxial testing and stress relaxation of asphalt concrete," *Mechanics of Materials*, vol. 36, pp. 849–864, 2004.

[84] H. Pradeep, J. M. Krishnan, K. R. Rajagopal, D. N. Little, and E. Masad, "Modelling constant displacement rate experiments of asphalt concrete using a thermodynamic framework," *International Journal of Pavement Engineering*, vol. 6, pp. 241–256, 2005.

[85] K. R. Rajagopal and A. R. Srinivasa, "Modeling anisotropic fluids within the framework of bodies with multiple natural configuration," *Journal of Non-Newtonian Fluid Mechanics*, vol. 99, pp. 109–124, 2001.

[86] ——, "Mechanics of the inelastic behavior of materials– Part I, theoretical underpinning," *International Journal of Plasticity*, vol. 14, pp. 945–967, 1998.

[87] ——, "Mechanics of the inelastic behavior of materials– Part II, inelastic response," *International Journal of Plasticity*, vol. 14, pp. 969–995, 1998.

[88] I. J. Rao and K. R. Rajagopal, "Phenomenological modeling of polymer crystallization using the notion of multiple natural configurations," *Interfaces and Free Boundaries*, vol. 2, pp. 73–94, 2000.

[89] ——, "A study of strain-induced crystallization of polymers," *International Journal of Solids and Structures*, vol. 38, pp. 1149–1167, 2001.

[90] K. Kannan, I. J. Rao, and K. R. Rajagopal, "A themomechanical framework for the glass transition phenomenon in certain polymers and its applications to fiber spinning," *Journal of Rheology*, vol. 46, pp. 977–999, 2002.

[91] S. C. Prasad, K. R. Rajagopal, and I. J. Rao, "A continuum model for the anisotropic creep of single crystal nickel-based superalloys," *Acta Materialia*, vol. 54, pp. 1487–1500, 2006.

[92] E. Masad, L. Tashman, N. Somedavan, and D. Little, "Micromechanics based analysis of stiffness anisotropy in asphalt mixtures," *Journal of Materials in Civil Engineering*, vol. 14, pp. 347–383, 2002.

[93] C. L. Monismith and K. E. Secor, "Viscoelastic behavior of asphalt concrete pavements," in *International Conference on the Structural Design of Asphalt Pavements Proceedings*. Ann Arbor, MI: University of Michigan, 476–498, 1962.

[94] R. L. Fosdick and A. S. Wineman, "On general measures of deformation," *Acta Mechanica*, vol. 6, pp. 275–295, 1968.

[95] A. S. Wineman, "Some comments on the mechanical response of elastomers undergoing scission and healing at elevated temperatures," *Mathematics and Mechanics of Solids*, vol. 10, pp. 673–689, 2005.

[96] A. Wineman and K. Rajagopal, "On a constitutive theory for materials undergoing microstructural changes," *Archives of Mechanics*, vol. 42, pp. 53–74, 1990.

[97] K. Ha and R. A. Schapery, "A three-dimensional viscoelastic constitutive model for particulate composites with growing damage and its experimental validation," *International Journal of Solids and Structures*, vol. 35, pp. 3497–3517, 1998.

[98] W. G. Knauss, "Quasi-elastic failure analysis of a solid-propellant rocket motor under thermal variations," *American Institute of Aeronautics and Astronautics Journal*, vol. 6, pp. 2101–2101, 1968.

APPENDIX A

CALIBRATION OF TORQUE SENSOR

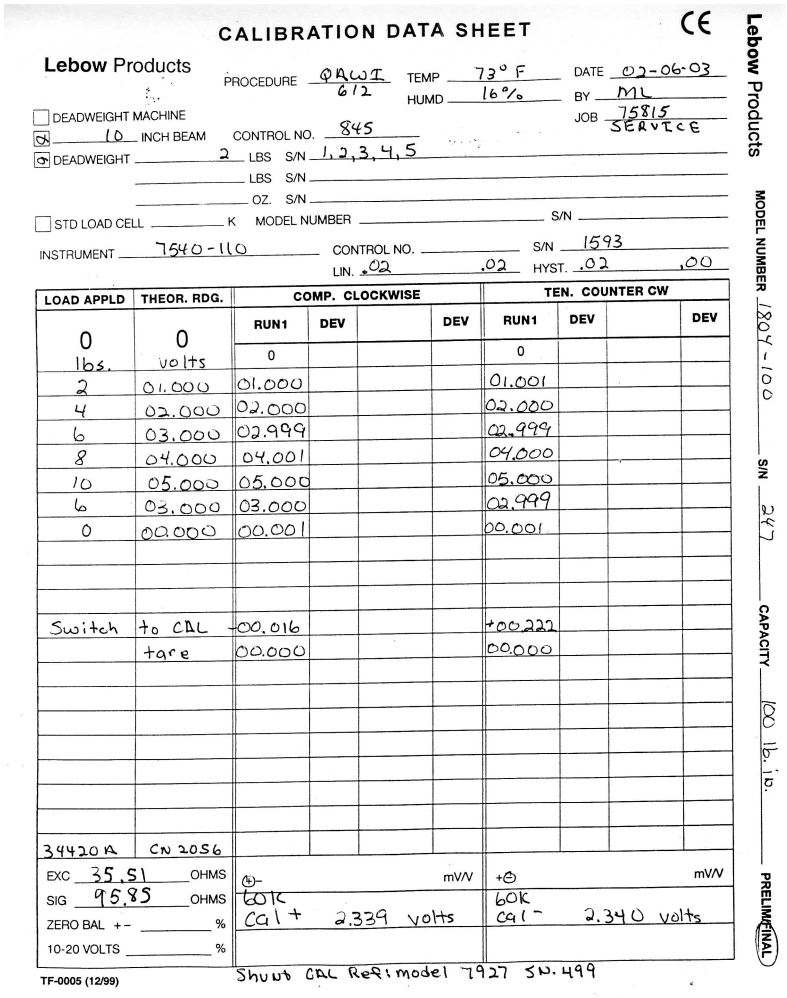

CALIBRATION DATA SHEET

Lebow Products

PROCEDURE QAQ1T 612 TEMP 73° F HUMD 16% DATE 02-06-03 BY ML JOB 75815 SERVICE

☐ DEADWEIGHT MACHINE
☒ 10 INCH BEAM CONTROL NO. 845
☒ DEADWEIGHT 2 LBS S/N 1,2,3,4,5
LBS S/N
OZ. S/N
☐ STD LOAD CELL K MODEL NUMBER S/N
INSTRUMENT 7540-110 CONTROL NO. S/N 1593
LIN. .02 .02 HYST. .02 .00

LOAD APPLD	THEOR. RDG.	COMP. CLOCKWISE RUN1	DEV		DEV	TEN. COUNTER CW RUN1	DEV		DEV
0 lbs.	0 volts	0				0			
2	01.000	01.000				01.001			
4	02.000	02.000				02.000			
6	03.000	02.999				02.999			
8	04.000	04.001				04.000			
10	05.000	05.000				05.000			
6	03.000	03.000				02.999			
0	00.000	00.001				00.001			
Switch	to CAL	-00.016				+00.222			
	tare	00.000				00.000			
34420A	CN 2056								

EXC 35.51 OHMS
SIG 95.85 OHMS
ZERO BAL +- % mV/V
10-20 VOLTS % mV/V

+⊖ 60K Cal + 2.339 volts
+⊖ 60K Cal - 2.340 volts

Shunt CAL Ref: model 7927 SN. 499

TF-0005 (12/99)

Lebow Products MODEL NUMBER 1804-100 S/N 247 CAPACITY 100 lb. in. PRELIM/FINAL

Fig. 44. Calibration sheet for the torque sensor

VITA

Parag Ravindran was born and brought up in Bangalore, India. After spending many wonderful years in Bangalore and obtaining a B.E. degree in mechanical engineering from Bangalore University (M. S. Ramaiah Institute of Technology), he came to College Station, Texas, in fall 1999. After spending a few more happy years in Aggieland, he obtained his M.S. and Ph.D. degrees in mechanical engineering from Texas A&M University in 2001 and 2006, respectively. He may be reached through Prof. K. R. Rajagopal, Department of Mechanical Department, Texas A&M University, College Station, TX 77843.

The typist for this dissertation was Parag Ravindran.